Master's thesis

Feed forward control of U anti-roll tanks

L.A. Immink

SDPO.21.004.m.

Delft University of Technology

Feed forward control of U anti-roll tanks

by

L.A. Immink

to obtain the degree of Master of Science
at the Delft University of Technology,
to be defended publicly on Friday March 19, 2021 at 13:00.

Student number:	4488733	
Project duration:	July 1, 2020 – March 19, 2021	
Involved company:	Royal IHC	
Thesis committee:	Prof. ir. H. Hopman,	TU Delft, chairman
	Ir. P. Naaijen,	TU Delft, supervisor
	MSc C. Lombardi,	Royal IHC, daily supervisor
	Dr. ing. S. Schreier,	TU Delft
	Prof. dr. ir. J.W. v. Wingerden,	TU Delft

This thesis is confidential and cannot be made public until March 19, 2021.

TU Delft Delft University of Technology

THE TECHNOLOGY INNOVATOR.

Contents

List of Figures

List of Tables

Nomenclature

Δ	Mass displacement of ship
ϵ	Phase angle
η_t	Non dimensional tank damping coefficient
Λ	Non dimensional frequency, $\omega/\omega_{0,\tau}$
λ	Root of transfer function
μ_t	Factor for GM free surface correction
∇	Volume displacement of ship
ω_0	Natural frequency
$\overline{H}_{1/3}$	Significant wave height
$\overline{P}_{b_{44}}$	Mean time-averaged power dissipated by the ship's damping coefficient
$\overline{P}_{b_{\tau\tau}}$	Mean time-averaged power dissipated by the ART's damping coefficient
$\overline{P}_{in}$	Mean time-averaged power input caused by the waves
$\overline{P}_p$	Mean time-averaged power delivered by the pump
$\Re(z)$	Real part of z
ρ_t	Density of fluid in the tank
ρ_{sw}	Density of seawater
τ	Fluid angle in tank
τ_{lim}	Statistical maximum of tank fluid angle for certain condition
τ_{max}	Physical maximum of tank fluid angle
θ	Wave slope
ζ	Wave amplitude
a	Added mass term in EoM
B	Beam of ship
b	Damping term in EoM
C	Coefficients for solution of differential equation
c	Spring term in EoM
F_p	Pump moment
$F_{4\tau}$	Moment on the ship due to the tank's motions
$F_{\tau 4}$	Moment on the tank due to the ship's motions
F_τ	External tank moment
$F_{p,a}$	Action part of pump moment
$F_{p,r}$	Reaction part of pump moment
F_{w40}	Wave moment on ship per unit of wave slope
F_{w4}	Wave moment on ship
G	Transfer function of system's plant
g	Gravitational acceleration
G_f	Gain factor
g_f	Amplification factor
G_{fb}	Gain factor of feedback loop
G_{ff}	Gain factor of feed forward loop
GM	Metacentric height (stability measure)
H	Transfer function of control part
h_t	Height of tank
I	Moment of inertia
k_{xx}	Mass radius of gyration around x-axis
L	Length of ship
N	Number of clockwise encirclements of $1+0i$
n	Local width of the tank
P	Number of open loop poles in RHP
P	Power
q	Friction coefficient

Q	Transfer function with derivative component
S	Sensitivity for certain model, either coupled or uncoupled.
s	Complex variable for Laplace transform
$S_{x,y}$	Transfer function of x per unit of y
T	Draft of ship
T	Period
t	Time
T_p	Peak period of wave spectrum
W	Work
w	Width of tank
x_i	Ship motion i: 1 = surge, 2 = sway, 3 = heave, 4 = roll, 5 = pitch, 6 = yaw
x_t	Tank length in the direction of the ship length
x_{i0}	Amplitude of x_i
Z	Number of closed loop zeros in RHP

Abstract

Within this thesis an attempt is made to improve the seakeeping of a Service Operation Vessel (SOV) by means of an active anti-roll tank (ART). For the active control it is researched if the addition of a wave prediction system can improve the ART's performance. As the seakeeping of the SOV is most important for the installed motion compensated gangway (required to transfer people to an offshore wind turbine), the workability is assessed for different control methods based on the design criteria of the SOV's gangway.

Method The computations have been made in frequency domain. Using the work of Lloyd (1989) equations of motion are derived for the behaviour of the ART. A one directional model is used with two degrees of freedom: the ship roll angle and the tank's fluid angle.

Due to the presence of a wave prediction system, a feed forward loop can be introduced in the control system. The feed forward loop is tuned by changing the phase angle of the pump with respect to the wave excitation moment. It is found that if the pump moment leads the wave excitation moment with a phase angle of about 30° - 45°, the tank's fluid will oscillate in a less power demanding way. This is caused by the interaction of the two forces that are caused by the pump. The action force on the ship's structure will always oppose the wave moment, but the force acting on the tank's fluid will only stabilise the vessel at certain frequencies.

To obtain a robust model, the feed forward loop is combined with the feedback controlled model developed by Alujević et al. (2020). The reason to combine the models is that a feedback loop is robust to model uncertainty. This is in contrast with the feed forward model, which requires high knowledge on the system's response for a certain input. So, by introducing a model with two degrees of freedom, the positive aspects of feedback and feed forward control are combined. To analyse the different properties of a feedback model and feed forward model, these two models are both kept within the analysis.

The stability of the models' feedback loop is assessed using Nyquist plots and sensitivity plots. It is found that for the damping factor belonging to the ART of the SOV, the feedback loop is unconditionally stable.

On topic of the powers related to the active ART the dissipated and actual power are analysed. Based on the dissipated powers it is found that for the same amount of dissipated power by the pump, the feed forward controlled model causes a lower root mean square value of the ship's roll in comparison with the feedback controlled model. This is explained by the better interaction of the forces generated by the pump.

Results Based on the obtained RAO for the roll motion, the workability of the SOV is assessed for a significant wave height of 3m. It is found that even though the seakeeping of the vessel increases due to the fact that the roll response decreases, the gangway motions aren't significantly affected by the active control of the ART. The reduction in roll response is not proportional to the reduction of the gangway motions since other vessel motions such as heave and sway also effect the gangway's motions.

Conclusion Adding a feed forward loop to the feedback controlled model developed by Alujević et al. (2020) improves the seakeeping of the SOV. However, to improve the workability of the SOV it is recommended to include a passive ART in the design, instead of an active ART. This is because the active control has little impact on the gangway's motions compared to the passive ART.

Preface

This thesis is written to obtain the degree of Master of Science at the Delft University of Technology. The work is developed in corporation with the TU Delft and Royal IHC. Therefore, I want to thank all supervisors and other involved people from Royal IHC and TU Delft.

- MSc C. Lombardi, for the daily supervision. Thank you for all the (online) meetings in which you helped me keep on track.
- Ir. P. Naaijen, for the supervision. Thank you for joining the various progress meeting and asking analytical questions to make the work more solid.
- Prof. ir. H. Hopman, for chairing the graduation committee.
- Prof. dr. ir. J.W. v. Wingerden, for taking part in the graduation committee and helping out with the control systems theory.
- Dr.ing S. Schreier, for taking part in the graduation committee.
- Ir. A. den Blanken, Ir. J. Clarenburg and Ir. J. van Stappen, for answering several questions during the process.

Hopefully this thesis will form a contribution to more safe and sustainable offshore operations.

1 - Introduction

In this Master's thesis research is performed on topic of U anti-roll tanks. The research subject is proposed by Royal IHC for the design of a Service Operation Vessel (SOV). Royal IHC is developing this vessel type for the offshore wind industry. According to Royal IHC (2020b) "the vessels feature a fully integrated service package with provisions for one motion compensated gangway, one active heave or motion compensated crane, daughter craft and step-less boat landing to allow for effective operations".

Figure 1.1: Example of a Service Operation Vessel.

1.1 Research context

1.1.1 Problem definition

Since the SOV is designed to perform operations at sea, the vessel motions at zero speed are an important aspect of the design. As conventional stabilisers such as bilge keels and fins provide little roll damping at zero speed, a U anti-roll tank is considered. If designed and controlled correctly, such a tank can reduce the vessel's roll motion and thereby increase the workability of the vessel. The design of the U-tank is dependent on the specific vessel data as well as the environment in which the vessel will operate. To maximise the positive effect on the vessel's roll motion the size, weight, location and control method of the tank must be determined.

For the initial design of the vessel seakeeping tests have been performed by MARIN. In these tests the operational limits of the gangway of the vessel have been determined. During the tests a passive anti-roll tank was included. To be able to improve these results a research study is proposed by Royal IHC.

After performing an initial literature study, it was found that improvements could possibly be achieved by introducing a wave prediction system. This allows to make use of a feed forward controlled model instead of a feedback controlled model (which is found frequently in literature on active anti-roll tanks). The goal of the thesis will be to assist the design question whether a feed forward controlled anti-roll tank can be beneficial for the workability of the SOV.

As mentioned, the gangway is the critical aspect of the workability of the vessel. If the motions of the vessel become to large, the motion compensation system of the gangway will be unable to keep the gangway connected to the offshore wind turbine. Since the overall operational limit of the vessel is set to a significant wave height of 3m, the gangway's motion compensation system will be assessed for this condition.

For convenience, the term 'anti-roll tank' will be abbreviated into 'ART'.

1.1.2 Research process

Before the writing of this thesis several steps have been taken. Initially a Research Proposal was written containing a first iteration of a gap analysis. Instead of focusing on the optimisation of the design of passive ARTs, it was found that research on topic of active ARTs had more value. Since papers describing the active control of ARTs mostly regarded feedback control systems, research on topic of feed forward control was underrepresented.

After discussing the Research Proposal during the kick-off meeting a Plan of Approach was written for the entire research project. The kick-off meeting together with the Plan of Approach resulted in a more detailed formulation of the research questions.

The Plan of Approach provided the framework for a literature study. In the Literature Study more information on the research questions is obtained.

1.1.3 Research questions

For the intended research the following research question is formulated:

What is the effect of using a wave prediction system for the control of an active U anti-roll tank on the workability of an SOV operating at zero speed?

To answer the research question, subquestions are formulated as well:

1. *What is the effect of a passive U anti-roll tank on a vessel's motion?*
2. *How can a passive U anti-roll tank be improved by making it active?*
3. *What type of model is most suitable to reduce the motions for the vessel with an active controlled U-tank?*
4. *What is the increase in workability due to the system?*
5. *What is the power demand for the active controlled U anti-roll tank?*

1.2 Types of anti-roll tanks

Before looking at any mathematical models of ARTs, an overview of the various types will be provided first. In general there are two types of ARTs: free surface tanks and U-shape tanks.

Free surface tank The free surface tank is also known as a 'flume' tank. According to Abdel Gawad et al. (2001) this tank was first investigated by Froude in 1874. The tank's width is normally equal to the vessel's beam and as the vessel rolls, the fluid will slosh back and forth. If the tank is excited in a certain frequency range, the tank will provide a stabilising moment on the vessel.

U-shaped ART The other type is the U-shaped ART that consists of two wing tanks connected by a duct. This tank was studied first by Frahm. The main benefit of a U ART with respect to a flume tank is the smaller free surface effect. In the duct of the U-ART a pump can be placed to actively control the tank. Therefore, a distinction can be made between passive and active ARTs.

Besides installing a pump, it is also possible to place valves in the duct to control the flow. This type of ART is defined as passive controlled and will not be discussed into further detail within this thesis.

1.3 Report structure

In this thesis the content will be addressed in different chapters.

- *Chapter 2 - Passive anti-roll tanks* - In Chapter 2 the working principles of a passive ART will be discussed. Also the mathematical model by Lloyd (1989) together with the notations and parameters of the vessel and ART will be introduced. Finally, the transfer functions and general properties of the ART based on the equations of motion will be computed.
- *Chapter 3 - Active anti-roll tank* - In Chapter 3 the mathematical model of a feedback controlled ART based on Alujević et al. (2020) will be introduced. Furthermore, the development of the feed forward controlled model and a 2DoF controlled model which is a combination of the feedback and feed forward model will be discussed.
- *Chapter 4 - Stability analysis* - In Chapter 4 the stability of the various models will be assessed. Once the models are considered stable, the further analysis can proceed.
- *Chapter 5 - Workability* - Chapter 5 regards the analysis of the transfer functions using a wave spectrum. The transfer functions will be assessed on the design criteria of the gangway.
- *Chapter 6 - Power dissipation and pump power requirement* - In Chapter 6 computations are made to determine the pump power required for the active control of the ART.
- *Chapter 7 - Results* - In this chapter the derived knowledge from the previous chapters will be combined in order to obtain the results of the thesis.
- *Chapter 8 - Discussion* - In this chapter the results of the thesis will be discussed. Also recommendations for further work are provided.
- *Chapter 9 - Conclusion* - Final conclusion of the work performed by answering the research question.

2 - Passive anti-roll tanks

2.1 Working principles

Basic working principles The basic working principles of a passive ART will be illustrated using Figure 2.1. The depicted scenario is for the working point of the tank in which the fluid motion leads the roll motion by a 90° phase angle. Note that, as stated by Holden et al. (2009), the weight of the tank fluid as well as the acceleration of the fluid (as per Newton's Second and Third Laws) contribute to stabilising moment due to the presence of the ART.

1. In the first sketch the vessel is horizontal, while the roll rate is at a maximum to starboard. For the optimum working of the tank, the fluid should now exert the maximum stabilising moment to port side.

2. In the second sketch, the roll rate is zero as well as the stabilising moment due to the tank. As the vessel rolls back to port side, the roll rate increases.

3. At the maximum roll rate (now in port side direction) the fluid exerts a maximum stabilising moment to star board. The fluid's centre of gravity is still at starboard side due to the inertia of the fluid.

4. Once the vessel is at its maximum roll angle to port side, the fluid angle will be zero with respect to the vessel to avoid amplification of the wave excitation moment.

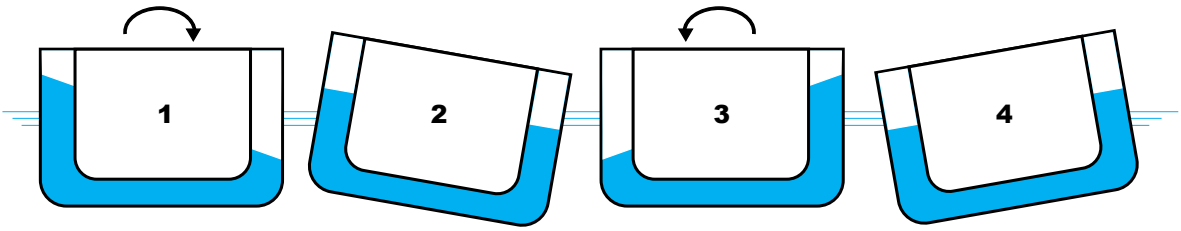

Figure 2.1: Working principle of a passive U anti-roll tank.

Rotations In order to study the effects of the U ART on the vessel motions, the following angles should be considered.

- τ: The tank's fluid angle has its centre of rotation at the centreline of the vessel. The fluid level above the datum level at a reservoir will always be equal to the fluid level below the datum level at the other reservoir.

- x_4: The axis about which the ship rolls, is not constant since the tank's fluid moves the transverse centre of gravity of the ship over time. However the assumption is made that the relative weight of the tank's fluid is small, as well as the rotations. Therefore, for the model it is assumed that the tank's fluid will not affect the location of the ship's centre of gravity. Therefore, it will be assumed that the ship rolls about the centre of gravity.

- θ: The wave slope is defined as the angle between a horizontal line and the surface of the sea water.

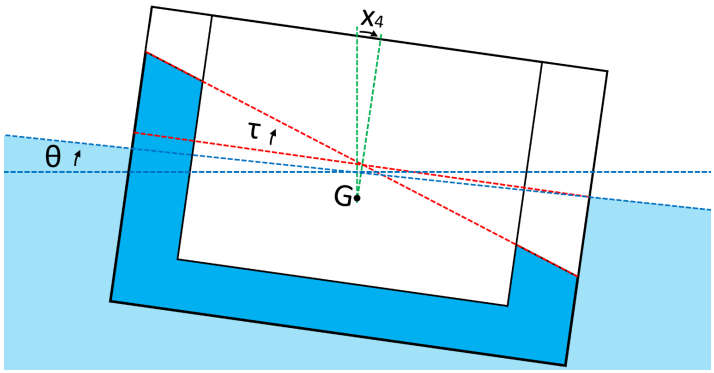

Figure 2.2: The ship's roll angle x_4, tank's fluid angle τ and wave slope θ.

Different working points For the ART to work optimal, the stabilising tank moment should counteract the roll moment. Since a ship will have the largest moment at its natural frequency, it is desirable to design the ART in such a way that it will provide the largest stabilising moment at the ship's natural frequency. As the ship's roll motion will lag the wave moment by 90° at its natural frequency, the ART's stabilising moment should lead the roll motion by 90° at that frequency in order to counteract the wave moment. As will be elaborated further on in this thesis, the excitation frequency at which the ART's fluid will lead the motion by 90° is the natural frequency of the ART. Therefore, the ART and the ship should have the same natural frequency.

For the behaviour of the ART for different phase angles between the tank's fluid angle and the ship's roll motion ϵ_{τ,x_4} an overview is given in Table 2.1. For an illustration of the phase angles see Figure A.1 in the appendix.

Table 2.1: Overview of phase angles ϵ_{τ,x_4}.

Phase	Effect	Description
0°	Positive	The water will stabilise the vessel. As the vessel rolls to its maximum angle, the water will flow in opposite direction. However, once the vessel is back in upright position, and rolls over again, the water (except for high frequencies) will have to be pumped up the reservoir to obtain the effect.
90°	Optimal	As the vessel rolls to its maximum position, the relative tank angle (τ) will become zero. As the vessel rolls back into the upright position, the water will flow to the other side, to act as a counterweight. This is the optimal stabilising working point.
180°	Negative	The water will act like a static free surface moment. As the vessel rolls to a side, the water will flow to that side as well. So, as the vessel rolls back to the upright position, the water will act as a counterweight (since it has flowed to the lowest reservoir) preventing the vessel to roll back.
270°	Worst	As the vessel rolls back into upright position, the water is in a place so that it adds to the righting moment, causing maximum amplification of the motion.

What can be concluded is that the presence of the ART will have the desired effect if the tank's fluid angle leads the ship's roll motion with a phase angle of about 0° to 90°. More detail on these phase angles will be given after the equations to describe the behaviour of the system have been derived.

2.2 Notations and parameters

Anti-roll tank To describe the tank, the notations as in Figure 2.3 are used. The tank's fluid angle τ is relative to the ship's roll angle x_4. The corresponding dimensions are given in Table 2.2.

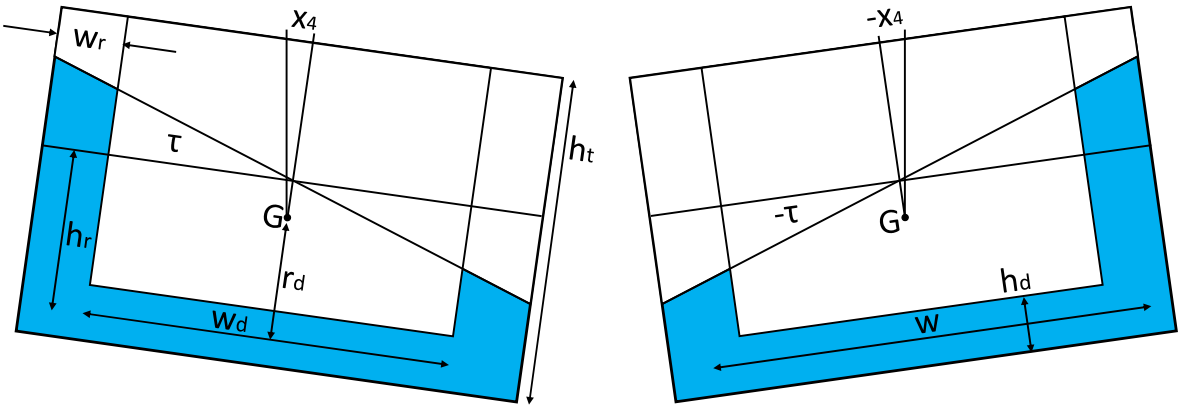

Figure 2.3: Notations for mathematical model.

Table 2.2: Parameters of the ART

Parameter	Value	Unit	Description
w_r	[redacted]	m	Reservoir width
w_d	[redacted]	m	Duct width
h_d	[redacted]	m	Duct height
h_t	[redacted]	m	Reservoir height
h_r	[redacted]	m	Fluid level in reservoir
r_d	[redacted]	m	Radius from CoG of ship to duct center
x_t	[redacted]	m	Length of the tank

Ship To analyse the ship motions, the hydrodynamic coefficients are used to obtain a linear model. For the use of the hydrodynamic coefficients a_{44} (added mass) and b_{44} (damping) it must be clear to what scenario they apply. If the coefficients apply to the situation with empty ART, they will change once the ART is filled due the change in displacement. However, if the hydrodynamic coefficients apply to a ship with filled ART, it is impossible to decouple the behaviour of the ART. As a solution, the hydrodynamic coefficients of the ship are based on a frozen tank fluid. In this way the weight of the fluid is taken in to account for the ship's properties, while the fluid's dynamics are accounted for in the coupled equations of motion.

The values for a_{44} and b_{44} used within this thesis are obtained by means of DIFFRAC which is a wave diffraction program built by MARIN. The program is based on potential flow theory. For the analysis the fluid is assumed to be inviscid, homogeneous, irrotational and incompressible (MARIN, 2020a).

Since a frozen tank is assumed, c_{44} must not be corrected for the free surface effect. The GM must only account for the weight of the fluid. The dynamics (which includes the free surface effect) is incorporated by means of a coupled set of equations, see §2.3. Only for static (loading) conditions, a correction of the GM can be made to correct for the free surface effect of the ART.

The moment of inertia is determined using the mass radius of gyration, see Equation 2.1a. This moment of inertia must be added tot the added mass term in the equation of motion. Furthermore, c_{44} is obtained based on the GM as shown in Equation 2.1b. For the ship the dimensions are used as in Table 2.3.

$$\text{(a)} \quad I_{44} = k_{xx}^2 \cdot \rho_{sw} \cdot \nabla \quad \left[\text{kg} \cdot \text{m}^2\right], \quad \text{(b)} \quad c_{44} = \rho_{sw} \cdot g \cdot \nabla \cdot GM \quad [\text{Nm/rad}] \tag{2.1}$$

Table 2.3: Parameters of the SOV

Parameter	Value	Unit	Description
L	[redacted]	m	Length
L_{pp}	[redacted]	m	Length between perpendiculars
B	[redacted]	m	Beam
T	[redacted]	m	Draft
GM	[redacted]	m	Metacentric height with 'frozen' ART
KG	[redacted]	m	Distance between keel and CoG
∇	[redacted]	m^3	Displacement
k_{xx}	[redacted]	m	Mass radius of gyration around x-axis

2.3 Equations of motion

Based on the model by Lloyd (1989) the equations of motion can be obtained as in Equation 2.2, with F_4 in Nm. Note that x_4, τ (and their derivatives) and F_4 are time dependent.

$$\begin{bmatrix} a_{44}+I_{44} & a_{4\tau} \\ a_{\tau 4} & a_{\tau\tau} \end{bmatrix} \begin{bmatrix} \ddot{x}_4 \\ \ddot{\tau} \end{bmatrix} + \begin{bmatrix} b_{44} & 0 \\ 0 & b_{\tau\tau} \end{bmatrix} \begin{bmatrix} \dot{x}_4 \\ \dot{\tau} \end{bmatrix} + \begin{bmatrix} c_{44} & c_{4\tau} \\ c_{\tau 4} & c_{\tau\tau} \end{bmatrix} \begin{bmatrix} x_4 \\ \tau \end{bmatrix} = \begin{bmatrix} F_4 \\ 0 \end{bmatrix} \tag{2.2}$$

Or written more compact:

$$(\mathbf{A}+\mathbf{I})\ddot{\mathbf{x}}(t) + \mathbf{B}\dot{\mathbf{x}}(t) + \mathbf{C}\mathbf{x}(t) = \mathbf{F}(t) \quad [\text{Nm}] \tag{2.3}$$

In this set of equations F_4 is the harmonically varying wave excitation moment. The acceleration and the rate of the ship's roll angle will be oscillating with the same harmonic frequency. This applies for the motions of the ship as well as for the motions of the tank's fluid. The coefficients below apply to Equation 2.2:

- $a_{\tau\tau} = Q_t\ w_r \left(\frac{w}{2h_d} + \frac{h_r}{w_r}\right) \quad \left[\text{Nm/(rad/s)}^2\right]$
- $b_{\tau\tau} = Q_t\ q\ w_r \left(\frac{w}{2h_d^2} + \frac{h_r}{w_r^2}\right) \quad [\text{Nm/(rad/s)}]$
- $c_{\tau\tau} = Q_t\ g = c_{\tau 4} \quad [\text{Nm/rad}]$
- $a_{\tau 4} = Q_t(r_d + h_r) \quad \left[\text{Nm/(rad/s)}^2\right]$
- $c_{\tau 4} = Q_t\ g \quad [\text{Nm/rad}]$

In the equations above Q_t is a common expression. It has no physical meaning in itself.

$$Q_t = \frac{\rho_t\ w_r\ w^2\ x_t}{2} \quad [\text{kg} \cdot \text{m}] \tag{2.4}$$

As can be seen from the set of equations, coupling takes place only via the roll motion. For the entire derivation of the equation of motion, Lloyd (1989) made the assumptions as listed in Table 2.4.

Table 2.4: Overview of assumptions.

ID	Assumption	Expression
1	The velocity of the tank's fluid is constant in the duct and constant in the reservoir; the flow will instantly change speed as it heads from the duct to the reservoir and vice versa.	$\frac{\partial v}{\partial y} = 0$
2	The tank's fluid and ship roll angle are small.	$\tan(\tau) = \tau$, $\tan(x_4) = x_4$
3	Laminar flow; resistance is proportional to the flow velocity.	$q \cong v$
4	Lateral forces of the ship on the tank are zero.	$\dot{x}_2 = \ddot{x}_2 = 0$
5	The tank will have no effect on the surge, heave or pitch moments.	$a_{i\tau} = b_{i\tau} = c_{i\tau} = 0,\ \forall\ (i = 1;\ i = 3;\ i = 5)$
6	The sway forces or yaw moments will be zero for steady state tank fluid angles (τ). Also the rate of change of the tank fluid angle ($\dot{\tau}$) has no significant effect on sway or yaw motions.	$b_{i\tau} = c_{i\tau} = 0\ \forall\ (i = 2;\ i = 6)$
7	Tank's length CoG is located at the ship's length CoG. Therefore acceleration of the tank fluid angle has no effect on yaw motions and vice versa.	$a_{6\tau} = a_{\tau 6} = 0$
8	Rate of the tank's fluid angle has no effect on the roll motions.	$b_{4\tau} = 0$

More details on the equation of motions have been provided in the Literature Study that was written in preparation for this thesis. Since the approach is based on the work of Lloyd (1989), more detail can be obtained by reading the work itself too.

Complex numbers Assuming harmonic oscillations of the moments and the responses, the equations of motion can be rewritten by using complex expressions ($i = \sqrt{-1}$).

$$x_4 = x_{40}\sin(\omega t + \epsilon) = \Re\left(x_{40}e^{-i(\omega t+\epsilon)}\right) = \Re\left(x_{40}e^{-i\epsilon}\cdot e^{-i\omega t}\right) = \Re\left(\hat{x}_{40}\cdot e^{-i\omega t}\right) \quad (2.5)$$

So now let $F_4(t) = \Re(\hat{F}_{40}e^{-i\omega t})$, $x_4(t) = \Re(\hat{x}_{40}e^{-i\omega t})$ and $\tau(t) = \Re(\hat{\tau}_0 e^{-i\omega t})$. Using these expressions properties of the ART can be obtained easily.

$$(\mathbf{A}+\mathbf{I})\ddot{\mathbf{x}}(i\omega) + \mathbf{B}\dot{\mathbf{x}}(i\omega) + \mathbf{C}\mathbf{x}(i\omega) = \mathbf{F}(i\omega) \quad [\text{Nm}] \quad (2.6)$$

2.4 Properties of the ART

For the ART multiple properties can be defined such as the natural frequency, the damping coefficient, the stabilising moment and the maximum fluid angle.

Block diagram To illustrate the different moments considered in the mathematical model a block diagram is made in Figure 2.4. This block diagram shows the wave moment (F_{w4}) as an input to the model. The ship motions (x_4) as a result of the waves are coupled to the ART, so the outgoing ship motions are an input to the ART. The coupling between the tank's fluid motion and the tank is shown by the moment $F_{4\tau}$, which is the moment exerted on the vessel due to the tank's fluid. In the equation of motion this moment can be seen back in the coupling terms $c_{4\tau}$ and $a_{4\tau}$ that relate the tank motions to the ship motions.

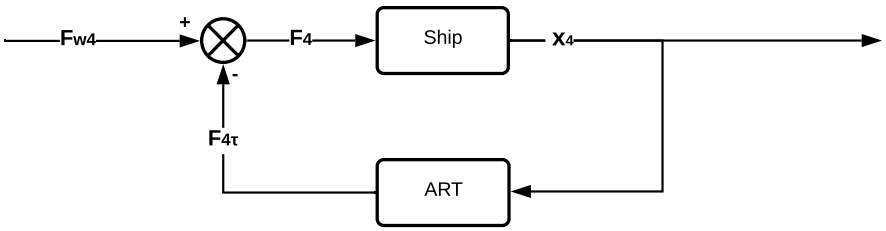

Figure 2.4: Block diagram of a passive U anti-roll tank.

Since the stabilising moment will be directly subtracted from the wave moment as seen in the block diagram, the ART will have the largest effect if the tank's stabilising moment is in phase with the wave moment. However, this is only partially true. Since this working point only occurs at high frequencies, the effect of the ART will be small, since the motions are small at high frequencies. This aspect will be discussed in more detail using Figure 2.7 further on.

Natural frequency The natural frequency of the ART can be determined similarly to a regular mass-spring system. Since the fluid level h_r contributes only little to the equation, the natural frequency of the tank is very much dependent on the initial design. Therefore, the tuning of the natural frequency should be performed before the tank is built.

$$\omega_{0,\tau} = \sqrt{\frac{c_{\tau\tau}}{a_{\tau\tau}}} = \sqrt{\frac{2gh_d}{w_r w + 2h_r h_d}} \quad [\text{rad/s}] \quad (2.7)$$

Damping coefficient The damping coefficient says something about how easily the tank's fluid can flow in the tank. Once again, this property is very much dependent on the initial design. Note that in reality the resistance is proportional to the velocity squared, but for the model a linearized coefficient is used. In §2.6 the value of damping coefficient is determined.

$$\eta_t = \frac{b_{\tau\tau}}{2\sqrt{c_{\tau\tau}a_{\tau\tau}}} = \frac{\sqrt{2}\,q\left(2\,h_r\,{h_d}^2 + w\,{w_r}^2\right)}{4\,w_r\sqrt{g\,{h_d}^3\,(2\,h_d\,h_r + w\,w_r)}} \quad [\text{-}] \tag{2.8}$$

Stabilising moment The stabilising moment exerted by the passive ART on the vessel is defined by the coupling terms. These coupling terms regard the mass coefficient $a_{4\tau}$ and the spring term $c_{4\tau}$. Note that in the equations of motion the stabilising moment is not an external moment acting on the ship, but merely a moment due to the coupling terms. To express it as a part of the external moment, it should be taken negative.

$$a_{4\tau}\ddot{\tau}(t) + c_{4\tau}\tau(t) = F_{4\tau}(t) \quad [\text{Nm}], \quad F_{stab} = -F_{4\tau} \quad [\text{Nm}] \tag{2.9}$$

Maximum fluid angle For the equations of motion to be valid, the fluid should not slosh against the top of the reservoir or be below the top of the duct. This gives the maximum value for the tank's fluid angle as below. Note that the linearisation of $\tan(\tau) \approx \tau$ is still acceptable. The approximated value is just 4.5% higher.

$$\tan(\tau_{max}) = \frac{h_t - h_d}{w} = 0.374 \quad [-] \quad \rightarrow \quad \tau_{max} = 0.358\ [\text{rad}] = 20.53^\circ \tag{2.10}$$

Loss in stability Since the fluid of the tank will cause a free surface effect, the loss in stability can be significant. For a static situation ($\omega \approx 0$) the righting moment F_4 for an applied moment is defined as below. The factor $(1 - \mu_t)$ is the loss in stability.

$$F_4 = \Delta \cdot g \cdot GM(1 - \mu_t) \cdot x_4 \quad [\text{Nm}], \quad \text{with } \mu_t = \frac{Q_t}{\Delta \cdot GM} \quad [-] \tag{2.11}$$

So, if the vessel has a certain GM for the case with frozen fluid in the ART, the value should be multiplied with $(1 - \mu_t)$ to correct for the free surface effect. Note that this only applies for static computations that make use of the vessel's GM. For dynamic computations, the free surface effect is included in the equations of motion.

2.5 Transfer functions

Based on the equations of motion the transfer functions with the corresponding phase angles can be obtained. The plots are made using the dimensions of the ART and SOV as given in Table 2.2 and Table 2.3.

General transfer functions The transfer function of the roll motion per unit of applied moment can be obtained as in the equations below. Building upon the complex equation of motion in Equation 2.6, the following expression can be found in which $\mathbf{S}(i\omega)$ is the dynamic stiffness matrix.

$$\mathbf{S}(i\omega)\mathbf{x}(i\omega) = \mathbf{F}(i\omega) \quad [\text{Nm}], \quad \mathbf{S}(i\omega) = -\omega^2(\mathbf{A} + \mathbf{I}) + i\omega\mathbf{B} + \mathbf{C} \quad [\text{Nm/rad}] \tag{2.12}$$

So the previous equation can also be expressed by the following matrix and vectors, using the dynamic stiffness matrix. Note that the elements in the vectors and matrix are functions of $i\omega$, however for convenience this will not be noted repeatedly.

$$\mathbf{S}(i\omega)\mathbf{x}(i\omega) = \mathbf{F}(i\omega) \rightarrow \begin{bmatrix} S_{F_4,x_4} & S_{F_4,\tau} \\ S_{F_\tau,x_4} & S_{F_\tau,\tau} \end{bmatrix} \begin{bmatrix} x_4 \\ \tau \end{bmatrix} = \begin{bmatrix} F_4 \\ F_\tau \end{bmatrix} \quad [\text{Nm}] \tag{2.13}$$

A solution for $\mathbf{x}(i\omega)$ can be obtained by inversion of $\mathbf{S}(i\omega)$.

$$\mathbf{x}(i\omega) = \mathbf{S}^{-1}(i\omega)\mathbf{F}(i\omega) \rightarrow \begin{bmatrix} x_4 \\ \tau \end{bmatrix} = \begin{bmatrix} S_{x_4,F_4} & S_{x_4,F_\tau} \\ S_{\tau,F_4} & S_{\tau,F_\tau} \end{bmatrix} \begin{bmatrix} F_4 \\ F_\tau \end{bmatrix} \quad [\text{rad}] \tag{2.14}$$

Since $\mathbf{S}^{-1}(i\omega)$ consists of the expressions that relate the rotations $\mathbf{x}(i\omega)$ to the applied moment $\mathbf{F}(i\omega)$, it is the transfer function of motions per unit of moment. Note that the components in the inverse matrix already incorporate the coupling behaviour between the ship and the ART. This can be understood by the fact that to invert a matrix, every matrix element is multiplied with the reciprocal of the determinant.

$$\begin{bmatrix} a & b \\ c & d \end{bmatrix}^{-1} = \frac{1}{ad - bc} \begin{bmatrix} d & -b \\ -c & a \end{bmatrix} \tag{2.15}$$

So for example, the response of the ship with passive ART to an excitation moment is determined using S_{x_4,F_4}. This expression is worked out below. By deriving the transfer function of the passive system based on the block diagram, the expression can be obtained too. This approach will be discussed into more detail in *Chapter 4 Stability analysis*.

$$S_{x_4,F_4} = \frac{1}{S_{F_4,x_4} \cdot S_{F_\tau,\tau} - S_{F_4,\tau} \cdot S_{F_\tau,x_4}} \cdot S_{F_\tau,\tau} \quad [\text{rad/Nm}] \tag{2.16}$$

Tank's fluid angle Another aspect to consider is the motion of the tank's fluid with respect to a fixed oscillating platform. This can be determined by solving Equation 2.13 for $F_\tau = 0$. The results are plotted in the left graph of Figure 2.5. These results are of use to determine the damping coefficient in §2.6 for example.

$$\begin{aligned} &S_{F_\tau,x_4} \cdot x_4 + S_{F_\tau,\tau} \cdot \tau = 0 \quad [\text{Nm}] \\ &S_{\tau,x_4,\text{uncoupled}} = \frac{\tau}{x_4} = -\frac{S_{F_\tau,x_4}}{S_{F_\tau,\tau}} \left(= \frac{S_{\tau,F_4}}{S_{x_4,F_4}} \right) \quad [\text{rad/rad}] \end{aligned} \tag{2.17}$$

To determine the coupled tank fluid angle per unit of ship roll angle, the coupled transfer function should be used from Equation 2.14. The results are plotted in the right graph of Figure 2.5.

$$\begin{aligned} &S_{F_\tau,x_4} \cdot x_4 + S_{F_\tau,\tau} \cdot \tau = 0 \quad [\text{Nm}] \\ &S_{\tau,x_4,\text{coupled}} = \frac{\tau}{x_4} = -S_{\tau,F_\tau} \cdot S_{F_\tau,x_4} \quad [\text{rad/rad}] \end{aligned} \tag{2.18}$$

Figure 2.5: Tank's fluid angle per unit of ship roll angle (Eq. 2.17 & 2.18).

The clear difference between the two graphs is the response around the natural frequency of the system. For the coupled response a large attenuation can be seen. This is caused by the fact that at the natural frequency of the ship a small moment is required to oscillate the ship. Therefore, only a small moment will act on the ART's fluid. So, the coupled response only regards the response of τ due to x_4. However, what is of interest is the comparison between the response of τ due to waves with x_4 due to waves. Therefore it can be concluded that the uncoupled response is of interest to analyse τ and x_4 due to waves.

Wave moment In order to obtain the transfer functions of the system per unit of wave slope or height, the wave moment is required. The wave moment will be approximated using an equation by Kornev (2012) for a vessel without ART. See Appendix A.2 for a derivation of the expression.

$$F_{w4} = -a_{44}\frac{\omega^4}{g}\zeta_0 \sin(\omega t) + b_{44}\frac{\omega^3}{g}\zeta_0 \cos(\omega t) + c_{44}\frac{\omega^2}{g}\zeta_0 \sin(\omega t) \quad [\text{Nm}] \tag{2.19}$$

The expression above can be rewritten into an expression of the wave moment per unit of wave slope. For the value of k the dispersion relation will be used ($\omega^2 = kg$). The wave slope is now as follows:

$$\theta = k \cdot \zeta = \frac{\omega^2}{g} \cdot \zeta \left(= \frac{\omega^2}{g} \cdot \zeta_a \sin(\omega t) \right) \quad [\text{rad}] \tag{2.20}$$

Substituting the above equation into the equation for the wave moment and rewriting to the complex notation gives:

$$F_{w4} = F_{w40} \cdot \theta = \theta \left(c_{44} + b_{44} \cdot i\omega - a_{44} \cdot \omega^2 \right) \quad [\text{Nm}] \tag{2.21}$$

Now the magnitude of the wave moment is as follows:

$$|F_{w4}| = \theta \sqrt{\left(c_{44} - a_{44}\omega^2\right)^2 + \left(b_{44}\omega\right)^2} \quad [\text{Nm}] \tag{2.22}$$

Ship's roll and tank's fluid angle per unit of wave slope The transfer function of the ship's roll motion per unit of wave moment can now be determined as below.

$$S_{x_4,\theta} = S_{x_4,F_4} \cdot \frac{F_{w40}}{\theta} \quad \text{[rad/rad]} \tag{2.23}$$

Similarly, the transfer function of the tank's fluid angle and the wave slope can be obtained.

$$S_{\tau,\theta} = S_{\tau,F_4} \cdot \frac{F_{w40}}{\theta} \quad \text{[rad/rad]} \tag{2.24}$$

The results of the latter two equations are plotted in Figure 2.6 for input where $\omega_{0,\tau} \approx \omega_{0,x4}$.

Figure 2.6: Ship's roll motion per unit of wave slope as in Eq. 2.23 and 2.24.

As expected the vessel's roll motion without ART will be equal to the wave slope for low wave frequencies, since the static behaviour will dominate. Around the natural frequency of the vessel a resonance peak can be seen. Furthermore, as seen in the graph, the ART will have a negative effect for low wave frequencies due to the free surface effect. Around the natural frequency of the vessel, the positive effect of the ART is spotted. For low damping coefficients η_t a double resonance peak occurs due to the additional degree of freedom. For high damping coefficients the ART's fluid will have very little movement causing the effect to decrease.

As the wave frequencies increase, the transfer function will go to zero since the waves are to short to excite the vessel in a significant way.

Phase angles Other important aspects of the ART are the various phase angles which can be obtained using the transfer functions. In Figure 2.7 the phase angles are plotted for $\eta_t = 0.25$.

$$\tan(\epsilon_{x_4,\theta}) = \frac{\Im(S_{x_4,\theta})}{\Re(S_{x_4,\theta})} \quad \text{[-]}, \quad \tan(\epsilon_{x_4,\tau}) = -\frac{\Im(S_{\tau,x_4})}{\Re(S_{\tau,x_4})} \quad \text{[-]} \tag{2.25}$$

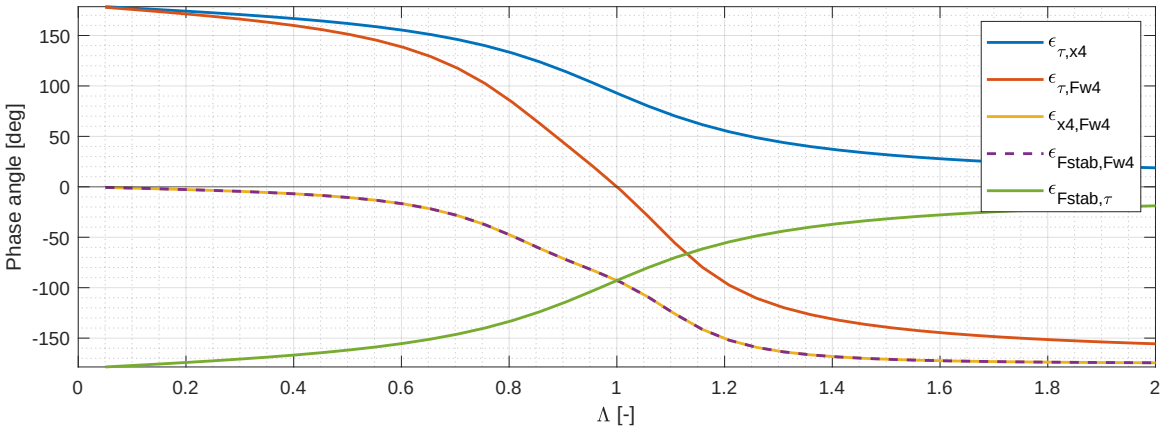

Figure 2.7: Phase angles using Eq. 2.25 for $\omega_{0,\tau} \approx \omega_{0,x4}$ and $\eta_t = 0.25$.

As seen, for low frequencies the vessel will oscillate in phase with the wave moment (yellow curve). This is because the static buoyancy force dominates the motions. For these low frequencies the stabilising moment is in phase with the moment (purple curve), meaning that the motions are amplified. This is caused by the free surface effect.

At the natural frequency of the vessel, the roll motion will lag the wave moment with a 90° phase angle (yellow curve). Since the tank's fluid angle leads the vessel's roll motion with a 90° phase angle (blue curve), the tank's fluid angle is in phase with the wave moment (red curve). This is the optimal working point as described in §2.1.

Note that even though the tank's fluid angle is in phase with the wave moment, the stabilising moment is not opposed to the wave excitation moment at the natural frequency (purple curve). This is due to the dynamic working principle of the ART. For higher frequencies, the stabilising moment is not exactly opposed to the tank's fluid angle anymore (green curve). The reason why the combined natural frequency of the ART and ship is still the optimal working point is because the phases together with the magnitude of the response is tuned best. (For the notations, see Figure 2.2.)

2.6 Determining the ART damping coefficient

The damping coefficient η_t of the ART is defined as in Equation 2.8. To determine the value of this coefficient the value of the friction coefficient q is required. Since this friction coefficient can't be determined analytically, use is made of a hexapod test, performed by MARIN (2020b). For this hexapod test a scale model of the ART is filled with water and oscillated with a certain amplitude and frequency.

Low frequencies For the low frequencies, the static behaviour of the tank will dominate since the dynamic response of the ART will be very small. In the model by Lloyd (1989) this means that the coefficient $c_{\tau\tau}$ will dominate. This coefficient is based on the static moment generated by the fluid in the wing tank of the ART.

$$F_{stab} = F \cdot r = \rho_t \, g \, \Delta h_r \, w_r \, x_t \cdot w/2 = \rho_t \, g \, (w \, x_4) \, w_r \, x_t \cdot w/2 \quad [\text{Nm}] \tag{2.26}$$

The approach of Lloyd (1989) differs from the approach of MARIN (2020b). For the static response MARIN uses the free surface moment based on the moment of inertia of the fluid's

surface. Since for small values $\tan(x_4) \approx x_4$, the free surface moment can be described as below. By simplifying it can be seen that the two approaches provide the same outcome.

$$\begin{aligned} F_{stab} &= \rho_t \; g \; I_{xx} \; x_4 = \rho_t \; g \; \frac{1}{12} \; x_t \; ((w + w_r)^3 - (w - w_r)^3) \; x_4 \quad [\text{Nm}] \\ &= \rho_t \; g \; \left(\frac{1}{2} w^2 \; w_r + \frac{1}{6} w_r^3 \right) x_4 \approx \rho_t \; g \; \frac{1}{2} w^2 \; w_r \; x_4 \quad [\text{Nm}] \end{aligned} \tag{2.27}$$

Hexapod The hexapod tests have been performed for a roll amplitude of 6°. This means that the moments are linearised at this roll amplitude. The affect of this linearisation is assessed by means of a paper written by Gunsing et al. (2014) on topic of experimental data on internal damping of an ART. In the paper it is found that for different roll amplitudes different peak damping moments are measured. However, the higher the roll amplitude, the lower the peaks are. So, if the ship's roll motion will have a roll response below 6°, a conservative approach is in place.

To find the moment caused by the ART, the data of the hexapod has been corrected for the transverse accelerations using Equation 2.28. In the equation I_{xx} is the radius of inertia in kgm^2 of the setup, a_ϕ is the rotational acceleration, G_{ART} is the CoG of the ART with respect to its bottom, and a_y is the transverse acceleration.

$$F_{stab} = I_{xx} \cdot a_\phi - m \cdot G_{ART} \cdot a_y \quad [\text{Nm}] \tag{2.28}$$

The measured moment by the hexapod has been translated into the moment that would be experienced by the vessel.

Figure 2.8: Comparison of data with model.

Plot By plotting the data of the test performed by MARIN together with the theoretical values based on Table 2.2, the damping coefficient is found. For the distance between the duct and the centre of gravity (r_d) the distance is taken as for the vessel. However, to match the data points, the value should (falsely) be taken negative. Since the only purpose of the hexapod is to obtain the damping coefficient, this has no further consequences for the calculations performed later on in this thesis. See Appendix A.3 for more elaboration.

Looking at Figure 2.8 it can be concluded that for the ART a damping coefficient η_t of 0.25 is a good approximation.

3 - Active anti-roll tank

As seen multiple times in the previous chapter, a passive ART will not behave optimal at all excitation frequencies. There are several unwanted effects:

- The optimal working point only occurs at the natural frequency of the ART.
- For low excitation frequencies the motions will be amplified.
- For low damping factors an extra resonance peak occurs.
- For high damping factors the effect of the tank becomes less significant.

Introducing the pump Using a pump these unwanted side effects can be reduced, or even entirely avoided. By introducing a pump to control the flow in the ART, the external moment F_τ acting on the tank's fluid will be non-zero. This external tank moment will affect the stabilising moment $F_{4\tau}$ caused by the coupling terms $a_{\tau 4}$ and $c_{\tau 4}$. Note that for complex notation $F_\tau(t) = \Re(\hat{F}_\tau e^{-i\omega t})$.

$$\begin{bmatrix} a_{44}+I_{44} & a_{4\tau} \\ a_{\tau 4} & a_{\tau\tau} \end{bmatrix} \begin{bmatrix} \ddot{x}_4 \\ \ddot{\tau} \end{bmatrix} + \begin{bmatrix} b_{44} & 0 \\ 0 & b_{\tau\tau} \end{bmatrix} \begin{bmatrix} \dot{x}_4 \\ \dot{\tau} \end{bmatrix} + \begin{bmatrix} c_{44} & c_{4\tau} \\ c_{\tau 4} & c_{\tau\tau} \end{bmatrix} \begin{bmatrix} x_4 \\ \tau \end{bmatrix} = \begin{bmatrix} F_4 \\ F_\tau \end{bmatrix} \tag{3.1}$$

Besides the effect of the pump on F_τ, the pump will also have an effect on F_4 since the vessel's structure will exert a reaction force on the pump. This is illustrated in Figure 3.1. The forces can be transformed into a moment by multiplying with the lever r_d.

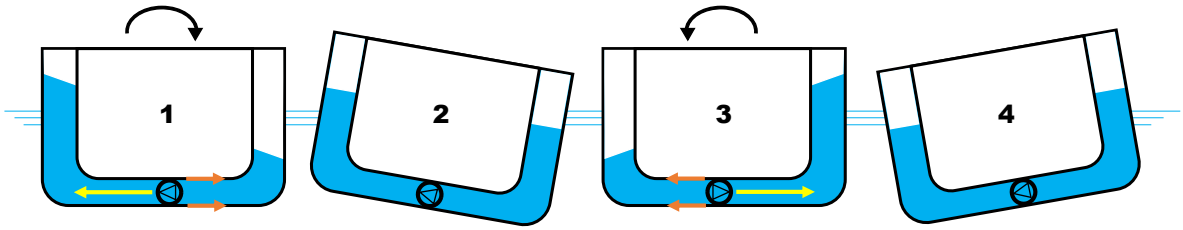

Figure 3.1: Two control forces acting on the ART.

So, as seen in the figure above, the pump will not only affect the tank's fluid motion but will also exert a stabilising moment directly on the tank's structure. Therefore, for active controlled ARTs the tank's fluid motion as well as the force on the ship's structure are of importance. In this chapter three different models to use the pump will be discussed.

1. Feedback controlled model based on Alujević et al. (2020)
2. Feed forward controlled model
3. 2DoF controlled model (combination of 1 & 2).

Pump properties For the analysis it is assumed that the transient behaviour of the pump is not a significant aspect of the active control. Since the motions are relatively slow and have a harmonic shape, the pump will have the necessary time to respond. Note that even though the pump is assumed to respond perfectly, this does not mean that the pump can instantly move the fluid without requiring very high powers.

3.1 Feedback controlled model

For the active control of an ART a common approach in literature is to apply feedback control based on the roll rate of the vessel. Alujević et al. (2020) and Holden et al. (2009) have developed and analysed such models. The frequency domain approach of Alujević et al. (2020) will be discussed below, before looking into feed forward control.

3.1.1 Mathematical model

Block diagram In the figure below a block diagram of the feedback controlled system is shown. This diagram shows the wave moment (F_{w4}) as an input to the model and the ship motions (x_4) as an output. In between the passive and the active feedback loops can be seen.

The passive loop regards the ship motions x_4 that are multiplied with a transfer function in order to arrive at the moments on the fluid due to the motions of the ship. These moments are caused by the coupling terms in the equation of motion ($a_{\tau 4}$ and $c_{\tau 4}$).

For the active feedback loop the ship's roll angle is fed into a roll rate sensor which gives a signal to the controller. The output of the controller is a certain power input for the pump. The pump's output is then the moment on the ship's structure and the moment on the ART's fluid. This will be made more clear by means of the following paragraphs.

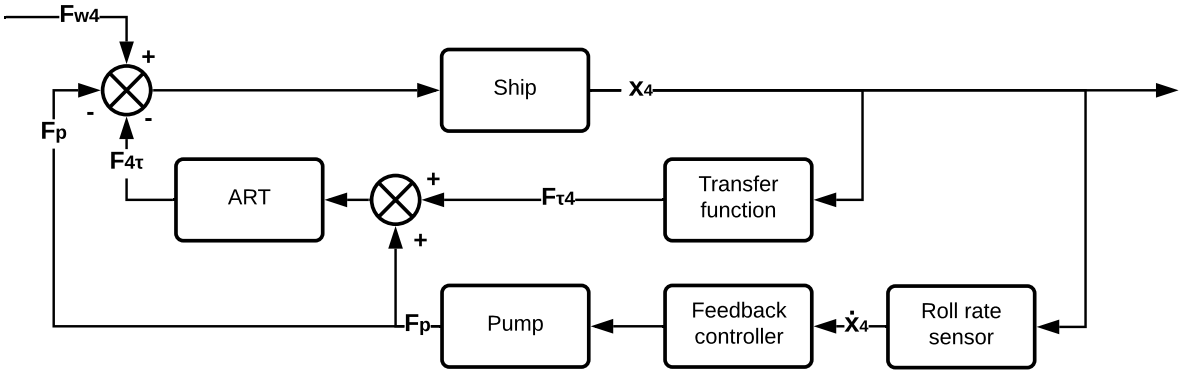

Figure 3.2: Block diagram of active feedback controlled ART.

The pump Via a negative feedback loop, the pump is controlled based on the roll rate. So, the (required) pressure difference generated by the pump is proportional to the roll rate.

$$\Delta p = -g_f \cdot \dot{x}_4 \quad [\text{Pa}] \tag{3.2}$$

As stated before, the pump exerts an action moment on the ship's structure ($F_{p,a}$) and a reaction moment on the tank's fluid ($F_{p,r}$), see Figure 3.1.

$$F_{p,a} = -G_f \cdot \dot{x}_4, \quad F_{p,r} = G_f \cdot \dot{x}_4 \quad [\text{Nm}] \tag{3.3}$$

In these two equations the feedback gain G_f is defined as the feedback amplification factor g_f (Pa · s/rad) multiplied with the cross-section area of the duct and the distance between the ship's CoG and the centre line of the duct. In this way, G_f is a moment per unit of rotation.

$$G_f = g_f \cdot h_d \cdot x_t \cdot r_d \quad [\text{Nms/rad}] \tag{3.4}$$

Transfer functions For the transfer functions use is made of the coupled equation of motion in Equation 2.14. By using this set of equations, the feedback control can be compared with respect to a passive ART. Note that since the coupled transfer functions from the equation of motion are used, the transfer functions will not be derived by writing out the expressions as depicted in Figure 3.2.

To control the pump based on the roll rate, the transfer function of the ship's roll rate is required per unit of moment.

$$\dot{\mathbf{x}}(i\omega) = i\omega \cdot \mathbf{S}^{-1}(i\omega)\mathbf{F}(i\omega) = \mathbf{Q}(i\omega)\mathbf{F}(i\omega) \quad [\text{rad/s}] \tag{3.5}$$

The matrix $\mathbf{Q}(i\omega)$ contains the transfer function of the roll rates per unit of excitation moment.

$$\mathbf{Q}(i\omega) = \begin{bmatrix} Q_{\dot{x}_4,F_4} & Q_{\dot{x}_4,F_\tau} \\ Q_{\dot{\tau},F_4} & Q_{\dot{\tau},F_\tau} \end{bmatrix} \quad \left[\frac{\text{rad}}{\text{Nm s}}\right] \tag{3.6}$$

The effects of the pump moments can now be determined.

$$\begin{bmatrix} \dot{x}_4 \\ \dot{\tau} \end{bmatrix} = \begin{bmatrix} Q_{\dot{x}_4,F_4} & Q_{\dot{x}_4,F_\tau} \\ Q_{\dot{\tau},F_4} & Q_{\dot{\tau},F_\tau} \end{bmatrix} \begin{bmatrix} F_{w4} - G_f \cdot \dot{x}_4 \\ G_f \cdot \dot{x}_4 \end{bmatrix} \tag{3.7}$$

Simplifying the matrix equations gives the following.

$$\begin{aligned} \dot{x}_4 &= Q_{\dot{x}_4,F_4} \cdot F_{w4} - Q_{\dot{x}_4,F_4} \cdot G_f \cdot \dot{x}_4 + Q_{\dot{x}_4,F_\tau} \cdot G_f \cdot \dot{x}_4 \quad [\text{rad/s}] \\ \dot{\tau} &= Q_{\dot{\tau},F_4} \cdot F_{w4} - Q_{\dot{\tau},F_4} \cdot G_f \cdot \dot{x}_4 + Q_{\dot{\tau},F_\tau} \cdot G_f \cdot \dot{x}_4 \quad [\text{rad/s}] \end{aligned} \tag{3.8}$$

Using the expression for the wave moment in Equation 2.21, the following transfer function is obtained.

$$Q_{\dot{x}_4,\theta} = \frac{\dot{x}_4}{\theta} = \frac{F_{w40} \cdot Q_{\dot{x}_4,F_4}}{1 + G_f\left(Q_{\dot{x}_4,F_4} - Q_{\dot{x}_4,F_\tau}\right)} \quad \left[\frac{\text{rad}}{\text{rad s}}\right] \tag{3.9}$$

The same procedure applies for the rate of the tank's fluid angle:

$$\begin{aligned} Q_{\dot{\tau},\theta} = \frac{\dot{\tau}}{\theta} &= F_{w40} \cdot Q_{\dot{\tau},F_4} + \frac{1}{\theta} \cdot G_f \cdot \dot{x}_4 \cdot \left(Q_{\dot{\tau},F_\tau} - Q_{\dot{\tau},F_4}\right) \\ &= F_{w40} \cdot Q_{\dot{\tau},F_4} + Q_{\dot{x}_4,\theta} \cdot G_f \cdot \left(Q_{\dot{\tau},F_\tau} - Q_{\dot{\tau},F_4}\right) \\ &= F_{w40}\left(Q_{\dot{\tau},F_4} + \frac{Q_{\dot{x}_4,F_4} \cdot G_f \cdot \left(Q_{\dot{\tau},F_\tau} - Q_{\dot{\tau},F_4}\right)}{1 + G_f\left(Q_{\dot{x}_4,F_4} - Q_{\dot{x}_4,F_\tau}\right)}\right) \quad \left[\frac{\text{rad}}{\text{rad s}}\right] \end{aligned} \tag{3.10}$$

The ship's roll and tank's fluid angle per unit of wave slope can now be obtained easily as well:

$$\mathrm{S}_{x_4,\theta} = \frac{x_4}{\theta} = \frac{Q_{\dot{x}_4,\theta}}{i\omega}, \quad S_{\tau,\theta} = \frac{\tau}{\theta} = \frac{Q_{\dot{\tau},\theta}}{i\omega} \quad \left[\frac{\text{rad}}{\text{rad}}\right] \tag{3.11}$$

The tank's fluid angle per unit of ship's roll can be determined using the previous equation.

$$S_{\tau,x_4} = \frac{S_{\tau,\theta}}{S_{x_4,\theta}} \quad \left[\frac{\text{rad}}{\text{rad}}\right] \tag{3.12}$$

In Figure 3.3 the results of Equation 3.11 and Equation 3.12 are plotted. As seen, the control is not effective over the entire frequency range. Since the roll rate is very small at the low frequencies, the control system will have minor effect. However, as the roll rate increases the stabilising effect of the pump is seen back. Especially at the natural frequency of the ship the system attenuates the motions significantly. However, at a certain frequency the motions are amplified due to the active control. This amplification can not be explained just by looking at the phase angle between the tank's fluid moment and the ship's roll angle, because at the frequencies where the motions are amplified, the phase angle is not below 0° yet. To obtain a better understanding of the amplifications, the stabilising moments are looked at.

Figure 3.3: Response of feedback controlled ART for different gain factors.

Stabilising moments To determine the response of the pump and the ART with respect to the waves it should be noticed that the force on the ship's structure will have no delay. The reaction force however will have a delay.

This reaction force results in a stabilising moment caused by the tank ($F_{4\tau}$) as determined in Equation 2.9. For the stabilising moment per unit of tank fluid angle the transfer function $S_{F_4,\tau}$ in Equation 2.13 is used. To express the stabilising moment as part of the external moment F_4, it should be brought to the right side of the equation, which means that it should be taken negative.

$$F_{4,\tau}/\theta = -F_{4\tau}/\theta = -S_{\tau,\theta} \cdot S_{F_4,\tau} \quad [\text{Nm/rad}] \tag{3.13}$$

Now the moments due to the pump consist of the force on the structure of the vessel and the moment generated by the tank's fluid.

$$S_{F_{4,stab},\theta} = F_{p,a}/\theta + F_{4,\tau}/\theta = -G_f \cdot Q_{\dot{x}_4,\theta} - S_{\tau,\theta} \cdot S_{F_4,\tau} \quad [\text{Nm/rad}] \tag{3.14}$$

The equation can also be given as the stabilising moment per unit of wave moment:

$$S_{F_{4,stab},F_{w4}} = \frac{-G_f \cdot Q_{\dot{x}_4,\theta} - S_{\tau,\theta} \cdot S_{F_4,\tau}}{F_{w40}} \quad \left[\frac{\text{Nm}}{\text{Nm}}\right] \tag{3.15}$$

The above equation is plotted in Figure 3.4. As seen in the right graph, the phasing of the total stabilising moment is best (± 180°) around the natural frequency of the system. For higher frequencies, the phase difference decreases, meaning that the stabilising moment is less effective.

Figure 3.4: Total stabilising moments for feedback controlled ART using Eq. 3.15.

For an overview, the model with its transfer functions is depicted in Figure A.5.

3.1.2 Downsides of feedback control system

As seen in the figures above, the active control of the ART can significantly reduce the ship's motions at certain excitation frequencies. Nevertheless, it is important to question whether the feedback control is as effective as it looks from the graphs. Since the frequency domain approach only regards the steady state response, the time domain response could be less promising: it could be that the system needs a long time to damp the motions before it arrives at the steady state response.

Even though feedback control is a powerful method to control a wide range of systems, it has a large downside. A feedback control model is namely unaware of future disturbances. On topic of the active ART, the pump can only correct for motions once they are measured by the roll rate sensor. This downside becomes even larger due to the fact that the pump can't move the tank's fluid very rapidly from side to side due to the inertia of the water.

To be able to correct for the future disturbances a feed forward loop is required in the control system. By using a feed forward loop, the gain factor can be based on the magnitude of the wave excitation moment. This will enable to stabilise the vessel for large moments, without experiencing large motions.

Waterbed effect From a more theoretical perspective the downsides of feedback control can be explained by considering Bode's integral formula using Astrom and Murray (2008). For a feedback controlled system (with no RHP poles of the open loop transfer function)

the Equation 3.16 applies. In the equation $S(i\omega)$ is the sensitivity function. If $|S(i\omega)| > 0$ the control system will amplify the disturbance and if $|S(i\omega)| < 0$ the control system will attenuated the disturbance. So in fact the equation states that if the control performance is improved at one frequency, it will be decreased at another. This property is also called the waterbed effect.

$$\int_0^\infty \log|S(i\omega)|d\omega = 0 \tag{3.16}$$

Bode's integral formula does not apply for feed forward controlled systems. Therefore the performance of a feedback controlled model can be improved by using feed forward control. More information on the sensitivity function is provided in *§4.1.2 Stability assessment.*

3.2 Feed forward controlled model

The goal of this thesis is to determine the effect of using a wave prediction system for the control of an active ART. By using a wave prediction system, a feed forward loop can be introduced. For this thesis it is assumed that a deterministic approach is adopted for the wave prediction, which means that the phases are resolved. Therefore, the time traces of the wave elevation are known.

3.2.1 Control objectives

In the preparatory literature study two possibilities have been defined as control objective for the feed forward controlled model:

1. Keep the stabilising tank moment $F_{\tau 4}$ in combination with the pump moments equal to the moment exerted on the vessel by the incoming waves F_{w4}.

2. Control the phase angle between the tank stabilising moment and the disturbing wave moment so that the tank will reduce the motions for all excitation frequencies.

The difference between these two control objectives is that if the control system will be tuned according to the first objective, the pump could for example increase the tank's fluid angle if the vessel is excited at its natural frequency. In this way, the maximum stabilising moment of a passive tank can be increased, to counteract the wave moment. This approach is also taken in the work of Moaleji (2006). However, since the work lacks clear mathematical derivations and expressions, no computations in this thesis are taken over.

If the pump is controlled according to the second objective, the objective is to make sure the tank will always contribute to the stabilising of the vessel. So the goal will be to improve the performance of the ART at excitation frequencies at which the passive ART is not effective in stabilising the vessel.

As a compromise a combination of the two control objectives will be adopted. The objective of the control is to use the pump in such a way that the ART will reduce the vessel motions over the entire frequency range by considering the phases, but also try to keep the stabilising moment equal in magnitude to the wave moment. This will be done by first looking into the magnitude of the stabilising moment in *§3.2.2 Control the stabilising moment* and then looking more closely to the the phasing of the control moment in *§3.2.3 Control the phase angle.*

System inversion To obtain a good feed forward model, the control should be based on the concept of model inversion as described by Astrom and Murray (2008). For perfect feed forward control, the control actuator must exert a moment based on the disturbance signal that will give the exact opposite response of the system compared to the system's response on the disturbance signal. So, to obtain the required control moment, the model must be inverted. However, due to the complexity of the interaction between the pump moment acting on the ship's structure and the flow of the tank's fluid, the model inversion is limited to the control objective of cancelling out the wave excitation moment. This approach will be further worked out in the following paragraphs.

Block diagram The block diagram of the feed forward system is schematically shown in Figure 3.5. One can see that the incoming wave moment (F_{w4}) will not only go to the ship to act as a disturbance, but will also be fed into the controller. The controller then determines the power input to the pump based on the wave moment. This is the main difference of the feed forward controlled model with respect to the feedback controlled model.

The output of the pump is again the moment on the ship's structure as well as the moment on the tank's fluid. The feedback loop of the passive part is also still visible. The moment generated by the ship on the tank's fluid ($F_{\tau 4}$) will be added to the output moment of the pump. These two moments combined will affect the tank's fluid motions. The final input to the ship consists of the tank's restoring moment ($F_{4\tau}$), the pump moment on the ship's structure and the wave moment.

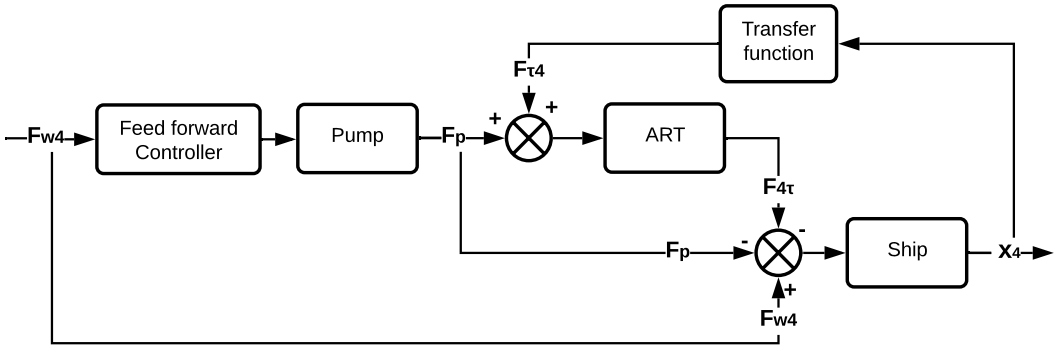

Figure 3.5: Control diagram of feed forward controlled ART.

3.2.2 Control the stabilising moment

The first aspect of the control objective is to assess the magnitude of the stabilising tank moment and have it equal to the moment exerted on the ship by the incoming waves.

The pump For this control objective the two control moments must be considered. The stabilising moment caused by the pump is as follows:

$$F_{stab,p} = F_p \cdot (S_{x_4,F_\tau} - S_{x_4,F_4}) \quad [\text{Nm}] \tag{3.17}$$

The parameter to determine the required pump pressure is the wave excitation moment F_{w4}. By adding a gain factor, the required pump pressure is defined as follows.

$$\Delta p = g_f \cdot F_{w4} \quad [\text{Pa}] \tag{3.18}$$

The two control moments consist of the force acting on the ship's structure and the force acting on the tank's fluid. The moments are obtained by multiplying with the cross-section area of the duct, and the distance between the ship's CoG and the centre line of the duct.

$$F_p = \Delta p \cdot h_d \cdot x_t \cdot r_d = g_f \cdot F_{w4} \cdot h_d \cdot x_t \cdot r_d = G_f \cdot F_{w4} \quad [\text{Nm}] \tag{3.19}$$

The following equation can now be obtained:

$$\begin{bmatrix} x_4 \\ \tau \end{bmatrix} = \begin{bmatrix} S_{x_4,F_4} & S_{x_4,F_\tau} \\ S_{\tau,F_4} & S_{\tau,F_\tau} \end{bmatrix} \begin{bmatrix} F_{w4} - F_p \\ F_p \end{bmatrix} \quad [\text{rad}] \tag{3.20}$$

This gives the following equation for the ship's roll angle and tank's fluid angle.

$$\begin{aligned} x_4 &= S_{x_4,F_4} \cdot F_{w4} + F_p \left(S_{x_4,F_\tau} - S_{x_4,F_4}\right) \quad [\text{rad}] \\ \tau &= S_{\tau,F_4} \cdot F_{w4} + F_p \left(S_{\tau,F_\tau} - S_{\tau,F_4}\right) \quad [\text{rad}] \end{aligned} \tag{3.21}$$

Transfer functions Using F_{w40} from Equation 2.21 gives the transfer function of the ship's roll per unit of wave slope in [rad/rad]. The equation gives the frequency response of the entire open loop from input to output. In Figure 3.6 the equation is plotted for different values of G_f.

$$S_{x_4,\theta} = F_{w40} \cdot \left(S_{x_4,F_4} + G_f \left(S_{x_4,F_\tau} - S_{x_4,F_4}\right)\right) \tag{3.22}$$

The tank's fluid motion per unit of wave slope can be determined similarly:

$$S_{\tau,\theta} = F_{w40} \cdot \left(S_{\tau,F_4} + G_f \left(S_{\tau,F_\tau} - S_{\tau,F_4}\right)\right) \tag{3.23}$$

The tank's fluid angle per unit of ship's roll can be determined using equations above.

$$S_{\tau,x_4} = \frac{S_{\tau,\theta}}{S_{x_4,\theta}} \quad \left[\frac{\text{rad}}{\text{rad}}\right] \tag{3.24}$$

Figure 3.6: Response of feed forward controlled ART based on Eq. 3.22 and Eq. 3.24.

Discussion In the figure above it can be seen in the left graph that as the gain factor increases above a certain point, the pump will have a negative effect on the ship's roll motion. This can be explained by looking at the corresponding phase angles in the plot on the right side. For a gain factor equal to 1, the phase angle ϵ_{τ,x_4} will be around 180° for low frequencies, meaning that the tank provides a large amount of power, but the tank's fluid will have a phase angle that lags the ship's roll in such a way that the motions will be amplified.

Therefore, it can be stated that the current control strategy is not very effective for high gain factors since the phase angles do not correspond to the optimal tank behaviour in which the tank's stabilising moment opposes the wave moment. Increasing the pump power not always leads to better performance of the system.

The difficulties of the phase angles result from the fact that the pump acts directly onto the vessel's structure, but the reaction force acts on the tank's fluid. The phase angle of the stabilising tank moment ($F_{4\tau}$) will depend on the excitation frequency. This causes an increased level of complexity in the pump control. In the next paragraph more elaboration will be given on topic of the phase angles of the system.

For an overview, the model with its transfer functions is depicted in Figure A.5.

3.2.3 Control the phase angle

Control objective As mentioned several times, the stabilising moment consists of the moment caused by the ART's fluid ($F_{\tau 4}$) and the moments caused by the pump. For the optimal performance of the tank not only the stabilising moment due to the force acting on the ship's structure should oppose the wave moment, but also the moment due to the ART's fluid.

Essentially, this control objective can be achieved by considering the current roll moment assisted by a feedback loop to the pump: by measuring the current roll moment, it can be determined what the desired control action is. The pump can then be used to manipulate the flow. However, as stated before, due to the fact that it takes time to manipulate the flow, the system might not be very effective. The system can effectively damp the vessel's motion after a certain wave has caused the motion, however it can not damp the first impact.

This is why a feed forward loop is required. Using a wave prediction system, it must be determined what the required behaviour of the pump would be to effectively control the pump to counteract the incoming wave moment.

Effect of the pump To be able to control the phase angle of the stabilising moment, first the effect of the pump will be analysed. For now the pump will be analysed without the waves disturbing the vessel. The pump moment is expressed as follows:

$$F_p = G_f \cdot F_{w4} \cdot \sin(\omega t + \epsilon_{F_p,F_{w4}}) = \Re\left(G_f \cdot F_{w4} \cdot e^{-i\epsilon_{F_p,F_{w4}}} \cdot e^{-i\omega t}\right) \quad \text{[Nm]} \tag{3.25}$$

For convenience the pump moment per unit of wave slope is defined as F_{p0}.

$$F_{p0} = \Re\left(G_f \cdot F_{w40} \cdot e^{-i\epsilon_{F_p,F_{w4}}} \cdot e^{-i\omega t}\right) \quad \text{[Nm/rad]} \tag{3.26}$$

To determine the phase angle of the moments generated by the pump with respect to the waves the moment on the ship's structure and the fluid moments should be considered. While

the force on the ship's structure will have no delay, the reaction force will cause a stabilising moment with a delay. This reaction moment can be determined using Equation 2.9.

So, to determine the phase angle the transfer function is derived of the moments due to the pump per unit of wave slope. First the tank's fluid angle due to the presence of the pump is determined:

$$S_{\tau,\theta} = F_{p0} \cdot (S_{\tau,F_\tau} - S_{\tau,F_4}) \quad [\text{rad/rad}] \tag{3.27}$$

The stabilising moment caused by the tank's fluid as defined in Equation 2.9 is equal to the coefficient $S_{F_4,\tau}$ in Equation 2.13. To express this moment as part of the external moment F_4, it should be brought to the right side of the equation, which means that it should be taken negative.

$$F_{4,\tau}/\theta = -F_{4\tau}/\theta = -S_{\tau,\theta} \cdot S_{F_4,\tau} \quad [\text{Nm/rad}] \tag{3.28}$$

Now the moments due to the pump consist of the force on the structure of the vessel and the moment generated by the tank's fluid.

$$S_{F_{4,stab},\theta} = -F_{p0} + F_{4,\tau} = -F_{p0}(1 + (S_{\tau,F_\tau} - S_{\tau,F_4}) \cdot S_{F_4,\tau}) \quad [\text{Nm/rad}] \tag{3.29}$$

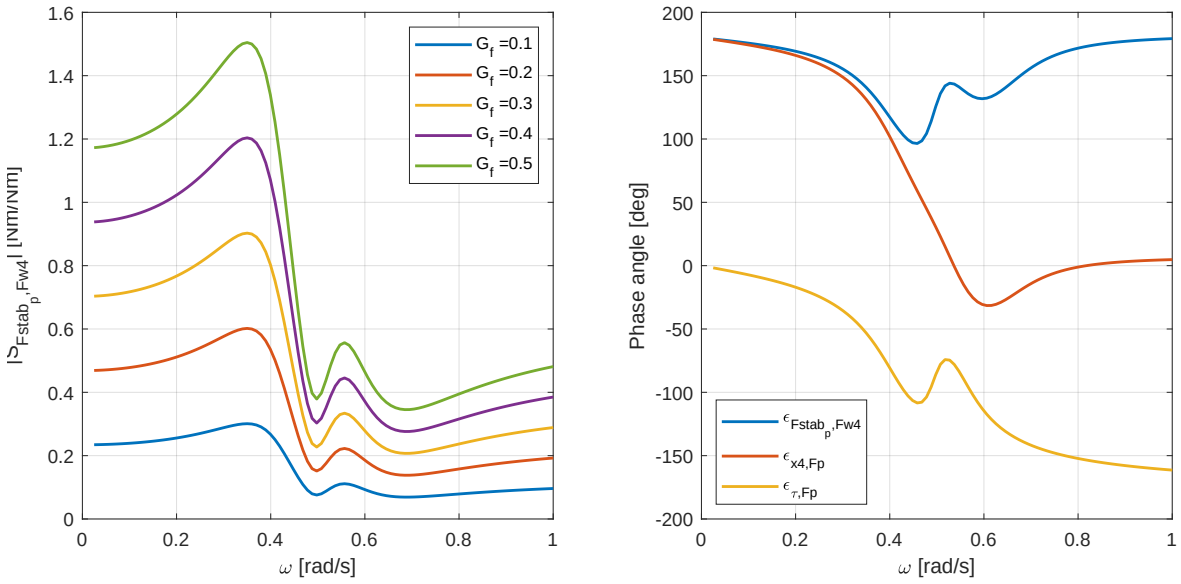

Figure 3.7: Stabilising moment due to pump for feed forward controlled ART using Eq. 3.29.

Effect of the pump + incoming waves The same approach can be adopted to determine the response of the active ART when it is excited by waves.

$$S_{\tau,\theta} = (F_{w40} - F_{p0}) \cdot S_{\tau,F_4} + F_{p0} \cdot S_{\tau,F_\tau} \quad [\text{rad/rad}] \tag{3.30}$$

$$\begin{aligned} F_{4,\tau}/\theta = -F_{4\tau}/\theta &= -S_{\tau,\theta} \cdot S_{F_4,\tau} \\ &= -((F_{w40} - F_{p0}) \cdot S_{\tau,F_4} + F_{p0} \cdot S_{\tau,F_\tau}) \cdot S_{F_4,\tau} \quad [\text{Nm/rad}] \end{aligned} \tag{3.31}$$

$$\begin{aligned} S_{F_{4,stab},\theta} &= -F_{p0} + F_{4,\tau} \\ &= -F_{p0} - ((F_{w40} - F_{p0}) \cdot S_{\tau,F_4} + F_{p0} \cdot S_{\tau,F_\tau}) \cdot S_{F_4,\tau} \quad [\text{Nm/rad}] \end{aligned} \tag{3.32}$$

The above equation can also be expressed as the stabilising moment per unit of wave moment in order to show which fraction of the wave moment is counteracted.

$$\begin{aligned} S_{F_{4,stab},F_{w4}} &= \frac{-F_{p0} - ((F_{w40} - F_{p0}) \cdot S_{\tau,F_4} + F_{p0} \cdot S_{\tau,F_\tau}) \cdot S_{F_4,\tau}}{F_{w40}} \\ &= -G_f - ((1 - G_f) \cdot S_{\tau,F_4} + G_f \cdot S_{\tau,F_\tau}) \cdot S_{F_4,\tau} \quad [\text{Nm/Nm}] \end{aligned} \tag{3.33}$$

Figure 3.8: Stabilising moment for wave excited feed forward controlled ART using Eq. 3.33.

Furthermore, as can be seen in the figure above, for a passive ART the moment caused by the tank's fluid will be in phase with the wave excitation moment, meaning that the motions of the vessel will be amplified. However, once the gain factor is increased, the moment will have a phase difference of about 180° with respect to the wave moment, which means that the ART acts as a stabiliser.

Results for different phases Now the results for different phase angles of the pump moment with respect to the incoming wave can be compared. The equations 3.22, 3.23 and 3.24 from §3.2.3 are used to plot the results.

In case the phase angle is out of the desired range as described in Table 2.1, the power demand will be affected significantly. This can be understood by the fact that the moment of the fluid will have different phases with respect to the ship's roll angle for different gains and frequencies. Even though the moment of the pump on the tank's structure will always be opposed to the wave moment, the tank's fluid moment due to the pump will not always be opposed to the wave moment. So, this means that the pump control can differ in effectiveness.

For ineffective control the power delivered to the pump will be wasted partially. This should be avoided by not only looking at the phase angle of the total stabilising moment with respect to the waves, but also to the phase angle of the tank's fluid angle with respect to the ship's roll angle.

Figure 3.9: Response of feed forward controlled ART with $\epsilon_{F_p,F_{w4}} = 0°$.

Figure 3.10: Response of feed forward controlled ART with $\epsilon_{F_p,F_{w4}} = -45°$

As seen in the figures above, the power used for the control will be used more effectively for the situation in which $\epsilon_{F_p,F_{w4}} = -45°$, since the phase angles lie more closely to 90°.

For a better analysis of the pump phase angle with respect to waves excitation moment,

the various phase angles have been plotted in one graph (Figure 3.11) for a gain factor of 0.25. It can be said that if the pump moment has a phase angle of -45° with respect to the wave moment, the system's response is best.

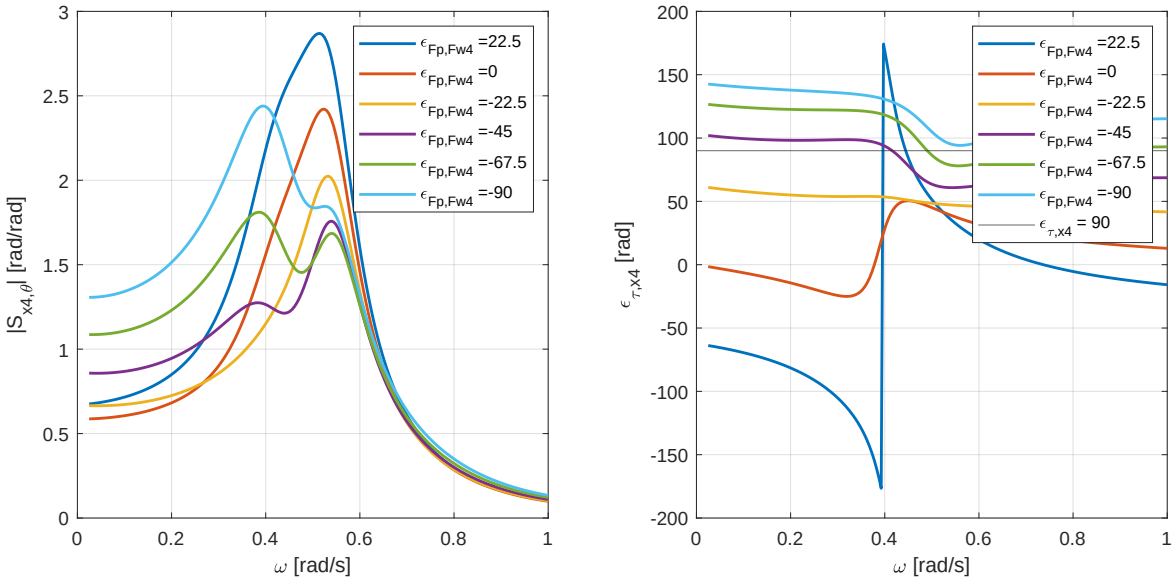

Figure 3.11: Response of feed forward controlled ART for different $\epsilon_{F_p,F_{w4}}$ with $G_f = 0.25$.

Looking back at the control objectives at the beginning of §3.2.1 it can be stated that the exact implementation of two separate and predefined objectives are not achieved. As to the first objective, the stabilising moment is not equal in size compared to the wave moment. As to the second objective it can be said that even though at some frequencies the passive ART's response is as desired, still the active control will insert power into the system. This is due to the limited complexity of the controller.

Nevertheless, the combined control objective is achieved. Due to the introduction of the feed forward controlled pump, the phase angle between the tank's stabilising moment and the disturbing wave moment is such that the tank will reduce the motions for all excitation frequencies.

For an overview, the model with its transfer functions is depicted in Figure A.6.

3.3 2DoF controlled model

In this section a model is discussed that is a combination of the feedback and feed forward models. A block diagram is shown in Figure 3.12. The green lines regard the feedback control and the blue line regards the feed forward control.

3.3.1 Combination of models

Instead of applying only feedback or feed forward control, a combination can capture the best of both worlds. Feedback control is very powerful in controlling a complex system since the exact response of a system to a certain gain factor is not required. The feedback control will

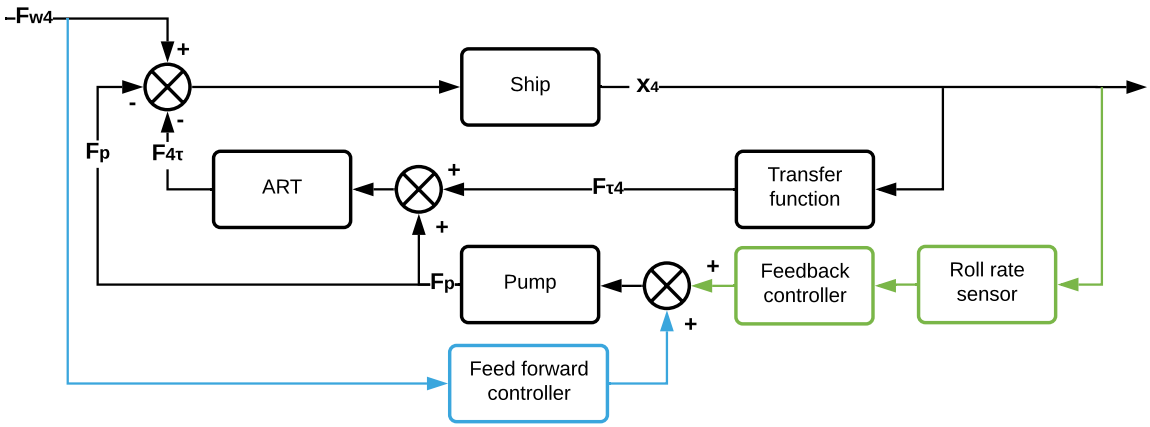

Figure 3.12: Block diagram of 2DoF controlled model.

enable to correct for the motions that occur, instead of the motions that are assumed to occur in the case of feed forward control. The presence of a feedback loop increases the robustness of the control method, without having to understand what the exact consequence of a certain control signal is, the ship can be stabilised. Of course, on the condition that the control loop is stable (see Chapter 4).

On the other hand, the feed forward control is very powerful in corrections for large incoming waves. So, by adding a feed forward loop to the feedback controlled model by Alujević et al. (2020), the system can become smarter.

Adding up the controller output signals By making use of two controllers the control based on the incoming wave signal can be added to the control based on the roll rate signal. The two signals can be added because their unit is the same. In the mathematical model it regards a moment, and in reality it would regard a power input to the pump. This can be a certain amount of fuel or electrical power, depending on the type of pump.

Since the two output signals are added up, it could also be that the signals cancel each other out. This could be the case if the ship rolls to port side (counterclockwise), while a large wave comes in from port side. In this case, the feedback loop would send a control signal to the pump for a clockwise moment. On the other hand, the feed forward loop would send a control signal for a counter clockwise moment. The result would be that no action from the pump is required and the ship would be stabilised due to the incoming wave.

The model For the feedback system the output of the controller for the pump is defined as follows:

$$F_{p,fb} = G_{fb} \cdot \dot{x}_4 = G_{fb} \cdot i\omega \cdot x_4 \quad [\text{Nm}] \tag{3.34}$$

For the feed forward system the output of the controller for the pump is defined as follows:

$$F_{p,ff} = G_{ff} \cdot e^{-i\epsilon_{F_p,F_{w4}}} \cdot F_{w4} \quad [\text{Nm}] \tag{3.35}$$

The following pump moment per unit of wave slope is obtained:

$$F_{p0} = G_{fb} \cdot i\omega \cdot S_{x_4,\theta} + G_{ff} \cdot e^{-i\epsilon_{F_p,F_{w4}}} \cdot F_{w40} \quad [\text{Nm/rad}] \tag{3.36}$$

For the gain factors the following expression is defined to determine the relation between the feedback and feed forward gains. This is a rather arbitrary model choice, since the robustness of the model should be assessed outside of the model's boundaries. Therefore, the optimal ratio of the feedback and feed forward control should be based on addition of disturbances or real life model tests.

$$G_f = c_{44} \cdot G_{fb} = G_{ff} \tag{3.37}$$

The pump moments can now be filled in in the equation of motion.

$$\begin{bmatrix} x_4 \\ \tau \end{bmatrix} = \begin{bmatrix} S_{x_4,F_4} & S_{x_4,F_\tau} \\ S_{\tau,F_4} & S_{\tau,F_\tau} \end{bmatrix} \begin{bmatrix} F_{w4} - F_{p,fb} - F_{p,ff} \\ F_{p,fb} + F_{p,ff} \end{bmatrix} \quad \text{[rad]} \tag{3.38}$$

The pump pressure is obtained by adding the pressures from the feedback loop and the feed forward loop.

$$\Delta p = g_{fb} \cdot \dot{x}_4 + g_{ff} \cdot F_{w4} = \frac{G_{fb} \cdot \dot{x}_4 + G_{ff} \cdot F_{w4}}{h_d \cdot x_t \cdot r_d} \quad \text{[Pa]} \tag{3.39}$$

3.3.2 Transfer functions

The transfer functions of the motions can now be determined using the derived equation of motion (Equation 3.38).

$$\begin{aligned} x_4 = S_{x_4,F_4} \cdot F_{w4} + G_{fb} \cdot i\omega \cdot x_4 \cdot (S_{x_4,F_\tau} - S_{x_4,F_4}) + \\ G_{ff} \cdot e^{-i\epsilon_{F_p,F_{w4}}} \cdot F_{w4} (S_{x_4,F_\tau} - S_{x_4,F_4}) \quad \text{[rad/s]} \end{aligned} \tag{3.40}$$

Rewriting gives the following:

$$\begin{aligned} x_4(1 - i\omega \cdot G_{fb} \cdot (S_{x_4,F_\tau} - S_{x_4,F_4})) = \\ F_{w4} \left(S_{x_4,F_4} + G_{ff} \cdot e^{-i\epsilon_{F_p,F_{w4}}} \cdot (S_{x_4,F_\tau} - S_{x_4,F_4}) \right) \quad \text{[rad/s]} \end{aligned} \tag{3.41}$$

Using the expression $F_{w4} = F_{w40} \cdot \theta$ (Equation 2.21) the following transfer function can be obtained.

$$S_{x_4,\theta} = \frac{x_4}{\theta} = \frac{F_{w40} \left(S_{x_4,F_4} + G_{ff} \cdot e^{-i\epsilon_{F_p,F_{w4}}} \cdot (S_{x_4,F_\tau} - S_{x_4,F_4}) \right)}{1 + G_{fb} \cdot (Q_{\dot{x}_4,F_4} - Q_{\dot{x}_4,F_\tau})} \quad \left[\frac{\text{rad}}{\text{rad}} \right] \tag{3.42}$$

For the tank's fluid motion the following equation is obtained:

$$\begin{aligned} \tau = S_{\tau,F_4} \cdot F_{w4} + G_{fb} \cdot i\omega \cdot x_4 \cdot (S_{\tau,F_\tau} - S_{\tau,F_4}) + \\ G_{ff} \cdot e^{-i\epsilon_{F_p,F_{w4}}} \cdot F_{w4} (S_{\tau,F_\tau} - S_{\tau,F_4}) \quad \text{[rad/s]} \end{aligned} \tag{3.43}$$

Using the above equation the transfer function of the tank's fluid angle per unit of wave moment can be defined.

$$\begin{aligned} S_{\tau,\theta} = S_{\tau,F_4} \cdot F_{w40} + G_{fb} \cdot i\omega \cdot S_{x_4,\theta} \cdot (S_{\tau,F_\tau} - S_{\tau,F_4}) + \\ G_{ff} \cdot e^{-i\epsilon_{F_p,F_{w4}}} \cdot F_{w40} (S_{\tau,F_\tau} - S_{\tau,F_4}) \quad \text{[rad/rad]} \end{aligned} \tag{3.44}$$

For the feed forward controlled model, the phase angle between the pump and the wave moment was considered best at 45°. To determine if the same value should be taken for the feed forward part of the 2DoF controlled model, the ship's response for different values is plotted in Figure 3.13. It can be seen that for a phase angle of -30° the response to waves is rather little and the phase angle between the tank's fluid angle and the ship's roll angle is close to the desired 90°. Therefore, $\epsilon_{F_p,F_{w4}} = -30°$ is considered best for $G_f = 0.16$.

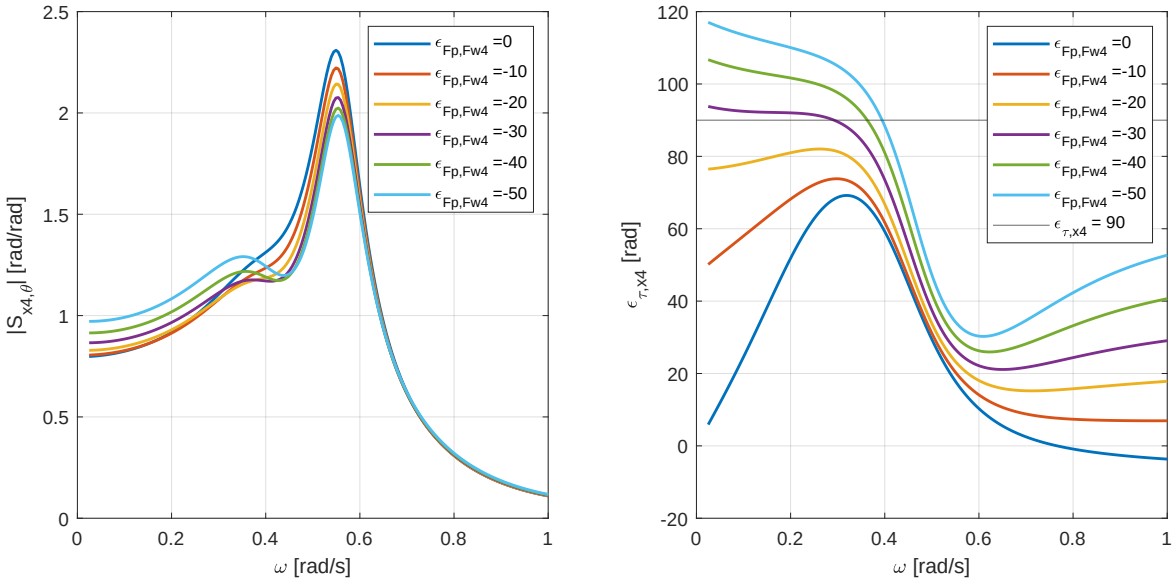

Figure 3.13: Response of 2DoF controlled ART for different $\epsilon_{F_p,F_{w4}}$ with $G_f = 0.16$.

Figure 3.14: Response of 2DoF controlled ART for different G_f with $\epsilon_{F_p,F_{w4}} = -30$.

In Figure 3.14 the response is plotted with a 30° phase difference for different gains. As

seen, for different gains the phase angle between the tank's fluid angle and the ship's roll angle change. Therefore, for a different gain factor a different phase angle might result in an improved performance of the active ART. Therefore, for the final gain factor that will be used, the optimal phase angle of the pump moment with respect to the wave moment must be determined.

Effect of the pump To obtain a better understanding of the system the effect of the pump is studied. As defined earlier, the stabilising fluid moment is as follows:

$$F_{4,\tau} = -F_{4\tau} = -S_{\tau,\theta} \cdot S_{F_4,\tau} \quad [\text{Nm}] \tag{3.45}$$

This moment is added to the stabilising moment by the pump on the ship's structure.

$$\begin{aligned} S_{F_{4,stab},\theta} &= -F_{p0} + F_{4,\tau} \\ &= -G_{fb} \cdot i\omega \cdot S_{x_4,\theta} - G_{ff} \cdot e^{-i\epsilon_{F_p,F_{w4}}} \cdot F_{w40} - S_{\tau,\theta} \cdot S_{F_4,\tau} \quad [\text{Nm/rad}] \end{aligned} \tag{3.46}$$

Or expressed as the stabilising moment per unit of wave moment:

$$S_{F_{4,stab},F_{w4}} = \frac{-G_{fb} \cdot i\omega \cdot S_{x_4,\theta} - G_{ff} \cdot e^{-i\epsilon_{F_p,F_{w4}}} \cdot F_{w40} - S_{\tau,\theta} \cdot S_{F_4,\tau}}{F_{w40}} \quad \left[\frac{\text{Nm}}{\text{Nm}}\right] \tag{3.47}$$

The above equation is plotted in Figure 3.15. It can be seen that due to the active control the stabilising moment will not act in phase with the wave moment.

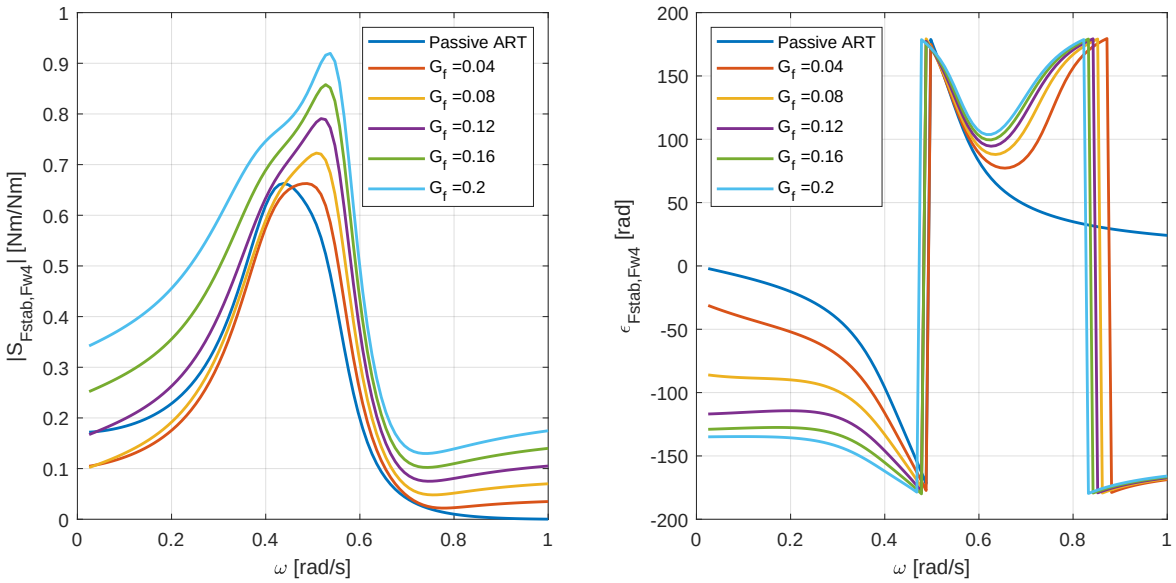

Figure 3.15: Stabilising moment for wave excited 2DoF controlled ART using Eq. 3.47 ($\epsilon_{F_p,F_{w4}} = -30°$).

For an overview of the equations related to the model see Figure A.7.

4 - Stability analysis

In the previous chapter response functions have been obtained for different control models. However, as stated by Alujević et al. (2020) the stability of control systems can't be seen from the response functions directly. Therefore, before any conclusions can be drawn from a set of response functions, it must be known whether they represent a stable system. An active ART is stable if for all input the output is bounded. So the ship's roll angle should not be ever increasing for a certain gain and frequency.

To build up the analysis, a brief introduction in control theory is provided first which is then applied to the passive ART. This will give insight the application of the control theory, as well as in the behaviour of the ART. Following, the stability of the feedback, feed forward and 2DoF controlled model will be assessed.

4.1 Control theory

In order to tune the ART use can be made of stability plots. These plots can be plotted easily using the Control System Toolbox in Matlab. This Matlab toolbox requires a transformation to the Laplace domain.

4.1.1 Transformation to Laplace domain

The transformation to the Laplace domain regards the conversion of the time dependent variable t into the complex variable $s = i\omega$.

Equation of motion Since complex phasor notations are already used within the thesis (see the equation of motion in Equation 2.6), the transformation to the Laplace domain can be performed by substituting $i\omega$ for s. This will give the following expression for the equation of motion:

$$(\mathbf{A} + \mathbf{I}) \cdot s^2 + \mathbf{B} \cdot s + \mathbf{C} = \mathbf{F}(s) \quad [\text{Nm}] \tag{4.1}$$

With the following expression for the wave excitation moment:

$$F_{w4}(s) = \left(a_{44} \cdot s^2 + b_{44} \cdot s + c_{44}\right) \theta \quad [\text{Nm}] \tag{4.2}$$

The above expressions can also be obtained by deriving the independent Laplace transforms of the harmonic oscillations of the time-domain equation of motion. The equation of motion is given below. In the equation $x(t) = \sin(\omega t)$. Also the wave moment consists of a harmonic oscillating function.

$$(\mathbf{A} + \mathbf{I})\ddot{\mathbf{x}}(t) + \mathbf{B}\dot{\mathbf{x}}(t) + \mathbf{C}\mathbf{x}(t) = \mathbf{F}(t) \quad [\text{Nm}] \tag{4.3}$$

The Laplace transform for $x(t) = \sin(\omega t)$ is given below. For the derivatives a multiplication with the complex variable s is required.

$$\mathcal{L}\{\sin(\omega t)\} = \frac{\omega}{s^2 + \omega^2}, \quad \mathcal{L}\left\{\frac{dx}{dt}\right\} = sX(s) \tag{4.4}$$

After substituting the Laplace transform, all terms (including the wave moment) will have the common expression $\omega/(s^2 + \omega^2)$. If this common expression is eliminated from the equation, the same expression as in Equation 4.1 will be obtained.

Phase shift For the feed forward controlled model a phase difference between the wave moment and the pump moment was introduced. This will result in a new expression for the Laplace transform.

$$\mathcal{L}\{\sin(\omega t + \epsilon)\} = \frac{s \cdot \sin(\epsilon) + \omega \cdot \cos(\epsilon)}{s^2 + \omega^2} \tag{4.5}$$

As a result the transfer function will be different for every frequency, since ω can't be eliminated. The pump moment is given below. The expression is already divided by the 'common' expression $\omega/(s^2 + \omega^2)$. In the equation below it can be seen that for $\epsilon = 0$, the frequency dependency is eliminated.

$$F_p(s) = G_f \cdot \left(\left(a_{44} \cdot s^2 + b_{44} \cdot s + c_{44} \right) \cdot \frac{s \cdot \sin(\epsilon) + \omega \cdot \cos(\epsilon)}{\omega} \right) \tag{4.6}$$

Note that the phase shift only applies for the feed forward loops, and therefore does not affect the closed loop stability.

Hydrodynamic coefficients To obtain a transfer function in the Laplace domain applicable to all frequencies to assess the closed loop stability, the frequency dependency of the hydrodynamic coefficients is neglected. For the value of a_{44} and b_{44} the values are taken of the constant part at low frequencies. The result of this simplification is that for higher frequencies the stability analysis looses its accuracy. However, as seen in Figure A.2, the hydrodynamic coefficients are relatively constant up to about $\Lambda = 1.5$. Therefore, the stability analysis based on fixed hydrodynamic coefficients gives a good approximation of the stability.

4.1.2 Stability assessment

General A simple feedback system is show in Figure 4.1. The block $G(s)$ is the transfer function of the system's plant. The block $H(s)$ is the transfer function of the control part. The closed loop transfer function in the Laplace domain is defined as follows:

$$\frac{x_4}{F_{w4}} = \frac{G(s)}{1 + G(s)H(s)} \tag{4.7}$$

In the equation $G(s)H(s)$ is the open-loop transfer function. The output of this open-loop part will be subtracted from the incoming disturbance, which is the wave excitation moment in the figure below.

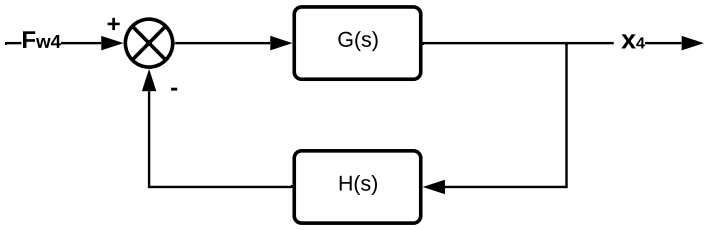

Figure 4.1: Simple block diagram of a feedback loop.

In order to have a stable system the roots of the denominator of the closed loop transfer function must be negative. If this is not the case, the control loop will amplify the error signal, resulting in an unbounded response. This will be made more clear in the following paragraph on topic of poles and zeros.

Using the open loop transfer function $G(s)H(s)$ the stability of the closed loop system can be assessed. The critical point of the system is when the denominator equals 0. This occurs when the magnitude of the open loop transfer function is 1 ($|G(s)H(s)| = 1$) at a phase shift of 180° ($\angle G(s)H(s) = 180°$). In this case the roots of the denominator of the closed loop transfer function will be on the imaginary axis. Using Nyquist's criteria it can be found on what side of the critical point the system will become unstable.

Poles and zeros In control theory the poles and zeros refer to the values for which, respectively, the denominator and the numerator of the transfer function are equal to zero. The transfer function is in fact a differential equation of a linear system (e.g. Equation 2.2). The homogeneous solution to this differential equation can be described as follows:

$$x_4(t) = \sum_{i=1}^{n} C_i e^{\lambda_i t} \quad \text{[rad]} \tag{4.8}$$

In this equation λ_i are the roots of the transfer function, which are equal to the system's poles. One can now see that for a bounded response, the system's poles should have a negative real value. Also, as the poles lie closer to the the imaginary axis, the system's damping factor will become lower, resulting in larger overshoots.

The values for C that are required for the time domain solution depend on the initial conditions of the system. Since a frequency domain analysis is adopted in this thesis, it will be disregarded.

At the frequencies corresponding to the systems zeros, the system's response will be zero. (MIT, 2004)

Nyquist plot A stability plot that is often used is the Nyquist stability plot. Using this plot, the closed loop stability can be determined based on the open loop stability. As stated by Astrom and Murray (2008), for a Nyquist plot the net number of clockwise encirclements of $-1 + 0i$ (N) equals the number of closed-loop poles in the RHP (Z) minus the number of open-poles in the RHP (P):

$$N = Z - P, \text{ or } Z = N + P \tag{4.9}$$

For closed-loop stability of a system there should be no closed-loop poles in the right half of the s-plane. So, Z should be zero. Once again for the overview:

- N: number of clockwise encirclements of $-1 + 0i$
- Z: number of closed-loop poles in the RHP
- P: number of open-loop poles in the RHP.

According to the paper by Alujević et al. (2020), the control system amplifies the motions as the Nyquist curve enters the unit circle with origin $-1+0i$. This can be explained by looking at the closed loop transfer function. Once the open loop part will be lower than zero, the

motions will be amplified. Since the evaluation of $1 + G(s)H(s)$ is performed by evaluating $G(s)H(s)$ at the point $-1 + 0i$, the term $1 + G(s)H(s)$ will be lower than 1 as the Nyquist curve enters a unit circle with the origin $-1 + 0i$.

Besides using a standard Matlab command, the Nyquist plot can also be obtained by plotting the real values of the open loop transfer function on the horizontal axis, and the imaginary values on the vertical axis.

Bode plot A bode plot gives almost the same information as a Nyquist plot, but in a different coordinate system. By plotting the magnitude and the phase of the frequency response the stability can be assessed. By looking at the phase angle of 180° and the magnitude of 1 of the open-loop transfer function, the stability margins can be obtained.

Sensitivity analysis To give a better representation of when the motions are amplified due to a controller, a sensitivity analysis can be made. There are different ways to explain the sensitivity plot.

One way to explain the sensitivity plot is to consider the Nyquist curve of the system's open loop transfer function. The sensitivity plot will show how far the Nyquist curve is located from the point of instability $-1 + 0i$. Since the open loop transfer function is $G(s)H(s)$, the distance will be $-1 - G(s)H(s)$. Since the system will be closer to instability for a small distance, the reciprocal of the distance is taken, to obtain a larger value of the sensitivity for a more stable system (Astrom and Murray, 2008).

Another way to look at the sensitivity is to consider the closed loop transfer function of a feedback system as in Equation 4.7. It can be seen that the sensitivity multiplied by the plant's transfer function $G(s)$ is equal to the closed loop transfer function. So, for a sensitivity greater than 1 the output will be amplified, while for a sensitivity smaller than 1 the output will be attenuated.

$$Sensitivity = \frac{1}{1 + G(s)H(s)} \quad [-] \tag{4.10}$$

As already addressed in the previous paragraph, the sensitivity function not only provides insight in the amplification and attenuation of signals, but also in the robustness of the control system. The higher the sensitivity function, the closer the system is to the point of instability. The maximum value of the sensitivity function (M_s) is the reciprocal of the shortest distance from the Nyquist curve of the loop transfer function to the point $-1 + 0i$.

$$M_s = \max_{0 \leq \omega < \infty} |Sensitivity| = \max_{0 \leq \omega < \infty} \left| \frac{1}{1 + G(s)H(s)} \right| \tag{4.11}$$

Model limits For the derived transfer functions, it must be determined to which frequencies they are applicable. Since the wave excitation moment diverges at high frequencies, the output of the feed forward loop will become very large too for high frequencies. The divergence of the wave excitation moment occurs when the static part of the moment is smaller than the acceleration part of the wave moment (see Equation 2.22). As a solution, the feed forward control will only be applied up to the frequency of the zero of the wave moment. Note that this will not affect the feedback loops.

4.2 Passive model

In this paragraph the stability of the passive ART is assessed. This analysis will provide knowledge of the system that will help to obtain a better understanding of the active controlled systems.

Transfer functions The transfer function of the closed loop block diagram (as in Figure 2.4) is derived from the equations of motion in Equation 2.14. Since there is no external moment acting on the tank fluid, the only matrix element of importance is the transfer function of the ship's roll motion per unit of external wave moment.

$$\frac{x_4}{F_{w4}} = S_{x_4,F_4} \quad [\text{rad/Nm}] \tag{4.12}$$

However, to know when the ART will amplify or attenuate the motions, the open loop system should be assessed. This will enable to analyse the stabilising moment of the ART. A block diagram of the open loop system is given in Figure 4.2. The expressions for the transfer functions have been derived in Equation 2.14.

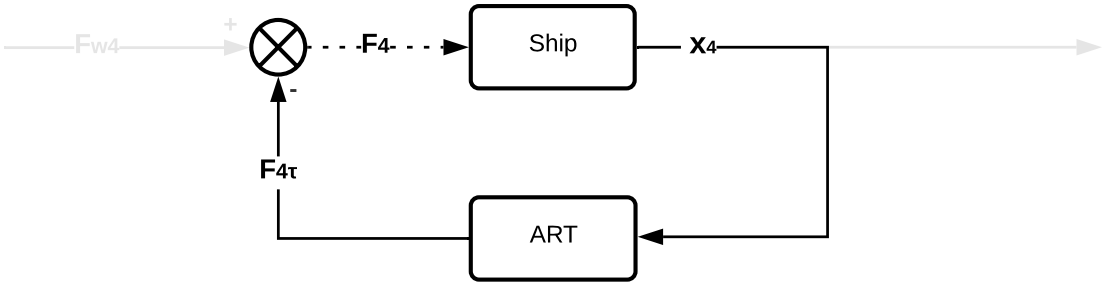

Figure 4.2: Block diagram of the open loop passive ART.

Derivations for OL transfer function To derive the OL transfer functions, the expressions for x_4 and F_4 are formulated and substituted. Using Figure 4.2 the following can be written:

$$\begin{aligned} x_4 &= (S_{F_4,x_4})^{-1} \cdot F_4 \quad [\text{rad}] \\ F_4 &= F_{w4} - x_4 \cdot S_{\tau,x_4,\text{uncoupled}} \cdot S_{F_4,\tau} \quad [\text{Nm}] \end{aligned} \tag{4.13}$$

The reason that $(S_{F_4,x_4})^{-1}$ is taken in the first equation is because the uncoupled response is required. This is in contrary with S_{x_4,F_4}, which gives the coupled response (For more elaboration on the coupled and uncoupled properties please see §2.5). The next step is to substitute the second equations into the first:

$$x_4 = (S_{F_4,x_4})^{-1} \cdot (F_{w4} - x_4 \cdot S_{\tau,x_4,\text{uncoupled}} \cdot S_{F_4,\tau}) \quad [\text{rad}] \tag{4.14}$$

Simplifying gives the following closed loop transfer function:

$$\frac{x_4}{F_{w4}} = \frac{(S_{F_4,x_4})^{-1}}{1 + (S_{F_4,x_4})^{-1} \cdot S_{\tau,x_4,\text{uncoupled}} \cdot S_{F_4,\tau}} \quad [\text{rad/Nm}] \tag{4.15}$$

Using Equation 2.17 the equation can be rewritten into the following:

$$\frac{x_4}{F_{w4}} = \frac{(S_{F_4,x_4})^{-1}}{1 + (S_{F_4,x_4})^{-1} \cdot \dfrac{-S_{F_\tau,x_4}}{S_{F_\tau,\tau}} \cdot S_{F_4,\tau}} \quad \text{[rad/Nm]} \tag{4.16}$$

So the open loop transfer function is as follows:

$$G(s)H(s) = S_{F_{4\tau},F_4} = (S_{F_4,x_4})^{-1} \cdot \frac{-S_{F_\tau,x_4}}{S_{F_\tau,\tau}} \cdot S_{F_4,\tau} \quad \text{[Nm/Nm]} \tag{4.17}$$

Note that even though the GM of the ship is affected by the presence of the ART due to the free surface effect of the tank's fluid, the case with and without ART can be compared. This is because the free surface effect is accounted for in the equations of motion since the tank's fluid and ship's roll motion are coupled. The correction of the GM is only required if static (loading) conditions are analysed without any consideration of the coupled equations of motion.

Nyquist plot By means of a Nyquist stability plot, the behaviour of a passive ART can be derived. The Nyquist plot is obtained by plotting the real values of the open loop transfer function on the horizontal axis, and the imaginary values on the vertical axis.

As expected from the RAO plots in Figure 2.6, the Nyquist plot shows that the ART amplifies the motions, since the plot enters the unit circle with radius $-1 + 0i$. However, the system is not unstable.

The reason that the system is not unstable is because there are no encirclements of the critical point and no open-loop poles in the RHP. So, for the passive system, the moment caused by the tank's fluid is not large enough to destabilise the ship. So even though the tank's fluid will amplify the incoming wave moment, the output will be bounded.

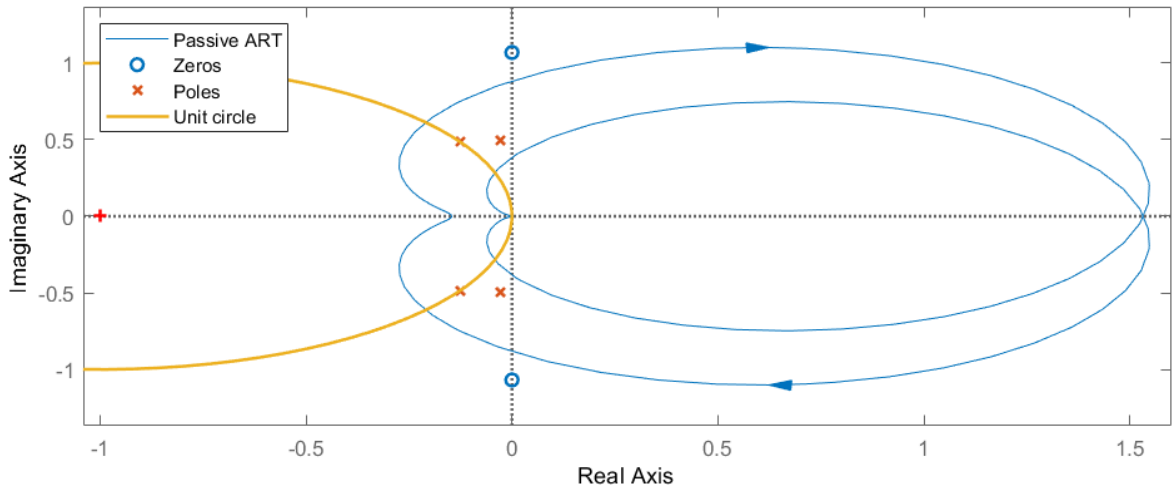

Figure 4.3: Nyquist plot of a passive ART using Eq. 4.17.

Sensitivity plot The sensitivity of the passive system is determined using the open loop transfer function as derived in Equation 4.17.

$$S_{P,U} = \frac{1}{1 + (S_{F_4,x_4})^{-1} \cdot \dfrac{-S_{F_\tau,x_4}}{S_{F_\tau,\tau}} \cdot S_{F_4,\tau}} \quad [-] \tag{4.18}$$

In Figure 4.4 the equation is plotted on the left. In the figure on the right the passive response of the ART is given for two cases; the case with, and the case without ART.

Figure 4.4: Sensitivity plot of a passive ART using Equation 4.18 (left) and comparison of the response of the passive ART (right).

4.3 Feedback controlled model

In the paper on topic of feedback control of U ARTs by Alujević et al. (2020), Nyquist stability plots are used. Since the ART of the SOV has different parameters, a stability assessment for the feedback controlled model is performed within this thesis. A block diagram of the open loop transfer function based on Figure 3.2 is given in Figure 4.5. The loop starts at the point where the moments are fed into the ship and ends at the stabilising moments.

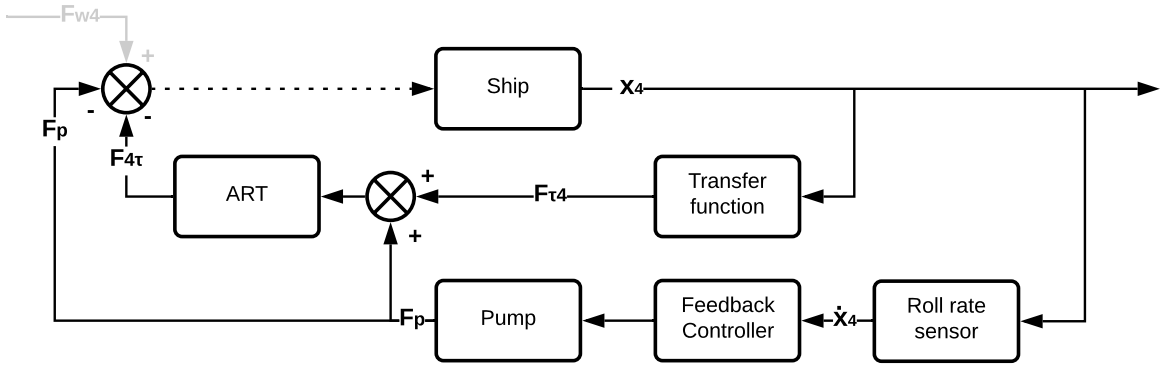

Figure 4.5: Block diagram of an open loop feedback controlled ART.

4.3.1 Transfer functions

Uncoupled transfer function The earlier defined transfer functions in the previous chapter (*§3.1 Feedback controlled model*) were based on the concept that the system's plant is the ship + passive ART. To compare the system with a ship without ART, the transfer function must be derived based on the uncoupled motions. This is performed in the derivations below. The signs and notation are based on the block diagram in Figure 4.5.

$$\begin{aligned} x_4 &= (S_{F_4,x_4})^{-1} \cdot F_4 \\ F_{4\tau} &= \Big(x_4 \cdot S_{\tau,x_4,\text{uncoupled}} + x_4 \cdot i\omega \cdot G_f \cdot (S_{F\tau,\tau})^{-1}\Big) \cdot S_{F_4,\tau} \\ F_p &= x_4 \cdot i\omega \cdot G_f \\ F_4 &= F_{w4} - F_{4\tau} - F_p \end{aligned} \tag{4.19}$$

Substitution gives the following:

$$\begin{aligned} x_4 &= (S_{F_4,x_4})^{-1} \cdot F_{w4} \\ &- x_4 \cdot (S_{F_4,x_4})^{-1} \cdot \Big(S_{\tau,x_4,\text{uncoupled}} \cdot S_{F_4,\tau} + i\omega \cdot G_f \cdot (S_{F\tau,\tau})^{-1} \cdot S_{F_4,\tau} + i\omega \cdot G_f\Big) \end{aligned} \tag{4.20}$$

$$\begin{aligned} x_4\Big(1 + (S_{F_4,x_4})^{-1} \cdot \Big(S_{\tau,x_4,\text{uncoupled}} \cdot S_{F_4,\tau} + i\omega \cdot G_f \cdot (S_{F\tau,\tau})^{-1} \cdot S_{F_4,\tau} + i\omega \cdot G_f\Big)\Big) \\ = (S_{F_4,x_4})^{-1} \cdot F_{w4} \end{aligned} \tag{4.21}$$

The final transfer function can now be obtained. Note that the characteristic formulation of a feedback transfer function is seen back.

$$\frac{x_4}{F_{w4}} = \frac{(S_{F_4,x_4})^{-1}}{1 + (S_{F_4,x_4})^{-1} \cdot \left(\dfrac{-S_{F_\tau,x_4}}{S_{F_\tau,\tau}} \cdot S_{F_4,\tau} + \dfrac{i\omega \cdot G_f \cdot S_{F_4,\tau}}{S_{F\tau,\tau}} + i\omega \cdot G_f\right)} \tag{4.22}$$

Coupled transfer function In the previous paragraph a derivation is given for the uncoupled system. This means that the ART is uncoupled from the ship's response. To

analyse the active control with respect to a passive system, the equations of motion as derived in *§3.1 Feedback controlled model* must be considered.

For a standard closed loop feedback model (as in Figure 4.1) the control loop is the equivalent of the output of the system multiplied with the control gain. If now the feedback controlled ART is considered, one can see in Figure 4.6 that the control loop consists of a gain factor multiplied with the system's output, but also a gain factor multiplied with the system's output acting on the ART's fluid. Therefore, to obtain a similar closed loop transfer function as in Equation 4.7, the two control parts have to be combined in one control loop that consists of the plant's transfer function multiplied with the control part's transfer function.

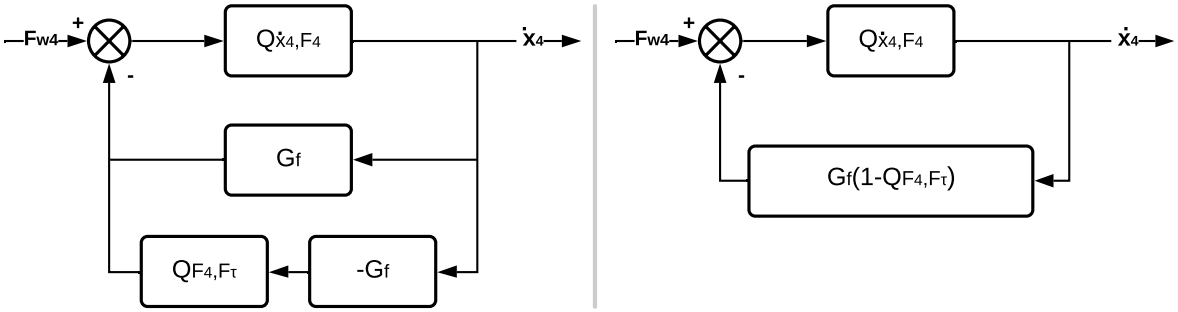

Figure 4.6: Equivalent block diagrams of an open loop feedback controlled ART.

Using the figure above, it can be demonstrated that the open loop transfer function can be determined as in the equation below. This is the same expression as defined by Alujević et al. (2020).

$$\begin{aligned} S_{F_{4,stab,p},F_{w4}} = G(s)H(s) &= Q_{\dot{x}_4,F_4} \cdot G_f \cdot (1 - Q_{F_4,F_\tau}) \\ &= Q_{\dot{x}_4,F_4} \cdot G_f \cdot \left(1 - Q_{\dot{x}_4,F_\tau} \cdot (Q_{\dot{x}_4,F_4})^{-1}\right) \\ &= G_f \cdot (Q_{\dot{x}_4,F_4} - Q_{\dot{x}_4,F_\tau}) \quad [\text{Nm/Nm}] \end{aligned} \tag{4.23}$$

In the above equation, the moment that is applied on the tank fluid is the gain factor multiplied with the response of the vessel to an external moment. This moment causes a motion of the vessel obtained by multiplying with $Q_{\dot{x}_4,F_\tau}$. This motion can be translated into an external force by multiplying with the uncoupled transfer function $(Q_{\dot{x}_4,F_4})^{-1}$. The uncoupled transfer function is taken because the only purpose is to know the force associated with the motion caused, no interaction of the system is required for this.

In the block diagram the system's plant is the ship with passive ART. The control loop only regards the active control part. This is different than the previously discussed uncoupled transfer function or the block diagram of the passive system, in which the system's plant is the ship without ART.

The steps in Equation 4.23 lead to the same open loop transfer function as can be seen back in the closed loop transfer function as derived in Equation 3.9. The equation is repeated below for convenience.

$$Q_{\dot{x}_4,\theta} = \frac{\dot{x}_4}{\theta} = \frac{F_{w40} \cdot Q_{\dot{x}_4,F_4}}{1 + G_f\,(Q_{\dot{x}_4,F_4} - Q_{\dot{x}_4,F_\tau})} \quad \left[\frac{\text{rad}}{\text{rad s}}\right]$$

4.3.2 Stability assessment

For the open loop transfer function of the coupled system (Equation 4.23) the Nyquist plot is given in Figure 4.7.

The active control amplifies the motions as the Nyquist curve enters the unit circle with origin $-1+0i$. This also matches with the RAO plots in Figure 3.3. As an example in the left graph of Figure 4.7, the frequency at which the Nyquist plot enters the unit circle is shown. For this gain and frequency the motions will indeed by amplified by the ART as seen in Figure 3.3.

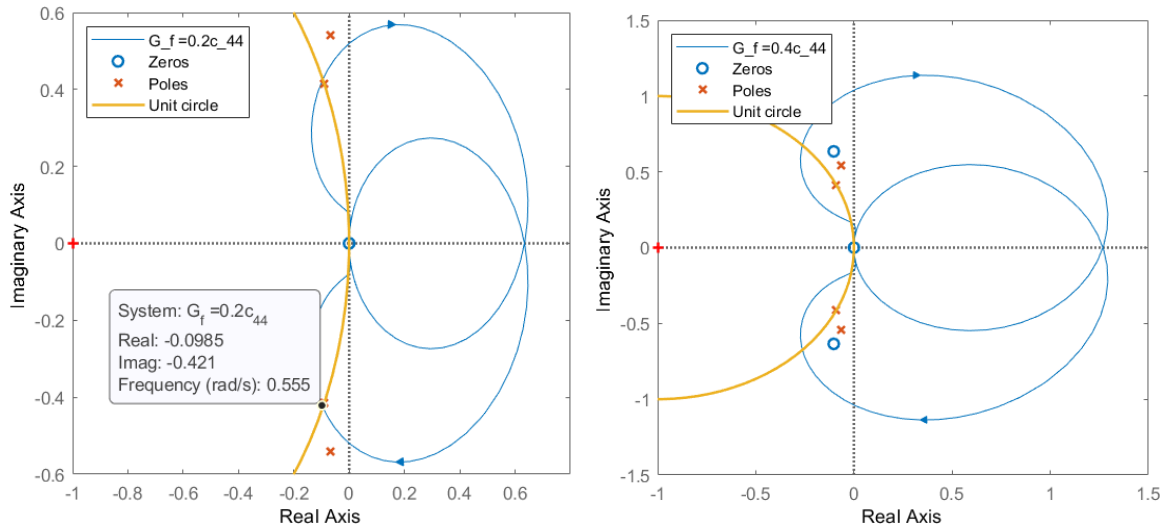

Figure 4.7: Nyquist plots for active part of open loop transfer function of feedback controlled system using Eq. 4.23.

For the closed loop system to be stable the equation $N = Z - P$ must satisfy with Z = 0 (see Equation 4.9). Since the are no open-loop poles in the RHP and no encirclements of $-1+0i$, the equation is satisfied. Since the Nyquist plot does not cross the negative real axis the system is unconditionally stable.

Sensitivity analysis To make more clear for which frequencies the active ART reduces the response of vessel, a sensitivity plot is made in Figure 4.8. To determine the sensitivity of the feedback controlled model Equation 4.10 is used. The expression below gives the sensitivity of the active control with respect to the ship with passive ART.

$$S_{fb,C} = \frac{1}{1+G(s)H(s)} = \frac{1}{1+G_f \cdot (Q_{\dot{x}_4,F_4} - Q_{\dot{x}_4,F_\tau})} \quad [-] \tag{4.24}$$

To analyse the effect of the active ART compared to a ship without ART, the sensitivity of the uncoupled transfer function is computed. The result is plotted in Figure 4.9.

$$S_{fb,U} = \frac{1}{1+(S_{F_4,x_4})^{-1} \cdot \left(\frac{-S_{F_\tau,x_4}}{S_{F_\tau,\tau}} \cdot S_{F_4,\tau} + \frac{i\omega \cdot G_f \cdot S_{F_4,\tau}}{S_{F\tau,\tau}} + i\omega \cdot G_f \right)} \quad [-] \tag{4.25}$$

Figure 4.8: Sensitivity plot of the active control of the ART using Equation 4.24 (left) and comparison of the response of the passive ART (right).

Figure 4.9: Sensitivity plot of the ART using Equation 4.25 (left) and comparison of the response of the ART (right).

As seen in the figure above, the feedback controlled amplifies the motions for the higher frequencies. Since the SOV is intended to operate in coastal areas, waves of higher frequencies are assumed to occur often. Therefore, the response amplification at frequencies around 0.6-0.8 rad/s is not good for the vessel's seakeeping.

Tank damping coefficient The analysis made applies to the obtained data of the SOV. However, for the sake of completeness, the model can also be analysed for different tank damping coefficients.

It is found that as long as the tank damping coefficient (η_t) is sufficiently high, the closed loop transfer function for the ship's roll remains stable. However, if the tank damping is significantly lower, the Nyquist curve will cross the negative real axis because the phase angle of the open loop transfer function will be shifted 180° so that it will act in phase with the incoming wave moment. This can be seen in Figure 4.10. In this figure the phase angle of the moment caused by the pump with respect to the wave moment is plotted for different ART damping coefficients and a gain factor of $G_f = c_{44}$.

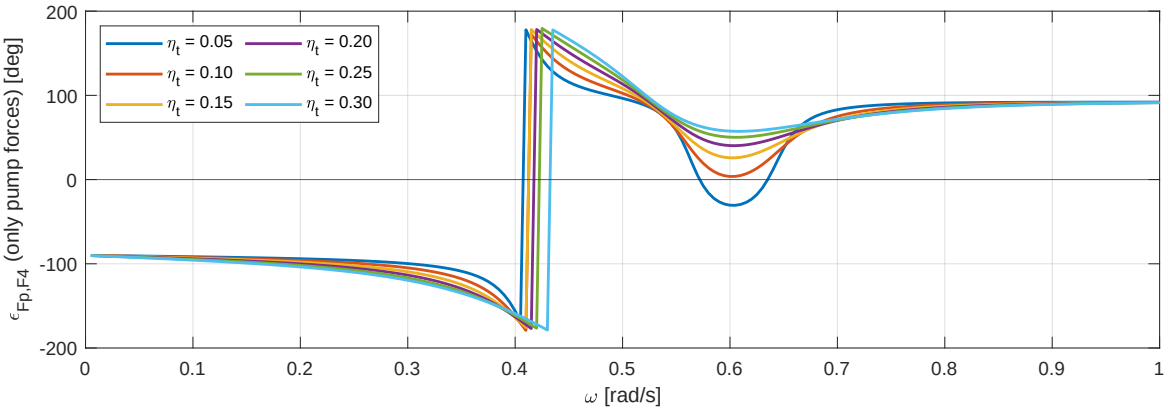

Figure 4.10: Phase of open loop transfer function (Eq. 4.23) for different η_t for feedback controlled ART.

In the case that the open loop transfer function is in phase with the excitation moment for certain frequencies, the system is conditionally stable. This aspect can be seen even easier in the root locus plot in Figure 4.11. For a certain gain factor the poles of the system with low tank damping will enter the right half plane, resulting in an unstable system.

Total system damping Besides the effect of the tank damping coefficient η_t on the stability of the system, also the total system damping is of interest. It can be seen that for both systems (with $\eta_t = 0.25$ and with $\eta_t = 0.05$) the system's damping is rather low because the poles are located relatively close to the imaginary axis. This will cause the system's time response to have a rather large overshoot.

To avoid large overshoots, the gain factor can be decreased. However, this is a trade-off, because a lower gain factor will reduce the effect of the control.

For the trade-off it should be noted that overshoots in roll motion for a ship are difficult to avoid. Especially at lower roll velocities, the roll damping is very little.

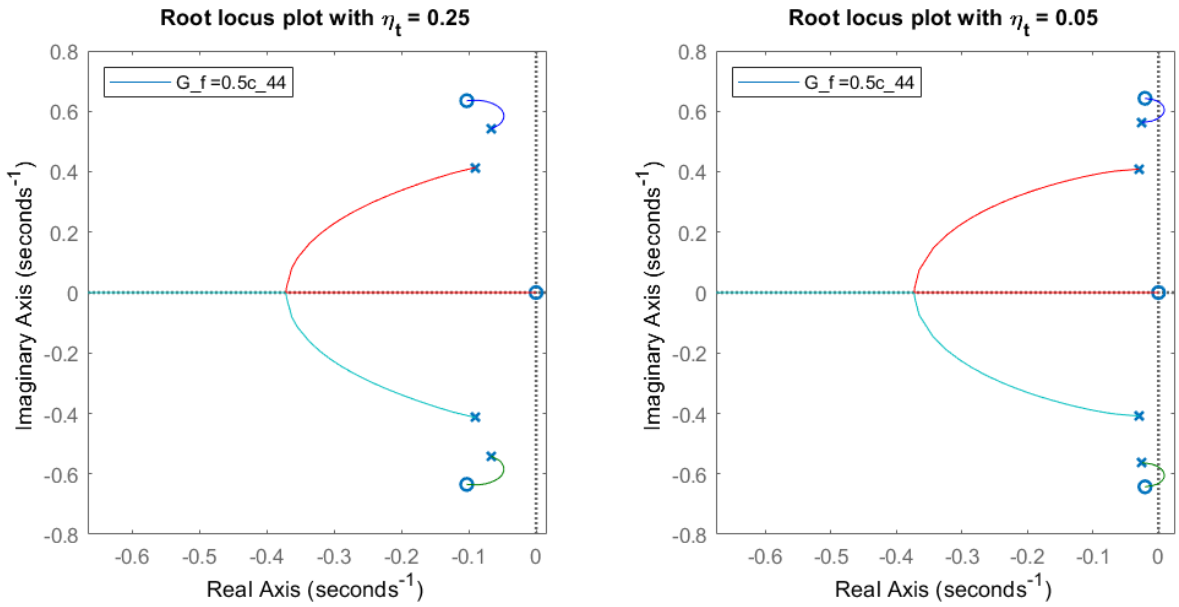

Figure 4.11: Root locus plot for feedback controlled ART with different η_t using Eq. 4.23.

Conclusion All in all, for the feedback controlled model, the system will not experience any issues with respect to the control system stability. However, the feedback control does cause an amplification of the motions at frequencies which will have a negative result for the seakeeping of the vessel.

The maximum allowable gain factor will depend on two aspects that have not been addressed in this paragraph. These two aspects are the limit for the tank's fluid angle due to structural limits and the maximum available pump power. In the following chapters these aspects will be analysed into further detail.

4.4 Feed forward controlled model

Since a feed forward model does not have a closed loop, the stability assessment will differ from the closed loop feedback system as there is no reason for instability. The only point of interest is whether the stabilising moment will not amplify the moments.

4.4.1 Transfer function

For the control of the feed forward model the open-loop transfer functions can be derived. The model to obtain the equations can be seen in Figure 4.12. Looking at the model it can be seen that the moments caused by the pump and ART will be subtracted from the wave moment.

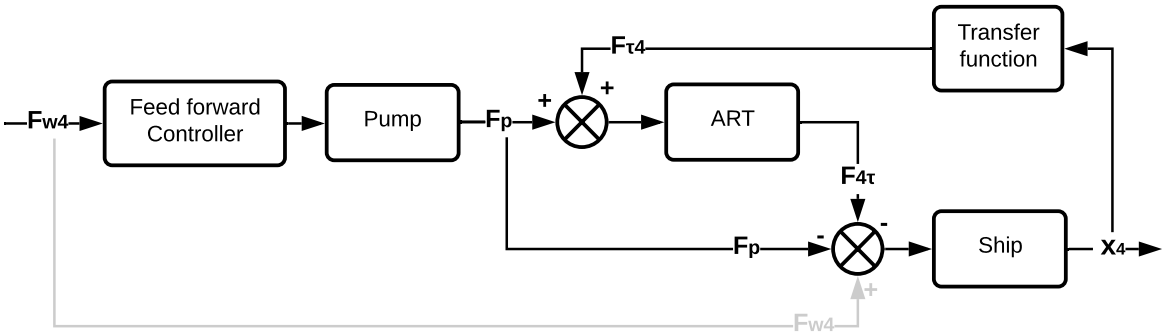

Figure 4.12: Open-loop control diagram for stability analysis of feed forward controlled ART.

By using Equation 3.33, the effect of changing the phase angle of the pump moment with respect to the waves can be analysed. The equation is repeated below for convenience:

$$S_{F_{4,stab},F_{w4}} = -G_f - ((1 - G_f) \cdot S_{\tau,F_4} + G_f \cdot S_{\tau,F_\tau}) \cdot S_{F_4,\tau} \quad [\text{Nm/Nm}]$$

4.4.2 Stability criteria

In general for a feed forward system the only point of interest is whether the stabilising moment has the correct phase and magnitude with respect to the disturbing moment. The phase difference of the stabilising moment should be around 180° with respect to the wave excitation moment. If the moments are in phase, the motions will be amplified.

Besides the phase angle of the stabilising moment, the magnitude is important as well. Even though the stabilising moment might oppose the wave moment, if it is larger than the disturbing moment, the active control is not as required since it will overreact the wave moment.

4.4.3 Stability assessment

Since there is no feedback loop, no use of Nyquist, Bode and Root locus plots is made. Instead, the response of the system is analysed using regular magnitude and phase plots.

Phase angle For a certain gain and frequency it could occur that the moments caused by the pump ($F_p + F_{4\tau}$) will act in phase with the wave moment. The analysis for when this could occur, is already made in §3.2.3. For the situation in which the action moment of the pump is exactly opposed to the wave moment (without a phase difference $\epsilon_{F_p,F_{w4}}$), the stabilising moments were opposed to the wave moment as the gain factor is increased (see Figure 3.8).

However, since the pump moment is based on the incoming wave moment, the response of the system can be manipulated by changing the phase angle between the wave moment and the pump moment. As found in Figure 3.11 the performance of the control was better for a phase angle of -45°. This can be supported by analysing the phase angles of the stabilising moment for different values of the phase angle of the pump moment (both with respect to the wave moment). As the ship's motions are the highest at the natural frequency of the ship, the phase angle of the stabilising moment with respect to the waves should be as close as possible to 180° at that point. This will give the largest real part of the stabilising moment that will counteract the wave moment.

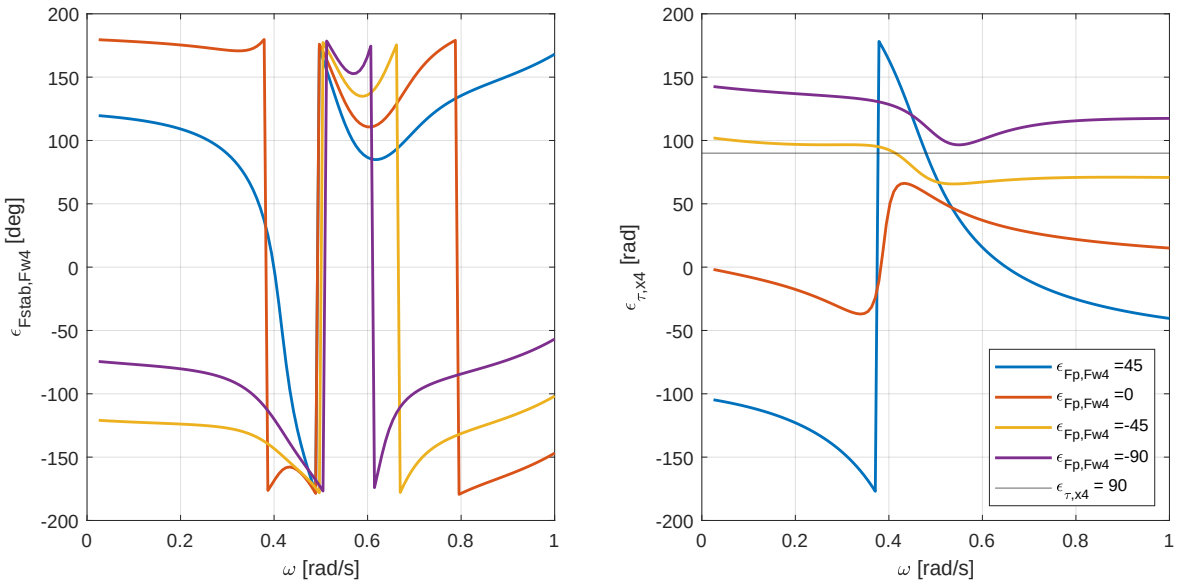

Figure 4.13: Phase angles of stabilising moment of feed forward controlled ART using Eq. 3.33 and 3.24 respectively for $G_f = 0.25$.

In Figure 4.13 the stabilising moment is plotted for different phases between the wave moment and pump moment. Since the natural frequency of the vessel with ART is about 0.5 rad/s, the curve for $\epsilon_{F_p,F_{w4}} = -45°$ is best. Note that the choice for a phase angle is a trade-off: The curve for $\epsilon_{F_p,F_{w4}} = -90°$ is even closer to the desired 180° around the natural frequency of the ship, however, the phase difference quickly decreases in size. Therefore, it is a less desirable model choice.

The power input effectiveness can be assessed by considering the phase angle between the tank's fluid and the ship's roll angle. As seen in Figure 4.13, the tank's fluid angle is within the desired range of about 90° for $\epsilon_{F_p,F_{w4}} = -45°$. For the best control effectiveness, the phase angle of the stabilising moment should be 180° with respect to the wave moment, and the phase angle of the tank's fluid angle should be 90° with respect to the ship's roll angle. The latter objective is only to reduce the required power. Therefore, it can also be achieved by considering the required power for different gain factors.

Magnitude To determine at which point the stabilising moment will overreact the disturbing wave moment the real part of the stabilising moment is plotted in Figure 4.14. The real part is plotted since that is the part that oscillates in phase with the wave moment.

In the left figure it can be seen that for a certain gain factor (about 0.4) the control overreacts the wave moment. The imaginary part shows the part of the stabilising moment that acts 90° out of phase with the wave excitation moment.

Just as for the feedback controlled model, there are no limits with respect to the stability. The control model can be optimised in terms of power requirement. For this optimisation the tank fluid angle with respect to the ship will be of importance. The closer the angle lies to the optimal 90° phase angle, the less power is required.

Furthermore, for an efficient use of power, the imaginary part of the stabilising moment should be as low as possible, since only the (negative) real part of the moment counteracts the wave moment.

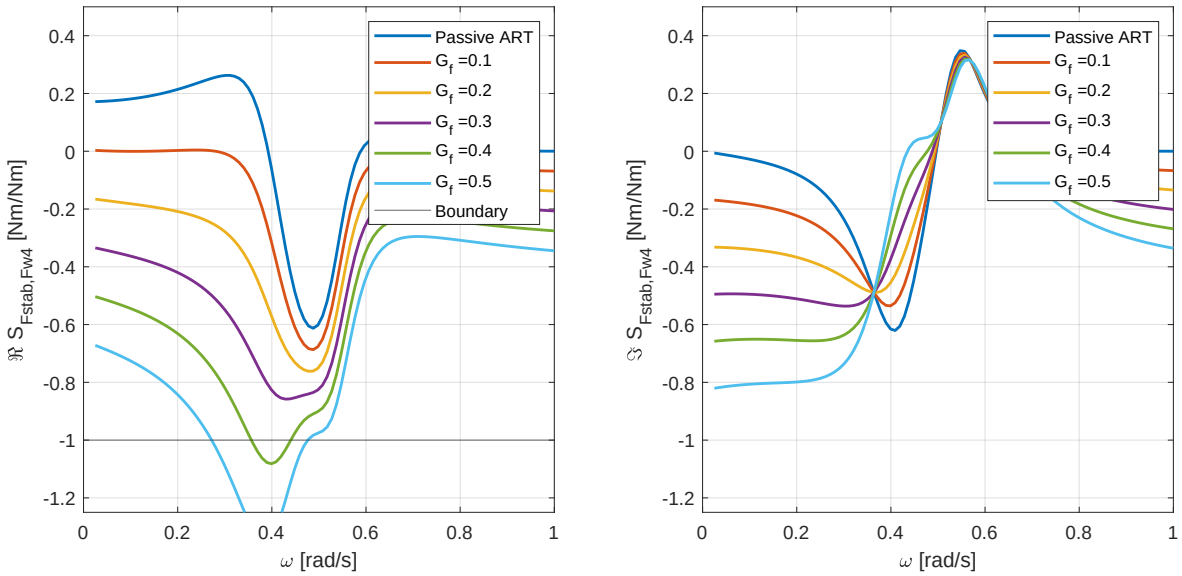

Figure 4.14: Stabilising moment for feed forward controlled ART using Eq. 3.33.

4.5 2DoF controlled model

A block diagram of the open loop transfer function for the 2DoF controlled model is shown in Figure 4.15. In this paragraph the stability will be assessed based on the previous two models, namely the feedback controlled model and feed forward controlled model.

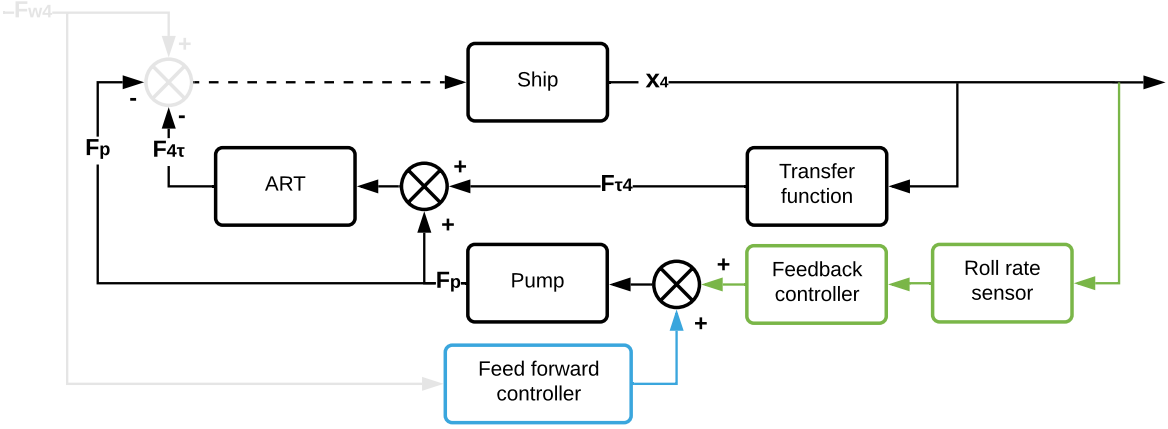

Figure 4.15: Block diagram of the open loop part of the 2DoF controlled model.

4.5.1 Transfer functions

Uncoupled transfer function Just as performed for the feedback controlled ART, the uncoupled transfer functions will be defined for the 2DoF controlled ART to compare the

system with a ship without ART.

$$\begin{aligned} x_4 &= (S_{F_4,x_4})^{-1} \cdot F_4 \\ F_{4\tau} &= \left(x_4 \cdot S_{\tau,x_4,\text{uncoupled}} + F_p \cdot (S_{F\tau,\tau})^{-1}\right) \cdot S_{F_4,\tau} \\ F_p &= x_4 \cdot i\omega \cdot G_{fb} + F_{w4} \cdot G_{ff} \\ F_4 &= F_{w4} - F_{4\tau} - F_p \end{aligned} \tag{4.26}$$

Substitution gives the following:

$$\begin{aligned} x_4 &= (S_{F_4,x_4})^{-1} \cdot F_{w4} \\ &- (S_{F_4,x_4})^{-1} \cdot \left(x_4 \cdot S_{\tau,x_4,\text{uncoupled}} + \left(x_4 \cdot i\omega \cdot G_{fb} + F_{w4} \cdot G_{ff}\right) \cdot (S_{F\tau,\tau})^{-1}\right) \cdot S_{F_4,\tau} \\ &- (S_{F_4,x_4})^{-1} \cdot \left(x_4 \cdot i\omega \cdot G_{fb} + F_{w4} \cdot G_{ff}\right) \end{aligned} \tag{4.27}$$

$$\begin{aligned} x_4\Big(1+(S_{F_4,x_4})^{-1} \cdot \Big(S_{\tau,x_4,\text{uncoupled}} \cdot S_{F_4,\tau} + i\omega \cdot G_{fb} \cdot (S_{F\tau,\tau})^{-1} \cdot S_{F_4,\tau} + i\omega \cdot G_{fb}\Big)\Big) \\ = (S_{F_4,x_4})^{-1} \cdot F_{w4} \cdot \left(1 - G_{ff} \cdot (S_{F_\tau,\tau})^{-1} \cdot S_{F_4,\tau} - G_{ff}\right) \end{aligned} \tag{4.28}$$

The transfer function of the entire system can now be obtained. Note that the characteristic formulation of a feedback transfer function is seen back.

$$\frac{x_4}{F_{w4}} = \frac{(S_{F_4,x_4})^{-1} \cdot (1 - G_{ff} \cdot (S_{F_\tau,\tau})^{-1} \cdot S_{F_4,\tau} - G_{ff})}{1 + (S_{F_4,x_4})^{-1} \cdot \left(\dfrac{-S_{F_\tau,x_4}}{S_{F_\tau,\tau}} \cdot S_{F_4,\tau} + \dfrac{i\omega \cdot G_{fb} \cdot S_{F_4,\tau}}{S_{F\tau,\tau}} + i\omega \cdot G_{fb}\right)} \tag{4.29}$$

Coupled transfer function The open loop transfer function is the transfer function between the incoming wave moment and the stabilising moments resulting from the ART and the pump ($F_p + F_{4\tau}$). The total stabilising moment per unit of wave moment as determined in Equation 3.47 is repeated below:

$$S_{F_{4,stab},F_{w4}} = \frac{-G_{fb} \cdot i\omega \cdot S_{x_4,\theta} - G_{ff} \cdot e^{-i\epsilon_{F_p,F_{w4}}} \cdot F_{w40} - S_{\tau,\theta} \cdot S_{F_4,\tau}}{F_{w40}} \quad \left[\frac{\text{Nm}}{\text{Nm}}\right]$$

However, only the feedback loop has a risk of becoming unstable. So to asses the stability the stabilising forces per unit of wave moment of the feedback loop are required. The open loop transfer function of this feedback part is the same as for the pure feedback controlled model (Equation 4.23) and is given below.

$$S_{F_{4,stab,p},F_{w4}} = G_{fb} \cdot (Q_{\dot{x}_4,F_4} - Q_{\dot{x}_4,F_\tau}) \quad [\text{Nm/Nm}] \tag{4.30}$$

This expression can also be obtained by substituting the transfer functions $S_{x_4,\theta}$ (Eq. 3.42) and $S_{\tau,\theta}$ (Eq. 3.44) in Equation 3.47 which is the repeated equation above. For the sake of brevity, the substitution is not given.

4.5.2 Stability criteria

For the stability of the 2DoF controlled model the feedback loop must be considered. For the feedback loop the same criteria applies as applied for the feedback model in §4.3. For the total stabilising moment caused by both loops it must be assessed whether the stabilising moment does not exceed the wave excitation moment. This is to avoid inefficient use of power.

4.5.3 Stability assessment

Feedback loop Since the feedback controlled model was stable, the feedback loop in the 2DoF model is stable too. For any gain and frequency the output of the loop will be bounded, as long is the input is bounded.

Total stabilising moment By plotting the real and imaginary part of Equation 3.47 it can be concluded that for a gain factor up to about 0.4, the presence of the pump positively affects the system. This can be explained for two reasons. Firstly, because of the fact that the real part of the stabilising moment is not larger than the wave moment. Secondly, the sign of the real part is negative, which means that the stabilising moment opposes the wave moment. The latter aspect could also already be seen in Figure 3.15 since the phase angle was about 180° for all excitation frequencies.

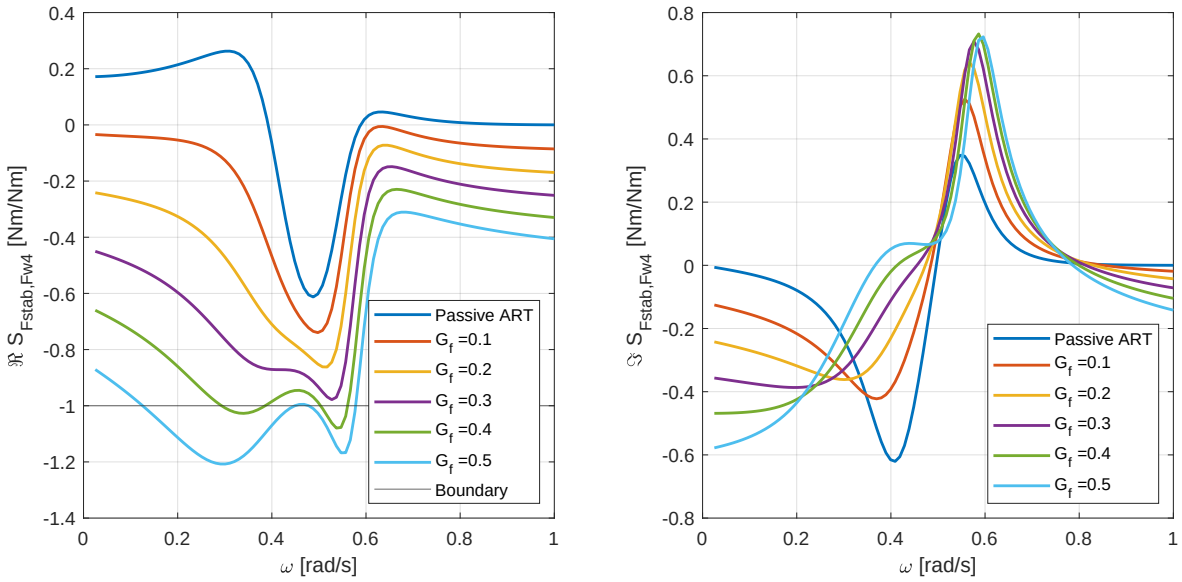

Figure 4.16: Stabilising moments due to the pump using Eq. 3.47.

The limit for the active control lies at the point where the stabilising moment is equal to the wave moment. Since there is no point at which the system will become unstable, the model can be optimised in terms of power requirement, without considering any stability limits.

4.6 Overview of stability conditions

After all the different control models have been analysed an overview can be made. In the Table 4.1 for every model the stability limitations are given.

Table 4.1: Overview of stability conditions.

Model	Stability	Remarks
Passive	Condition-ally stable	Motions are amplified, but system remains stable. However, if the ART is increased by increasing the length of the ART, the system can become unstable. This is because the stabilising moment will increase as the ART's size increases.
Active feedback	Uncondition-ally stable	Instability can occur if the ART damping coefficient turns out to be significantly lower than measured during the hexapod tests.
Active feed forward	Uncondition-ally stable	The stabilising moment will always oppose the wave excitation moment, however, the effectiveness deteriorates once the stabilising moment is larger than the wave excitation moment.
Active 2DoF	Uncondition-ally stable	Since the 2DoF model is a combination of the feedback and feed forward models, the remarks on that models also apply tho the 2DoF model.

5 - Workability

The workability of the SOV is mainly related to the operational criteria for the gangway on board the vessel. The goal of the workability study is to determine if the SOV is able to operate at 3m significant wave height. So, only the limiting environmental condition is assessed based on the design requirements.

5.1 Gangway properties

Dimensions The motion compensated gangway is attached to the ship by means of a vertical column, called the pedestal. At the ship's design draft, the vertical location of the connection point of the gangway with the pedestal is equal to the vertical location of the platform in case of calm water. For the height of the platform a wind turbine operation point is assumed of 26m above the calm waterline. Furthermore, in rest, the length of the gangway L_{gw} equals 25m. Also, the root of the gangway is above the centre line of the vessel.

Table 5.1: Gangway properties.

Gangway property	Symbol	Unit	Value
Length	L_{gw}	m	[redacted]
Longitudinal location connection point with pedestal	L_{cp}	m	[redacted]
Vertical location connection point with pedestal	H_{cp}	m	[redacted]
Transverse location connection point with pedestal	B_{cp}	m	[redacted]

Figure 5.1: Example of a motion compensated gangway (Royal IHC, 2020a).

Gangway limitations The motions of the gangway can be described as shown in Figure 5.2. These parameters all have a maximum value, given in Table 5.2. As the SOV is intended to operate at a maximum significant wave height of 3m, the ship motions must be such that the gangway will not exceed its design constraints.

Table 5.2: Gangway criteria for operation in maximum H_s of 3m at zero speed.

Gangway property	Symbol	Unit	Criterion
Length	L_{gw}	m	[redacted] < L_{gw} < [redacted]
Telescoping speed (variation of length)	$\dot{L}_{gw}$	m/s	< [redacted]
Slewing angle (horizontal plane)	β	deg	< [redacted]
Slewing speed	$\dot{\beta}$	deg/s	< [redacted]
Luffing angle (vertical plane)	α	deg	< [redacted]
Luffing speed	$\dot{\alpha}$	deg/s	< [redacted]

The equations below can be used to determine the values of the gangway properties. In the equations the origin is the connection point of the gangway with the pedestal.

$$L_{gw} = \sqrt{(x_p)^2 + (y_p)^2 + (z_p)^2} \quad [\text{m}], \quad \dot{L}_{gw} = \frac{dL_{gw}}{dt} \quad [\text{m/s}] \tag{5.1}$$

$$\beta = \text{atan}\left(\frac{x_p}{y_p}\right) - x_5 \quad [\text{deg}], \quad \dot{\beta} = \frac{d\beta}{dt} \quad [\text{deg/s}] \tag{5.2}$$

$$\alpha = \text{asin}\left(\frac{z_p}{L_p}\right) + x_4 \quad [\text{deg}], \quad \dot{\alpha} = \frac{d\alpha}{dt} \quad [\text{deg/s}] \tag{5.3}$$

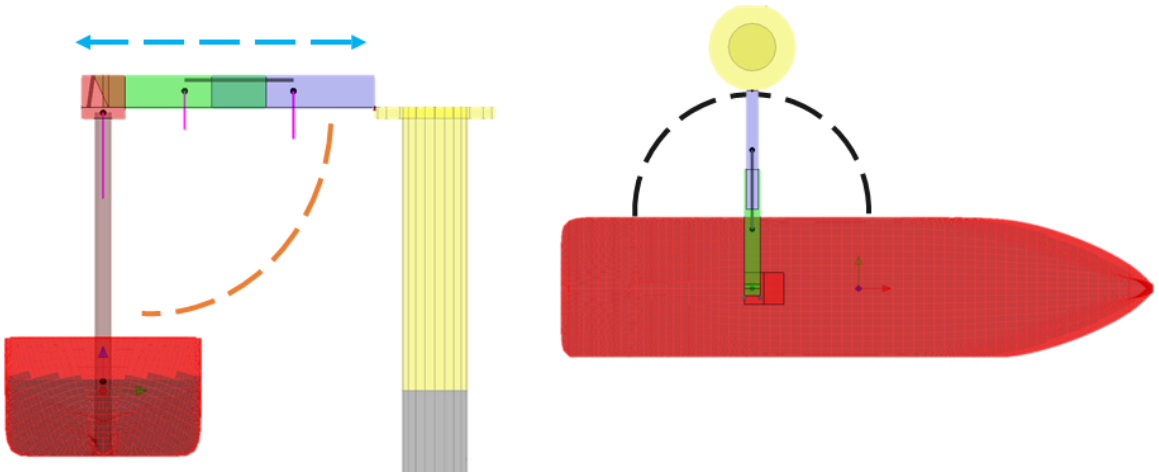

Figure 5.2: Telescope motion (blue), luffing motion (orange) and slewing motion (black).

5.2 Wave spectra

To analyse the waves use can be made of wave energy spectra, or shortly, wave spectra. In this paragraph it will be discussed how to obtain the response of the SOV to a certain sea state. (Journée and Massie, 2001).

5.2.1 Wave energy spectrum

Definition A wave spectrum shows, if integrated over a certain frequency range and multiplied with ρg, the energy of the waves for a certain frequency range. In the following equation the wave spectrum of the wave elevation is given.

$$S_\zeta(\omega_n) \cdot d\omega = \frac{1}{2}\zeta_{0_n}^2 \quad [\mathrm{m}^2] \tag{5.4}$$

By not only considering the wave elevation, but also the wave length, the wave spectrum of the wave slope can also be obtained. In the equation below k is the wave number. This parameter includes the property of the wave's length.

$$S_\theta(\omega_n) \cdot d\omega = \frac{1}{2}\theta_{0_n}^2 = \frac{1}{2}\zeta_{0_n}^2 \cdot k^2 = \frac{1}{2}\zeta_{0_n}^2 \cdot \frac{\omega_n^4}{g^2} \quad [\mathrm{rad}^2] \tag{5.5}$$

JONSWAP As input for the model, a JONSWAP spectrum will be used, which is based on the Bretschneider spectrum. The Bretschneider spectrum is also known as the modified Pierson-Moskowitz spectrum and describes the waves at the open ocean. The JONSWAP spectrum is an adapted form of the Bretschneider spectrum and describes the waves in more coastal areas. In these coastal areas the waves are less developed, which causes the spectrum to cover a smaller frequency range.

In the below equations γ is the peak enhancement value. The lower the gamma value, the wider the frequency wave spectrum.

$$S_{J\zeta}(\omega) = 0.658 \cdot \gamma^J \cdot S_{B\zeta}(\omega) \tag{5.6}$$

$$S_{B\zeta}(\omega) = \frac{A}{\omega^5} \cdot \exp\left(\frac{-B}{\omega^4}\right) \quad [\mathrm{m}^2/(\mathrm{rad/s})] \tag{5.7}$$

$$A = 487 \cdot \frac{\overline{H}_{1/3}^2}{T_0^4} \quad [\mathrm{m}^2/\mathrm{sec}^4], \quad B = \frac{1949}{T_0^4} \quad [\mathrm{sec}^{-1}] \tag{5.8}$$

$$J = \exp\left(\frac{-1}{2\sigma^2}\left(\frac{\omega \cdot T_p}{2\pi} - 1\right)^2\right) \tag{5.9}$$

In the above equation $\sigma = 0.07$ for $\omega < 2\pi/T_p$ and $\sigma = 0.09$ for $\omega > 2\pi/T_p$. The values for $\overline{H}_{1/3}$ and T_p as defined by the World Meteorological Organization (Alujević et al., 2020) can be found in Table 5.3. In Figure 5.3 the wave height and wave slope spectrum are plotted for sea state 5.

Table 5.3: Average sea state properties.

Sea state	1	2	3	4	5	6	7	8	9
$\overline{H}_{1/3}$ [m]	0.050	0.300	0.875	1.875	3.250	5.000	7.500	11.50	15.00
T_p [s]	2.0	4.0	5.5	7.0	8.0	9.5	12.0	15.0	21.0

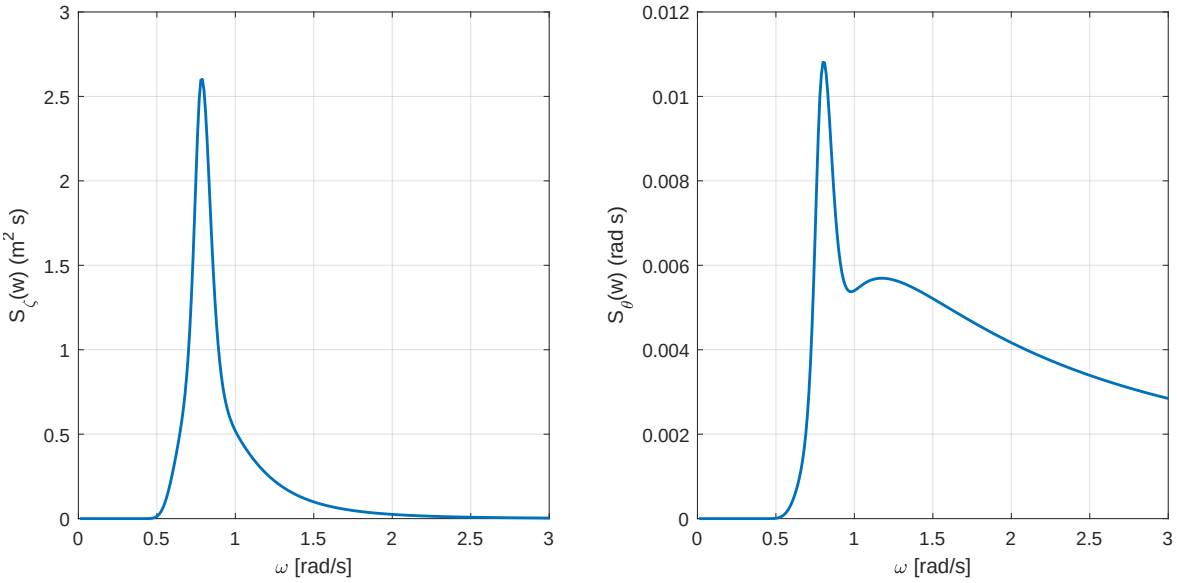

Figure 5.3: Wave height and wave slope spectrum for sea state 5.

5.2.2 Response energy spectrum

The response of the vessel can be determined using the wave spectrum, the RAO squared should be multiplied with the wave energy spectrum to obtain the response energy.

$$S_{x_4}(\omega) = |S_{x_4,\theta}(i\omega)|^2 \cdot S_\theta(\omega) \quad [\text{rad} \cdot \text{s}] \tag{5.10}$$

$$S_\tau(\omega) = |S_{\tau,\theta}(i\omega)|^2 \cdot S_\theta(\omega) \quad [\text{rad} \cdot \text{s}] \tag{5.11}$$

Significant amplitude The significant roll amplitude ($\overline{x_{40}}_{1/3}$) gives the mean value of the highest one-third part of the roll amplitudes. First the moments of the energy response function must be determined, which relate to the variance of the spectrum. In the equation below $n = 0$ relates to the roll angle, $n = 2$ relates to the roll rate, and $n = 4$ relates to the roll acceleration.

$$m_{nx_4} = \int_0^\infty \left(S_{x_4}(\omega) \cdot \omega^n\right) d\omega \quad [\text{rad}^2/\text{sec}^n], \quad n = 0, 2, 4 \tag{5.12}$$

$$\overline{x_4}_{1/3} = 2\sqrt{m_{0x_4}} \quad [\text{rad}] \tag{5.13}$$

Besides the significant roll amplitude, the root mean square of the roll motion can be obtained as well. The RMS of a signal with a zero mean is equal to the standard deviation.

$$\text{RMS}_{x4} = \sqrt{m_{0x_4}} = \frac{\overline{x_4}_{1/3}}{2} \quad [\text{rad}] \tag{5.14}$$

The same procedure also applies for the response of the tank's fluid angle.

$$\overline{\tau}_{1/3} = 2 \cdot \int_0^\infty S_\tau(\omega)\, d\omega \quad [\text{rad}], \quad \text{RMS}_\tau = \frac{\overline{\tau}_{1/3}}{2} \quad [\text{rad}] \tag{5.15}$$

5.3 Vessel response for different models

5.3.1 Transfer functions

Using the obtained transfer functions, the response of the SOV in different sea states can be determined. The following transfer functions are used:

Feedback controlled model Using Equation 3.11:

$$\text{S}_{x_4,\theta} = \frac{1}{i\omega} \cdot \frac{F_{w40} \cdot Q_{\dot{x}_4,F_4}}{1 + G_f\left(Q_{\dot{x}_4,F_4} - Q_{\dot{x}_4,F_\tau}\right)} \quad \left[\frac{\text{rad}}{\text{rad}}\right]$$

Feed forward controlled model Using Equation 3.22:

$$S_{x_4,\theta} = F_{w40} \cdot \left(S_{x_4,F_4} + G_f\left(S_{x_4,F_\tau} - S_{x_4,F_4}\right)\right) \quad \left[\frac{\text{rad}}{\text{rad}}\right]$$

2DoF controlled model Using Equation 3.42:

$$S_{x_4,\theta} = \frac{F_{w40}\left(S_{x_4,F_4} + G_{ff} \cdot e^{-i\epsilon_{F_p,F_{w4}}} \cdot \left(S_{x_4,F_\tau} - S_{x_4,F_4}\right)\right)}{1 + G_{fb} \cdot \left(Q_{\dot{x}_4,F_4} - Q_{\dot{x}_4,F_\tau}\right)} \quad \left[\frac{\text{rad}}{\text{rad}}\right]$$

5.3.2 Validity of the model

For the model to be valid, the tank's fluid angle should be considered. If the tank's fluid angle will be larger than physically possible due to the limited height of the reservoirs, the model will give an invalid output.

Defining the limit To asses the fluid level in the reservoirs, the response spectrum of the tank's fluid angle is considered. Now if for example the significant tank fluid angle amplitude would be equal to the maximum tank's fluid angle as determined in Equation 2.10, the water would slosh against the top of the reservoir in 13.5% of the waves (Holthuijsen, 2007). This is still quite often, so a higher limit should be defined.

Since the exact limit is rather arbitrary because it is not a big issue if the tank's fluid angle will slosh against the top of the reservoir once in a while, a limit is considered of 1 in every 1000 waves ($N_w = 1000$). This is based on the number of waves in a 3 hour storm. The reason that this limit is rather high is because the model must be valid to analyse safety constraints of the gangway. This will be discussed in *§5.4 Probabilistic exceedance of gangway limitations*.

Rayleigh distribution Using the expression for the Rayleigh probability density function as defined by Journée and Massie (2001) and Holthuijsen (2007), a limit for the tank's fluid angle is obtained in Equation 5.16.

The Rayleigh probability density function is based on the combination of two independent random variables following a normal distribution. The two variables are the two wave directions in the horizontal plane. Therefore, for the computation, normal distributed wave elevations are assumed. Since harmonic linear oscillations are assumed, the type of probability density function of the tank's fluid angle will be the same as the type of probability density function of the wave amplitudes.

$$P(\tau > \tau_{lim}) = \exp\left(-2\left(\frac{\tau_{\text{lim}}}{\overline{\tau}_{1/3}}\right)^2\right) = \frac{1}{N_w} \rightarrow \tau_{lim} = \sqrt{-\frac{\ln(1/N_w)}{2}} \cdot \overline{\tau}_s \quad \text{[rad]} \tag{5.16}$$

To put it briefly, τ_{lim} should remain below the maximum allowable tank fluid angle in order to consider the results valid. Filling in the above equation for $N_w = 1000$ gives:

$$\tau_{lim} = \sqrt{-\frac{\ln(1/1000)}{2}} \cdot \overline{\tau}_{1/3} = 1.86 \cdot \overline{\tau}_{1/3} \quad \text{[rad]} \tag{5.17}$$

In a similar way, the amplification factor for the significant wave height in a 3h storm can be obtained.

$$H_{storm} = \sqrt{-\frac{\ln(1/1000)}{2}} \cdot \overline{H}_{1/3} = 1.86 \cdot \overline{H}_{1/3} \quad \text{[m]} \tag{5.18}$$

5.4 Probabilistic exceedance of gangway limitations

Since when analysing the ship's response to the waves a statistical approach is adopted, a certain probability of exceedance is required for the maximum allowed roll motion. Based on this probability of exceedance it can be determined if the ship can still operate in a certain sea state.

To analyse the structural design and strength criteria is provided by DNV GL (2017). It is stated that for the accelerations of the gangway a probability of exceedance of 10^{-8} is a typical value to analyse the extreme values. This means that the gangway's design criteria on topic of accelerations would only be exceeded once every 10^8 oscillations ($N_w = 10^8$).

However, since the gangway's limits as defined in Table 5.2 are not in terms of accelerations because they are not on topic of structural integrity, the 10^{-8} probability of exceedance is not suitable. Instead, the gangway's limits are in terms of angles and velocities because they are on topic of maximum displacements.

Since gangway operations are performed with good visibility, the master of the ship is able to detect large incoming waves that could cause the gangway to disconnect. In case of a large incoming wave, the master can stop the operations to guarantee the safety of the personnel on board. Therefore, the probability of exceedance is limited to 10^{-3} which is an approximation for once in every 3 hour storm. Using the Rayleigh distribution again gives the expression as below.

$$P(x > x_{lim}) = \exp\left(-2\left(\frac{x_{\text{lim}}}{\overline{x}_{1/3}}\right)^2\right) = \frac{1}{N_w} \rightarrow x_{lim} = 1.86 \cdot \overline{x}_{1/3} \quad \text{[rad]} \tag{5.19}$$

So, to meet the design requirements on topic of gangway displacements, the significant amplitude of a motion multiplied by 1.86 should be lower than the design limit. Note that the structural integrity of the gangway is not assessed by means of this approach.

The assumption made for this approach is that the extremes still follow the Rayleigh distributions. This might not be the case since for higher waves non linearity occurs due to for example wave breaking. Nevertheless, it does give a decent approximation since the extremes in a 3h storm are not expected to be highly non-linear.

5.5 Workability tool

Using a workability analysis tool developed by Royal IHC the design criteria for the gangway are assessed. By making a model of the gangway and implementing the RAOs of the SOV for the different models, results are obtained.

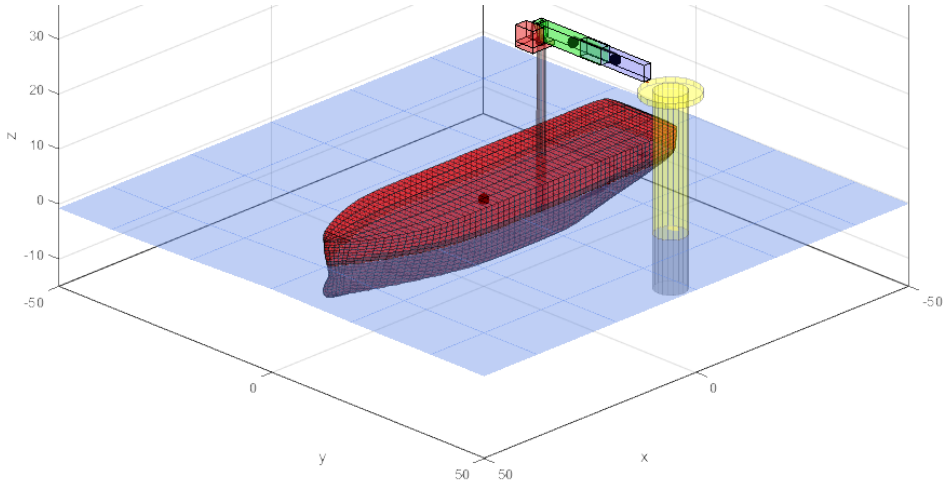

Figure 5.4: Gangway model of SOV in the workability tool.

Time domain analysis The gangway's limitations are most easy to assess in time domain due to non linear properties of the gangway motions. The non linearity is caused by the fact that the motions can easily become too large to linearise the trigonometric functions. Therefore, the workability analysis tool transforms the frequency domain results to the time domain. Based on a time trace of the motions, the kinematic computations are made to obtain the position, velocity and accelartion of the gangway with respect to the offshore wind turbine.

To go from the frequency domain towards the time domain, the workability tool uses the Cummins equation. This equation determines the hydrodynamic reaction forces by means of impulse response functions. The impulsive displacement during a short time interval will affect the motions at the interval itself, but also the motions after the interval. In this way, an irregular wave can be considered more accurate.

Frequency domain analysis As stated before, the gangway's design criteria may only be exceeded once every 1000 oscillations. To apply a proper probabilistic approach, a transformation back to the frequency domain is made.

6 - Power dissipation and pump power requirement

Since the ART will be active, there is a power requirement. This power is required to activate the pump(s). In this chapter the power requirements for the system will be addressed. This will be done for the feedback, feed forward, and 2DoF controlled model.

To obtain more insight in the power flow, the mean time-averaged power dissipation will be determined. This gives an expression for the effectiveness of the different models. After this, the pump power will be determined based on the flows and pressures.

This sequence of the analysis is chosen since the paper by Alujević et al. (2020) provides an approach to analyse the dissipated powers. Based on the approach to determine the dissipated powers, the pump power can be determined too.

6.1 Power dissipation

As stated by Alujević et al. (2020) the mean time-averaged total power input caused by the waves must be equal to the power dissipated by the ship, the ART and the pump over time. Therefore, the mean time-averaged power input caused by the waves ($\overline{P}_{in}$) is the sum of the power dissipated due to the tank ($\overline{P}_{b\tau\tau}$), ship damping ($\overline{P}_{b44}$) and power delivered by the pump ($\overline{P}_p$).

$$\overline{P}_{in} = \overline{P}_{b_{44}} + \overline{P}_{b_{\tau\tau}} + \overline{P}_p \quad [\text{W}] \tag{6.1}$$

If the pump delivers power, the pump power will be negative. This can be understood by considering that the damping coefficients of the ship (b_{44}) and ART ($b_{\tau\tau}$) will always dissipate power and thereby always be positive. Since the pump (in general) does not dissipate power, but will insert power to the system, the pump power will thus have the opposite sign.

However, there is a situation in which the dissipated power of the pump will be positive. This is the theoretical case in which the pump will act as a sort of generator. For low frequencies, the performance of the ART can be improved by slowing down the fluid flow. This will cause power to be generated. See §8.2 *Further research* for more elaboration on this concept.

6.1.1 Detailed analysis

The fact that only the damping is considered for the mean time-averaged power can be explained by considering the amount of energy that is dissipated by each term in the equation of motion. Based on the approach by Journée and Massie (2001) the amount of energy dissipated due to the mass, damping and spring force components can be expressed as below, using the relation that power equals work divided by time ($P = W/t$). Harmonic oscillations in the form $x_4 = x_{40}\sin(\omega t + \epsilon)$ are assumed. Note that the same approach applies for the ART's equation of motion too. In the equations below T stands for one period.

$$\begin{aligned}\overline{P}_{a_{44}} &= \frac{1}{T}\int_0^T (a_{44} + I_{44})\ddot{x}_4 \, dx_4 = \frac{1}{T} \cdot (a_{44} + I_{44}) \int_0^T \ddot{x}_4 \cdot \dot{x}_4 \, dt \\ &= \frac{1}{T} \cdot (a_{44} + I_{44}) \int_0^T -\omega^2 \cdot x_{40}\sin(\omega t + \epsilon) \cdot \omega \cdot x_{40}\cos(\omega t + \epsilon) dt = 0 \quad [\text{W}]\end{aligned} \tag{6.2}$$

$$\begin{aligned}\overline{P}_{b_{44}} &= \frac{1}{T}\int_0^T b_{44}\cdot\dot{x}_4\,dx_4 = \frac{1}{T}\cdot b_{44}\int_0^T \dot{x}_4\cdot\dot{x}_4\,dt \\ &= \frac{1}{T}\cdot b_{44}\int_0^T \omega\cdot x_{40}\cos(\omega t+\epsilon)\cdot\omega\cdot x_{40}\cos(\omega t+\epsilon)dt = \\ &= \frac{1}{T}\cdot b_{44}\cdot\omega^2\cdot x_{40}^2\int_0^T\left(\frac{1}{2}+\frac{\cos(2\omega t+\epsilon)}{2}\right)dt = \frac{1}{2}\cdot b_{44}\cdot x_{40}^2\cdot\omega^2 \quad [\mathrm{W}]\end{aligned} \tag{6.3}$$

$$\begin{aligned}\overline{P}_{c_{44}} &= \frac{1}{T}\int_0^T c_{44}\cdot x_4\,dx_4 = \frac{1}{T}\cdot c_{44}\int_0^T x_4\dot{x}_4\,dt \\ &= \frac{1}{T}\cdot c_{44}\int_0^T \sin(\omega t+\epsilon)\cdot\omega\cos(\omega t+\epsilon)dt = 0 \quad [\mathrm{W}]\end{aligned} \tag{6.4}$$

So, as can be seen from the equations, only the damping contributes to the mean time-averaged power.

Complex equations Using the complex expressions for the motions the mean time-averaged power can be defined as well. The reason that this is of interest is because within this thesis complex notations are used instead of the time dependent harmonic oscillations as in the derivations in the previous paragraph. So, instead of using $x_4(t) = x_{40}\sin(\omega t+\epsilon)$ to describe the harmonic oscillations, now $x_4(t) = \Re\left(\hat{x}_{40}\cdot e^{-i\omega t}\right)$ is used.

$$\begin{aligned}x_4(t) &= \Re\left(\hat{x}_{40}\cdot e^{-i\omega t}\right) \rightarrow x_{40} = |\hat{x}_{40}| \\ \dot{x}_4(t) &= \Re\left(-i\omega\cdot\hat{x}_{40}\cdot e^{-i\omega t}\right) \rightarrow x_{40} = |-i\omega\cdot\hat{x}_{40}|\end{aligned} \tag{6.5}$$

The above expression can now be substituted for $x_{40}^2\cdot\omega^2$.

$$\overline{P}_{b_{44}} = \frac{1}{2}\cdot b_{44}\cdot x_{40}^2\cdot\omega^2 = \frac{1}{2}\cdot b_{44}\cdot|-i\omega\cdot\hat{x}_{40}|^2 \quad [\mathrm{W}] \tag{6.6}$$

Or making the derivation all the way from the beginning will give the expressions below. Note that the following properties of complex identities are required and that the asterisk * denotes the complex conjugate.

$$\Re(z) = \frac{z+z^*}{2} \quad \rightarrow \quad \Re(z)^2 = \frac{z^2+2zz^*+z^{*2}}{4} = \frac{z^2+2|z|^2+z^{*2}}{4} \tag{6.7}$$

$$\begin{aligned}\overline{P}_{b_{44}} &= \frac{1}{T}\int_0^T b_{44}\cdot\dot{x}_4\,dx_4 = \frac{b_{44}}{T}\int_0^T \dot{x}_4\cdot\dot{x}_4\,dt \\ &= \frac{b_{44}}{T}\int_0^T \Re\left(-i\omega\cdot\hat{x}_{40}\cdot e^{-i\omega t}\right)^2 dt \\ &= \frac{b_{44}}{4T}\int_0^T\left(\left(-i\omega\cdot\hat{x}_{40}\cdot e^{-i\omega t}\right)^2+2\left|-i\omega\cdot\hat{x}_{40}\cdot e^{-i\omega t}\right|^2+\left(-i\omega\cdot\hat{x}_{40}\cdot e^{-i\omega t}\right)^{*2}\right)dt \\ &= \frac{b_{44}}{4T}\int_0^T\left(-\omega^2\cdot\hat{x}_{40}^2\cdot e^{-2i\omega t}+2\cdot\omega^2\cdot\hat{x}_{40}^2-\omega^2\cdot\hat{x}_{40}^2\cdot e^{-2i\omega t}\right)dt \\ &= \frac{1}{2}\cdot b_{44}\cdot\omega^2\cdot\hat{x}_{40}^2 \quad [W]\end{aligned} \tag{6.8}$$

The last step can be taken based on the fact that the integral over one period for the time dependent terms equals zero.

Looking at Equation 6.7 and 6.8, it can be seen that the z^2 and z^{*2} terms do not contribute to the mean time-averaged power. Only the term $zz^* = |z|^2$ contributes.

6.1.2 Feedback control system

Equations The approach to determine the powers in the paper by Alujević et al. (2020) is analogue to determining the complex power of an electrical circuit. In Equation 6.9 the expression for the complex power is given (Alexander, 2005). In the equation the factor 1/2 comes from the fact the root mean square amplitudes are taken of the harmonic signals, which result in a factor $\sqrt{2}$ for V and I. By taking the complex conjugate of I, the complex power does not have a reference angle anymore. For example, if V and I have the same phase angle, by taking the complex conjugate of I the phase angle of the product will be zero, as desired.

$$S = \frac{1}{2} \cdot V \cdot I^* \quad \text{[VA]} \tag{6.9}$$

The real power now is the real part of the complex power.

$$P = \Re(S) = \frac{1}{2} \cdot \Re(V \cdot I^*) \quad \text{[W]} \tag{6.10}$$

For the dissipated powers related to the ship with the ART the following relation is stated by Alujević et al. (2020):

$$P = \frac{1}{2} \cdot \Re(F^* \cdot \dot{x}) \quad \text{[W]} \tag{6.11}$$

The above equation can also be explained by looking at Equations 6.7 and 6.8. In case the two harmonic signals are not the same, than $z_1 \cdot {z_2}^*$ and ${z_1}^* \cdot z_2$ can not be simplified to $|z|^2$. Therefore, for the time independent parts of the power dissipation, $z_1 \cdot {z_2}^*$ and ${z_1}^* \cdot z_2$ have to be considered. Since $\Re(z_1 \cdot z_2^* + z_2 \cdot z_1^*) = \Re(2 \cdot z_1 \cdot z_2^*)$, the equation above can be expressed as it is.

Using the obtained expressions, the dissipated powers can now be rewritten into the following equations:

$$P_{b_{44}} = \frac{1}{2} \cdot \Re\Big(b_{44} \cdot \dot{x}_4^* \cdot \dot{x}_4\Big) = \frac{1}{2} \cdot b_{44} \cdot |\dot{x}_4|^2 \quad \text{[W]} \tag{6.12}$$

$$P_{b_{\tau\tau}} = \frac{1}{2} \cdot \Re\Big(b_{\tau\tau} \cdot \dot{\tau}^* \cdot \dot{\tau}\Big) = \frac{1}{2} \cdot b_{\tau\tau} \cdot |\dot{\tau}|^2 \quad \text{[W]} \tag{6.13}$$

$$\begin{aligned} P_p &= \frac{1}{2} \cdot \Re\Big({F_{p,a}}^* \cdot \dot{x}_4 - {F_{p,r}}^* \cdot (\dot{x}_4 + \dot{\tau})\Big) \\ &= \frac{1}{2} \cdot \Re\Big(G_f \cdot \dot{x}_4^* \cdot \dot{x}_4 - G_f \cdot \dot{x}_4^* \cdot (\dot{x}_4 + \dot{\tau})\Big) \\ &= -\frac{1}{2} \cdot G_f \cdot \Re\Big(\dot{x}_4^* \cdot \dot{\tau}\Big) \\ &= -\frac{1}{4} \cdot G_f \left(|\dot{x}_4 + \dot{\tau}|^2 - |\dot{x}_4|^2 - |\dot{\tau}|^2\right) \quad \text{[W]} \end{aligned} \tag{6.14}$$

Explanation Note that in the equation for the power dissipation of the pump, the action moment is taken positive and the reaction moment is taken negative. This is in contrast to there definitions. The reason for this is in that the force of the pump on the ship's structure will cause power to be dissipated, just as for the damping terms of the ship and the tank's fluid. On the contrary, the force of the pump on the tank's fluid will cause an increase in power and therefore is negative.

As seen in the equation above, for the reaction moment of the pump the rate of the absolute tank angle ($\dot{x}_4 + \dot{\tau}$) is used. This is required in order to comply with Newton's 3$^{\text{rd}}$ law; In the theoretical condition in which the tank fluid is frozen it must move together with the ship. This means that the rate of the relative tank angle is zero, which causes the net power dissipation to be zero since there is no velocity.

The fact that the power dissipation due to the reactive moment component is nonzero for $\dot{\tau} = 0$ is correct because this reactive moment component acts on a rotating body, and, mathematically this does result in a non-zero power. However, the other component of the moment acts on the rotating body having the opposite sign and also results in a non-zero power, where mathematically this power component has the opposite sign and cancels the power due to the reactive moment.

Plots In Figure 6.1 the powers are plotted using Equations 6.12 - 6.14 and the transfer functions of the motions. In the left plot it can be seen that due to the ART, and even more due to the active control, the input power will decrease. Since, the waves can supply less power into the system the ART and it's control do not only dissipate power, but also decrease the input power.

In the plot on the right side the negative values indicate that the power dissipated by the pump is negative, so the pump has to supply power.

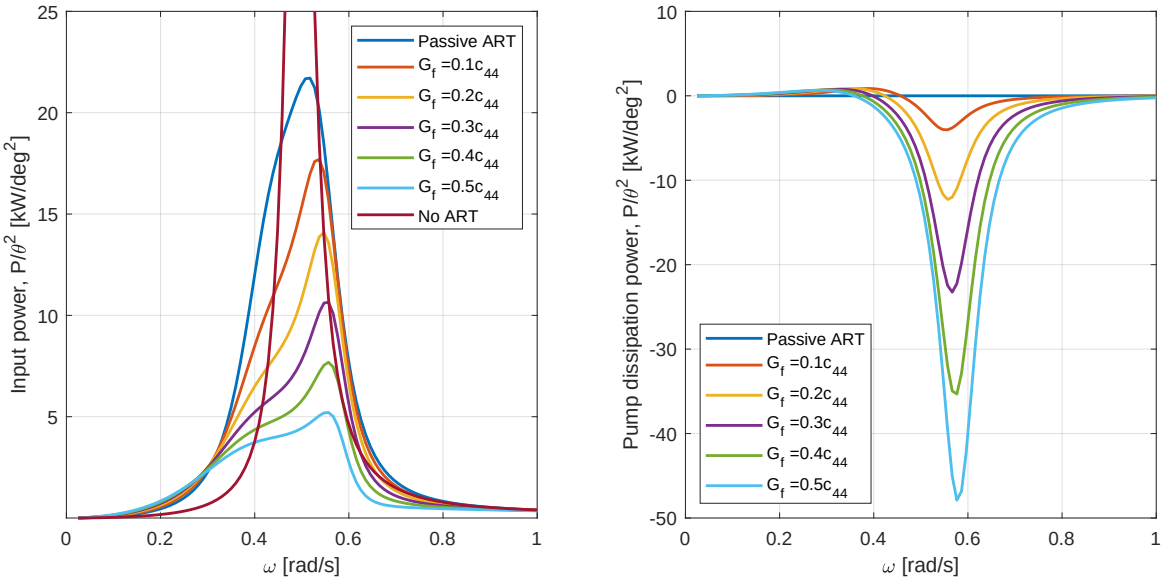

Figure 6.1: Input and pump power for feedback controlled model using Eq. 6.12 - 6.14.

Time averaged power Using wave spectra the expected value for the various rotational velocities can be obtained in order to derive the mean time averaged expressions.

$$\begin{aligned} E\left[|\dot{x}_4+\dot{\tau}|^2\right] &= \int_0^\infty \left(|Q_{\dot{x}_4,\theta}+Q_{\dot{\tau},\theta}|^2 \cdot S_\theta\right) d\omega \quad [(\text{rad/s})^2] \\ E\left[|\dot{x}_4|^2\right] &= \int_0^\infty \left(|Q_{\dot{x}_4,\theta}|^2 \cdot S_\theta\right) d\omega \quad [(\text{rad/s})^2] \\ E\left[|\dot{\tau}|^2\right] &= \int_0^\infty \left(|Q_{\dot{\tau},\theta}|^2 \cdot S_\theta\right) d\omega \quad [(\text{rad/s})^2] \end{aligned} \tag{6.15}$$

This will give the following expression for the dissipated power by the pump for the feedback controlled model:

$$\overline{P}_p = -\frac{G_f}{4}\left(E\left[|\dot{x}_4+\dot{\tau}|^2\right] - E\left[|\dot{x}_4|^2\right] - E\left[|\dot{\tau}|^2\right]\right) \quad [\text{W}] \tag{6.16}$$

6.1.3 Feed forward control

Pump moment For the feed forward controlled model, the expression for F_p is different. The moment delivered by the pump to manipulate the flow of the tank's fluid is determined in Equation 3.19. The equation is repeated below for convenience.

$$F_p = \Delta p \cdot h_d \cdot x_t \cdot r_d = g_f \cdot F_{w4} \cdot h_d \cdot x_t \cdot r_d = G_f \cdot e^{-i\epsilon_{F_p,F_{w4}}} \cdot F_{w4} \quad [\text{Nm}]$$

The pump moment per unit of wave slope F_{p0} is obtained by using the wave moment per unit of wave slope F_{w40}.

Power dissipation Using the expression for the moment generated by the pump, the power dissipation can be determined. Note that $F_{p,a}$ is the action moment of the pump action on the ship's structure and $F_{p,r}$ is the reaction moment of the pump on the tank's fluid. Since these moments are equal they can also be expressed as F_p.

$$\begin{aligned} P_p &= \frac{1}{2}\Re\Big({F_{p,a}}^* \cdot \dot{x}_4 - {F_{p,r}}^* \cdot (\dot{x}_4+\dot{\tau})\Big) \\ &= \frac{1}{2}\Re\Big({F_p}^* \cdot \dot{x}_4 - {F_p}^* \cdot (\dot{x}_4+\dot{\tau})\Big) \\ &= \frac{1}{2}\Re\Big(-{F_p}^* \cdot \dot{\tau}\Big) \\ &= -\frac{1}{4}(|F_p+\dot{\tau}|^2 - |F_p|^2 - |\dot{\tau}|^2) \quad [\text{W}] \end{aligned} \tag{6.17}$$

In Figure 6.2 the total input power as well as the equation above is plotted. The negative values indicate that the power dissipated by the pump is negative, so the pump has to supply power.

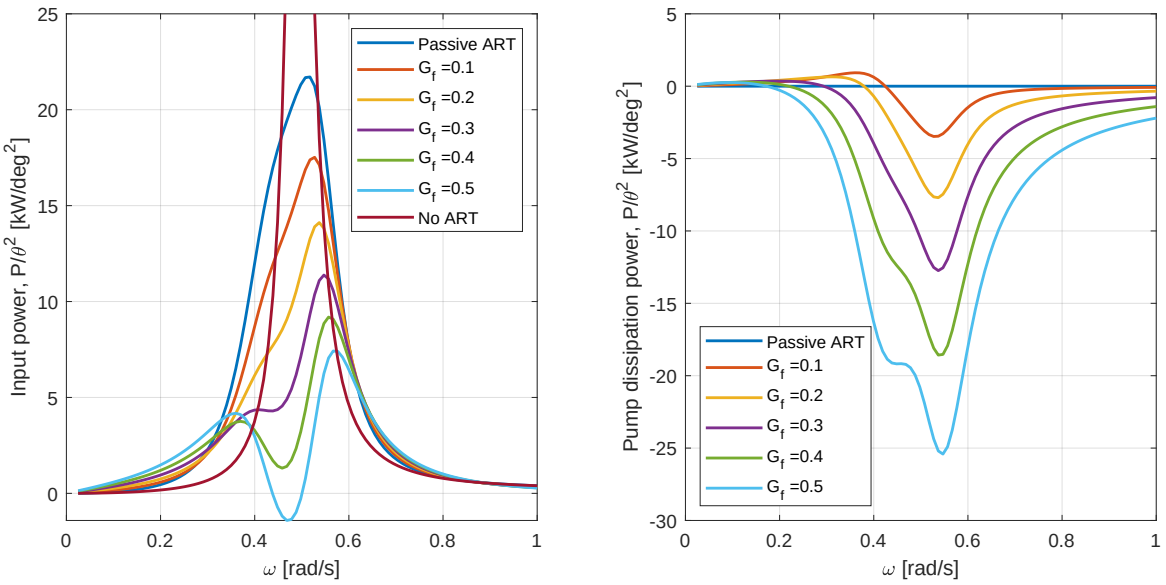

Figure 6.2: Input and pump power for feed forward controlled model using Eq. 6.12, 6.13 and 6.17.

Time averaged power To obtain the time averaged power dissipation the response energy must be integrated over the frequency range.

$$\begin{aligned} E\left[|F_p + \dot{\tau}|^2\right] &= \int_0^\infty \left(|F_{p0} + Q_{\dot{\tau},\theta}|^2 \cdot S_\theta\right) d\omega \quad [\text{rad}] \\ E\left[|F_p|^2\right] &= \int_0^\infty \left(|F_{p0}|^2 \cdot S_\theta\right) d\omega \quad [\text{rad}] \\ E\left[|\dot{\tau}|^2\right] &= \int_0^\infty \left(|Q_{\dot{\tau},\theta}|^2 \cdot S_\theta\right) d\omega \quad [\text{rad}] \end{aligned} \tag{6.18}$$

This will give the following expression for the pump power dissipation of the feed forward controlled model:

$$\overline{P}_p = -\frac{1}{4}\left(E\left[|F_p + \dot{\tau}|^2\right] - E\left[|F_p|^2\right] - E\left[|\dot{\tau}|^2\right]\right) \quad [\text{W}] \tag{6.19}$$

6.1.4 2DoF controlled model

For the 2DoF controlled model the moment F_p is determined based on Equation 3.36:

$$F_p = G_{fb} \cdot \dot{x}_4 + G_{ff} \cdot e^{-i\epsilon_{F_p,F_{w4}}} \cdot F_{w4} \quad [\text{Nm/rad}] \tag{6.20}$$

The pump power dissipation again consists of the action moment and the reaction moment:

$$\begin{aligned} P_p &= \frac{1}{2}\Re\Big(F_{p,a}{}^* \cdot \dot{x}_4 - F_{p,r}{}^* \cdot (\dot{x}_4 + \dot{\tau})\Big) \\ &= \frac{1}{2}\Re\Big(-F_p{}^* \cdot \dot{\tau}\Big) \quad [\text{W}] \\ &= \frac{1}{2}\Re\left(\left(G_{fb} \cdot \dot{x}_4 + G_{ff} \cdot e^{-i\epsilon_{F_p,F_{w4}}} \cdot F_{w4}\right)^* \cdot \dot{\tau}\right) \quad [\text{W}] \end{aligned} \tag{6.21}$$

The equation above contains the feedback and the feed forward control aspect. Therefore, it can be rewritten using the expressions obtained earlier for the feedback and feed forward models.

$$\begin{aligned} P_{p,fb} &= -\frac{1}{4} \cdot G_{fb} \left(|\dot{x}_4 + \dot{\tau}|^2 - |\dot{x}_4|^2 - |\dot{\tau}|^2 \right) \quad [\mathrm{W}] \\ P_{p,ff} &= -\frac{1}{4} \left(|G_{ff} \cdot e^{-i\epsilon_{F_p,F_{w4}}} \cdot F_{w4} + \dot{\tau}|^2 - |G_{ff} \cdot e^{-i\epsilon_{F_p,F_{w4}}} \cdot F_{w4}|^2 - |\dot{\tau}|^2 \right) \quad [\mathrm{W}] \end{aligned} \tag{6.22}$$

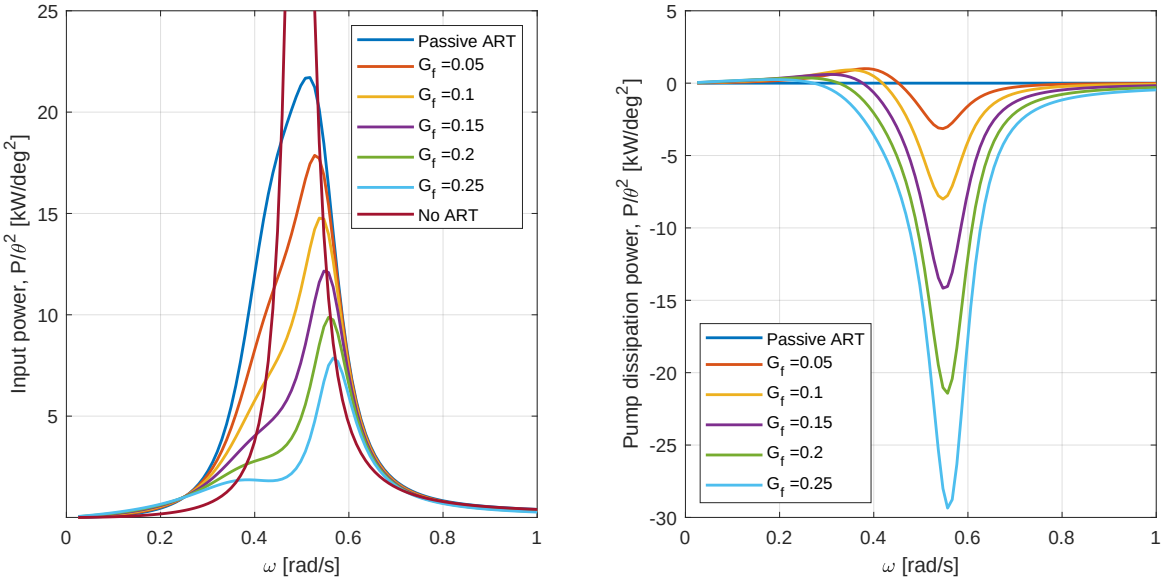

Figure 6.3: Input and pump power for 2DoF controlled model using Eq. 6.12, 6.13 and 6.22.

6.1.5 Comparison of models on pump dissipation power

In Figure 6.4 on the left side the pump power dissipation for the different models is plotted. On the right side the total input power is plotted.

What can be seen in the left graph is that the dissipated power for a certain RMS value of the roll motion is much lower for the feed forward controlled model with phase angle of $\epsilon_{F_p,F_4} = -45°$ compared to the other models. This can be explained by the fact that the tank's fluid angle with respect to the ship's roll motion is tuned better. By maintaining a 90° phase angle between the tank's fluid angle and the ship's roll motion, the situation is avoided that the reaction component of the pump moment has a negative effect on the seakeeping of the SOV. Since the latter situation does occur at the other models, the power dissipated by the pump has a smaller effect on the roll motion.

From the graph on the right side the same can be concluded, the models in which the pump has a phase angle with respect to the wave moment are more efficient. For a certain root mean square value of the roll motion, those models have less input power.

Looking at the curves for the 2DoF model with phase angle of $\epsilon_{F_p,F_4} = -30°$, it can be seen that it is indeed a compromise between the feedback and feed forward model since the curves lie between the pure feedback model and the pure feed forward model. Nevertheless, as mentioned before in §3.3, a 2DoF model is preferred above a pure feed forward model since

Figure 6.4: Comparison of pump power dissipation for different models.

the latter model will be less robust. Without a feedback loop included, the model would rely too heavily on the theoretically expected motions.

6.2 Pump power

In the previous paragraphs the pump dissipation power is discussed. In addition to this, the actual pump power will be discussed below. The actual pump power regards the power that is required for the defined control moments within the models.

6.2.1 Pump power for the different models

For the velocity in the reservoirs the assumption is made that the angle of the fluid (τ) will be small;

$$v_r = \frac{d}{dt}\left(\frac{z}{2}\right) = \frac{w\ \dot{\tau}}{2} \quad [\mathrm{m/s}] \tag{6.23}$$

As seen in the equation above, the rate of the tank's fluid angle is required. Using the transfer functions of the tank's fluid angle per unit of wave slope, the rate of the tank's fluid angle can be obtained by multiplying with $i\omega$. To obtain the flow rate the flow velocity must be multiplied with the cross-sectional area.

$$Q = v \cdot w_r \cdot x_t \quad [\mathrm{m^3/s}] \tag{6.24}$$

For the pump power the expression as below is used. The expressions for the pressure (Δp) are obtained in Chapter 3.

$$P_p = Q \cdot \Delta p \quad [\mathrm{W}] \tag{6.25}$$

Feedback model The power can be determined using the following equation:

$$P_{p,fb} = Q \cdot \Delta p = \left(\frac{w \ \dot{\tau}}{2} \cdot w_r \cdot x_t \right) \cdot g_{fb} \cdot \dot{x}_4 \quad [\mathrm{W}] \tag{6.26}$$

Now the transfer function of the power multiplied with the wave spectrum (S_θ) is as in Equation 6.27. Due to the fact that the transfer function of the pump power is per unit of wave moment *squared*, the transfer function is not squared before multiplication with the wave spectrum. The fact that the pump power transfer function is per unit of θ^2 is because the transfer functions $S_{\dot{\tau}_4,\theta}$ and $S_{\dot{x}_4,\theta}$ are part of the expression.

In contrast with the computations for the dissipated powers, now the absolute value of the transfer function of the pump moment is taken directly. This means that the case in which the pump would theoretically be able to absorb power of the system, is not considered. This is because it is assumed that a first implementation of the system will not have power absorption capabilities.

$$S_{p,fb}(\omega) = \left| \frac{w \cdot S_{\dot{\tau}_4,\theta}}{2} \cdot w_r \cdot x_t \cdot g_{fb} \cdot S_{\dot{x}_4,\theta} \right| \cdot S_\theta \quad \left[\frac{\mathrm{W} \cdot \mathrm{s}}{\mathrm{rad}} \right] \tag{6.27}$$

By integration of the spectrum, the mean power is already obtained.

$$\overline{P}_{p,fb} = \int_0^\infty S_{p,fb}(\omega) \ d\omega \quad [\mathrm{W}] \tag{6.28}$$

Feed forward model The power for the feed forward model is as follows:

$$P_{p,ff} = Q \cdot \Delta p = \left(\frac{w \ \dot{\tau}}{2} \cdot w_r \cdot x_t \right) \cdot g_{ff} \cdot F_{w4} \quad [\mathrm{W}] \tag{6.29}$$

$$S_{p,ff}(\omega) = \left| \frac{w \cdot S_{\dot{\tau}_4,\theta}}{2} \cdot w_r \cdot x_t \cdot g_{ff} \cdot F_{w40} \right| \cdot S_\theta \quad \left[\frac{\mathrm{W} \cdot \mathrm{s}}{\mathrm{rad}} \right] \tag{6.30}$$

$$\overline{P}_{p,ff} = \int_0^\infty S_{p,ff}(\omega) \ d\omega \quad [\mathrm{W}] \tag{6.31}$$

Now on topic of the actual pump power of the feed forward model, an improvement can be made by limiting the frequency range over which the pump will exert a control moment. Up till now the only model limit defined on this aspect is that the for the control moment the wave excitation moment will only be considered up to the frequency of the zero of the moment's transfer function (see §4.1.2 *Stability assessment*). However, since the required pump power is rather high for frequencies above the natural frequency of the ART while the effect of the ART is small, an improvement can be made by only applying the feed forward control moment up till a frequency of about 20% above the ART's natural frequency.

In Figure 6.5 the effect of this approach is visualised. In the left graph, it is seen that the transfer function of the ship's roll per unit of wave slope for the cases with active ART will differ little from the case with passive ART. Nevertheless, as seen in the right graph, it will save a significant amount of power if the pump power is not integrated over the entire frequency range. In Figure 6.6 the effect is shown for a sea state with $\overline{H}_{1/3} = 3\mathrm{m}$ and $T_p = 13\mathrm{s}$.

Figure 6.5: Power limit for feed forward controlled ART.

Figure 6.6: Power limit comparison for feed forward controlled ART.

2DoF model Since the 2DoF model is a combination of the feedback and feed forward models, the pump power can easily be obtained by adding the expressions for the independent models.

$$\overline{P}_{p,hb} = \overline{P}_{p,fb} + \overline{P}_{p,ff} \quad [\text{W}] \tag{6.32}$$

Comparison of different models In Figure 6.7 the results are plotted for the different models. As expected the feed forward model has the lowest required pump power for a certain RMS roll motion.

Figure 6.7: Root mean square value of pump power for different models.

6.2.2 Maximum pump power in a storm

Due to the approach in the previous paragraph, the root mean square value has not been derived, since it has no meaning. This also implies that the probabilistic calculations can not be performed as usually performed in spectral analyses. However, to be able to say something about the expected peak powers, the spectra of the flow and pressure are considered independently. This will provide root mean square values. The power can then be determined based on the simplification that the power and flow are two independent variables.

$$\begin{aligned} S_Q &= |1/2 \cdot w \cdot w_r \cdot x_t \cdot S_{\dot{\tau},\theta}|^2 \cdot S_\theta \quad \left[\frac{\mathrm{m}^6}{\mathrm{s} \cdot \mathrm{rad}}\right] \\ S_{\Delta p} &= |g_{fb} \cdot S_{\dot{x}_4,\theta}|^2 \cdot S_\theta \quad \left[\mathrm{Pa}^2 \cdot \mathrm{s/rad}\right] \end{aligned} \tag{6.33}$$

$$\begin{aligned} Q_{rms} &= \sqrt{\int_0^\infty S_Q(\omega)\, d\omega} \quad \left[\mathrm{m}^3/\mathrm{s}\right] \\ \Delta p_{rms} &= \sqrt{\int_0^\infty S_{\Delta p}(\omega)\, d\omega} \quad [\mathrm{Pa}] \end{aligned} \tag{6.34}$$

Maximum power in a 3h storm Now the highest required power during a storm of 3h with about 1000 waves can be determined using the root mean square values. In Equation 5.18 the maximum amplification of the significant motion is determined as 1.86.

$$P_{p,storm,FB} = 1.86 \cdot 2 \cdot Q_{rms} \cdot 1.86 \cdot 2 \cdot \Delta p_{rms} = 13.8 \cdot Q_{rms} \cdot \Delta p_{rms} \quad [\mathrm{W}] \tag{6.35}$$

Based on this expression, the pump power for a 3h storm can also be expressed based on the combined power spectrum. In this way the information on the relative phase angles will not be lost in the computations.

$$P_{p,storm,FB} = 13.8 \cdot \overline{P}_{p,fb} \quad [\mathrm{W}] \tag{6.36}$$

Other models The expressions for the maximum powers for the feedback controlled model can be used for the feed forward and 2DoF models too.

7 - Results

For the results of the workability analysis, the discussed aspects of the ART should be combined. Namely, the maximum tank fluid angle, the stability analysis and the maximum available pump power. The results of the performance analysis of the following three models will be given:

- Feedback controlled model
- Feed forward controlled model with $\epsilon_{F_p,F_{w4}} = -45°$
- 2DoF controlled model with $\epsilon_{F_p,F_{w4}} = -30°$.

Parameter selection To give the results it must first be determined what parameters will used. For the different parameters a substantiation is given.

- The average pump power is set to 100kW. This gives a maximum pump power in a 3h storm of about 1400kW.
- The tank's fluid angle must remain below the physical limit of 20.53° as defined in Equation 2.10.
- Since the operational limit of the SOV is set to a significant wave height of 3m, beam waves with $H_s = 3$m are considered. To assess the worst case scenario, a peak period equal to the resonance period of the system (±13s) is used as input for the wave spectrum.

Results of ship and tank fluid motions Based on the input as stated above, the results are obtained using a MATLAB script. These results are for the 1-directional model with two degrees of freedom as discussed within this thesis. There is no coupling of the other motions. The results can be seen in Table 7.1.

Table 7.1: Results for different models for $T_p = 13$s.

Model	Gain factor	RMS of x_4 [deg]	RMS of τ [deg]	Max τ in 3h storm [deg]
No ART	[redacted]	[redacted]	[redacted]	[redacted]
Passive ART	[redacted]	[redacted]	[redacted]	[redacted]
FB model	[redacted]	[redacted]	[redacted]	[redacted]
FF model with phase	[redacted]	[redacted]	[redacted]	[redacted]
2DoF model with phase	[redacted]	[redacted]	[redacted]	[redacted]

As seen in the table above, all maximum values of τ are below the maximum value of 20.53° as determined in Equation 2.10. Therefore, the results are considered valid.

Results of gangway motion criteria The results of the gangway motions are obtained by means of the workability tool developed by Royal IHC. As input the RAOs of the SOV are given. The RAO for roll is computed based on this thesis (see Figure 7.1), while the RAOs for the other 5 degrees of freedom are based on the SOV without ART. The output of the tool is a time trace. From this time trace a spectrum in frequency domain is made. By integration of the spectrum the root mean square values are obtained.

Note that the workability tool is only used for the gangway's motions since the workability tool developed by IHC does not provide the possibility to analyse the tank's fluid. Furthermore, it is assumed that there are no second order wave drift forces. In reality this would mean that the vessel's dynamic positioning system corrects for the drift forces.

Figure 7.1: RAOs for roll as used for the input of the workability tool.

In the tables the below the following abbreviations are used (see Figure 5.2 for notations):

- LA = Luffing angle
- LS = Luffing speed
- TL = Telescope length
- TS = Telescope speed
- SA = Slewing angle
- SS = Slewing speed

Table 7.2: RMS values of gangway motions for different models for $T_p = 13$s.

Model	LA [deg]	LS [deg/s]	TL [m]	TS [m/s]	SA [deg]	SS [deg/s]	x_4 [deg]
Limit	**32**	**8**	**5**	**2.5**	**270**	**6**	n/a
No ART	[redacted]	[redacted]	[redacted]	[redacted]	[redacted]	[redacted]	[redacted]
Passive ART	[redacted]	[redacted]	[redacted]	[redacted]	[redacted]	[redacted]	[redacted]
FB model	[redacted]	[redacted]	[redacted]	[redacted]	[redacted]	[redacted]	[redacted]
FF model	[redacted]	[redacted]	[redacted]	[redacted]	[redacted]	[redacted]	[redacted]
2DoF model	[redacted]	[redacted]	[redacted]	[redacted]	[redacted]	[redacted]	[redacted]

Based on the assumption that the gangway motions can be described by the Rayleigh distribution, the maximum values are approximated. The maximum values are defined for an extreme wave occurring once every 3h storm.

Table 7.3: Maximum gangway motions in 3h storm for different models for $T_p = 13$s.

Model	LA [deg]	LS [deg/s]	TL [m]	TS [m/s]	SA [deg]	SS [deg/s]	x_4 [deg]
Limit	**32**	**8**	**5**	**2.5**	**270**	**6**	n/a
No ART	[redacted]	[redacted]	[redacted]	[redacted]	[redacted]	[redacted]	[redacted]
Passive ART	[redacted]	[redacted]	[redacted]	[redacted]	[redacted]	[redacted]	[redacted]
FB model	[redacted]	[redacted]	[redacted]	[redacted]	[redacted]	[redacted]	[redacted]
FF model	[redacted]	[redacted]	[redacted]	[redacted]	[redacted]	[redacted]	[redacted]
2DoF model	[redacted]	[redacted]	[redacted]	[redacted]	[redacted]	[redacted]	[redacted]

Analysis of gangway motions What can be seen is that even though the roll response decreases due to the active control of the ART, the gangway motions do not decrease proportionally. To determine whether this pattern applies for different peak periods of the wave spectrum as well, an analysis is made for the 2DoF controlled model.

In Figure 7.3 the extreme values of the gangway motions are given for different peak periods. As seen, the roll motion is only partially responsible for the reduction of the gangway motions. The reduction in roll motion caused by the passive ART has a significant effect on the gangway motions. However, the further reduction in roll motion caused by the active control of the ART does not affect the gangway's motions significantly anymore.

Figure 7.2: Ship's roll for sea state with $H_s = 3$m and different T_p.

Figure 7.3: Gangway motions for sea state with $H_s = 3$m and different T_p.

8 - Discussion

The goal of this discussion is to provide more context to the performed research by discussing the model type and interpreting the results. This will be supported by giving suggestions for further research.

8.1 Remarks on research aspects

To place the research performed within this thesis into context, several statements on topic of type of model and the application of the model are made.

8.1.1 Frequency domain and time domain

Within this thesis a frequency domain approach is adopted. Since the only aspect of time in a frequency domain model is the wave period, the model does not require a long time trace of the incoming wave in order to model feed forward control. The maximum amount of seconds that the wave should be predicted in advance, is not more than the wave period of the low frequency components in the incoming waves. However, in practice additional time will be required to make the computations.

Assuming that a wave prediction system is capable of reading the waves up to several minutes, it could be stated that due to the frequency domain approach the full capabilities of a wave prediction system will not be used. By using a model in time domain the motions of the vessel could be reduced in a more advanced way. However, the downside of a model in time domain is the complexity of the computations. A part of the time that the waves are predicted up front would be lost in computation time. The consequence is that the accuracy of the model might be even worse compared to a fast frequency domain model. This is supported by the fact that if a shorter prediction time is required, the model input can be made more accurate.

8.1.2 Model linearity

For the computations within this thesis a linear model is used. The used expression for the wave moment is proportional to the wave amplitude ζ_0. Also the ship's and tank's fluid angles are linearised. Instead of using trigonometric functions, the equations are proportional to the angles, which is based on small values of the angles ($\tan(x_4) = x_4, \tan(\tau) = \tau$).

Now within literature models have been defined to assess the nonlinear behaviour of ARTs on the ship's motions. Examples are the models of Neves et al. (2009) and Holden and Fossen (2012). As stated in the papers, the nonlinear models are more accurate to assess high-amplitude motions. Such nonlinear models are required to assess parametric roll for example. When a ship experiences parametric roll, the roll motion can become very large within just a few oscillations. Since for the SOV this specific case is left out of consideration and only small roll angles are assessed, the linearised model is considered sufficiently accurate.

8.1.3 Control system

In this paragraph several remarks will be made with respect to the control aspect of the various models.

Feedback model Within this thesis an attempt has been made to improve the active control of U ARTs. Even though this is considered a relevant research subject, the same objective could have pursued by improving the performance of the control system for the feedback controlled model.

Another interesting remarks is the difference in stability performance between the feedback model within this thesis and the feedback model of Alujević et al. (2020). For the latter model the authors concluded that the natural frequency of the ART should be half the natural frequency of the ship in order to obtain a stable feedback loop. The reason that this is not required for the ART on board the SOV is due to the difference in tank damping coefficient (η_t). The damping coefficient that is determined using the hexapod tests at MARIN is higher to such an extent that the control system's stability is not an issue. The values for ${}^{b_{\tau\tau}}/_{a_{\tau\tau}}$ and ${}^{b_{\tau\tau}}/_{c_{\tau\tau}}$ are about 2.5 times higher for the SOV compared to the ship in the paper by Alujević et al. (2020). Therefore, an ART with a lower natural frequency than the ship is not required for the design of the SOV.

Proportional gain For all models analysed and developed within this thesis a proportional gain is used. By using a proportional gain for the control of the system, the model is not able to correct for any inaccuracies in the system's actuator. The output of the pump for example will change over time due to the physical nature of a technical system. For example, the blades of the pump can have wear, the level of lubrication might differ or the fuel lines might become contaminated. All these aspects affect the pump's real output with respect to its expected output. The result of this is that the control system might loose its effect over time. By adding derivative and integrator parts to the control system, the problem can be avoided.

Non constant phase angle In the developed models within this thesis a constant phase angle between the wave excitation moment and the pump moment is used. For an even better response of the system it could also be possible to use a non constant phase angle. The phase angle should be such that the total stabilising moment will oppose the wave moment with exactly 180°.

8.1.4 Analysis of extreme values for gangway limits

For the gangway of the SOV certain limits have been defined. A safety constraint is that these limits may only be exceeded once every 3h storm. Using probabilistic properties of the waves and the responses, it can be approximated what for example the required power and tank fluid angle would be for an extreme wave.

Non linearity of extreme values Now the first point of discussion is the aspect of non linearity. For high waves, non linear phenomena can occur such as wave breaking. The result of this is that the extreme values do not necessarily follow the used Rayleigh distribution. Therefore, additional research is required to determine how the safety constraints of the gangway can be considered best.

High margins The difficulty of the safety constraint is that the system's capabilities must be rather large for the extreme responses in comparison with the mean responses. Due to

the high capabilities of the active system required to obtain a model that is valid for extreme values, it is suggested not to design the ART for the extreme conditions. The design of the ART is more effective if it is only intended to damp the roll motion up to a certain level.

8.1.5 Considered wave conditions

To assess the workability of the SOV, the worst case scenario has been analysed, namely a sea state with a peak period equal to the resonance frequency of the ship. For the significant wave height the required 3m is selected. However, looking at the sea states defined by the World Meteorological Organization as shown in Table 5.3, the common peak period for a sea state with $\overline{H}_{1/3}$ is about 8s. This is far lower than the 13s used for the workability analysis.

Reduce natural period of the ART Due to the low peak period of the expected sea state, it could be beneficial to tune natural frequency of the ART to the expected peak period. In this way, the ART will have the largest effect on the workability. In the current case, the ART might not be very effective, since the SOV is unlikely to operate in a sea state with $T_p = 13$s.

Reduce natural period of the ART + vessel Now instead of reducing the roll period of just the ART, it could also be possible to reduce the natural period of the vessel as well. In this way, the vessel can be designed smaller, reducing costs. So by using the ART it can be avoided that a ship needs to have a certain size in order to avoid sea states that could cause resonance.

In the suggested case it is very much possible that the vessel will be excited at lower frequencies than the natural frequency of the ART. As shown multiple times within this thesis, a passive ART will amplify the motions at these frequencies. Therefore, it is desirable to use an active ART since there is no amplification of the motions for excitation frequencies below the natural frequency of the ART.

8.2 Further research

On top of the research performed within this thesis, additional steps can be taken to obtain a better model of the ART and to obtain more knowledge on the application of ARTs. In this paragraph multiple suggestions for further research are given.

Improving accuracy of model For the research performed within this thesis several simplifications are made. To improve the model the following aspects could be added.

- A pump model. This can be done by means of a transfer function of the pump pressure with respect to a certain input signal.
- The effects of inaccuracies in wave prediction system. This will give a more realistic indication of the active ART's performance compared to a passive ART.
- Sway motion. Within this thesis only the roll motion is considered. However, there is also a small coupling effect between the tank's fluid and the sway motion of the ship for the acceleration components in the equations of motion.

- Instead of defining a power requirement, as performed within this thesis, it could be analysed if it is more effective to define a power availability. Based on this available power, the pumps of the ART could then be controlled. This will increase the utilisation of the system.

Interaction between the gangway and ship motions The results of the gangway motions showed that the active control of the ART doesn't reduce the gangway motions significantly with respect to the passive ART. This can be explained by the fact that the ship is not only subjected to roll motion. Also the other ship motions affect the gangway motions.

Now by analysing the effect of the roll motion of the ship on the gangway motions, more insight can be obtained to determine the optimal size of the ART. This insight is valuable since a smaller ART will cause a smaller reduction of the GM due to the free surface effect caused by the tank's fluid.

Effect of roll reduction on ship size As stated in §8.1.5, the roll reduction caused by the presence of an (active) ART could be used to decrease the size of a vessel. As a research project it could be determined what benefit this would have in terms of design and costs.

Energy harvesting Another interesting topic for further research is the concept of energy harvesting. It is found that the effect of the ART is rather large at low frequencies. For these frequencies, the flow in the ART should be slowed down. Instead of adding power to slow down the fluid, it could possibly be done by extracting the energy of the fluid by means of some kind of generator which functions as an energy harvesting device.

9 - Conclusion

The research question for this thesis was formulated as follows:

What is the effect of using a wave prediction system for the control of an active U anti-roll tank on the workability of an SOV operating at zero speed?

By answering the sub-questions first, the answering of the main question is supported.

RQ 1 *What is the effect of a passive U anti-roll tank on a vessel's motion?*

A passive ART will decrease the ship's roll response at the natural frequency of the SOV. However, the roll response will be increased at low frequencies due to the free surface effect. Also, for low damping factors, the ART will cause two new resonance peaks, resulting in response amplification.

From the power dissipation analysis it is found that the input power decreases for two reasons: the tank's fluid dissipates power and the waves can supply less power into the ship.

RQ 2 *How can a passive U anti-roll tank be improved by making it active?*

By introducing a pump at the centre of the duct, the flow can be manipulated. The flow must be adjusted in a way that it will have a better phasing with respect to the ship and the wave excitation moment.

The pump will cause two control moments. One due to the force on the ship's structure and one due to the force acting on the tank's fluid. Using a controller the two control moments must be such that the ship's roll response decreases and no power is wasted due to inefficient interaction of the control moments. This inefficient interaction occurs when only the force on the ship's structure has a positive effect on the seakeeping performance, while the force on the tank's fluid causes a moment in phase with the wave excitation moment.

RQ 3 *What type of model is most suitable to reduce the motions for the vessel with an active controlled U-tank?*

Within this thesis three models have been analysed with each a different control method. The first control method regards a feedback controlled model as defined in available literature. In addition to this, two methods have been developed: a feed forward controlled model and a 2DoF controlled model. The latter model is a combination of the feed forward model and the feedback model. By combining a feedback loop and a feed forward loop, the robust properties of feedback control can be combined with the possibility to control for future disturbances with feed forward control. Also, the application of feed forward control will eliminate the waterbed effect caused by Bode's sensitivity integral. So, it is found that a model with a feedback and a feed forward loop gives the best performance.

RQ 4 *What is the increase in workability due to the system?*

For the workability analysis use is made of the design constraints of the gangway. It has been found that if a passive ART is included in the design of the SOV, the motions are reduced such that the gangway's limits are not exceeded anymore for sea states with $\overline{H}_{1/3} = 3\text{m}$.

Even though the active models provide significant roll reduction with respect to the passive model, not all the gangway's motions are improved. Therefore, there is no significant increase in workability due to the active system in terms of gangway motions.

RQ 5 *What is the power demand for the active controlled U anti-roll tank?*

All models have been analysed for a mean power demand of 100kW. This gives a peak power requirement of about 1400kW. This peak power is assumed to be exceeded once every storm of 1000 waves.

Main question All in all, it is found that by using a wave prediction system the performance of the active control can be increased since the phasing of the control moment with respect to the wave excitation moment can be controlled. Due to the improved performance of the control system the seakeeping performance of the SOV is also improved since the roll motions are attenuated.

Looking at the gangway motions, it is found that the design requirements are exceeded for the SOV without ART. However, even though the seakeeping performance of the vessel is improved due to the active control of the ART, the gangway motions aren't reduced proportionally. This can be explained by the fact that besides the roll motion of the ship, the surge, sway, heave, yaw and pitch motions also effect the gangway motions. Since the ART only affects the roll motion, the gangway motions can only be reduced partly by reducing the roll motion of the ship.

Therefore, it is suggested to use a passive ART for the design of the SOV instead of an active ART.

Bibliography

Abdel Gawad, A., Ragab, S., Nayfeh, A., and Mook, D. (2001). Roll stabilization by anti-roll passive tanks. *Ocean Engineering*, Vol. 28:457–469.

Alexander, C. K. (2005). *Fundamentals of Electric Circuits*, volume 473-477. McGraw-Hill.

Alujević, N., Ćatipović, I., Malenica, , Senjanović, I., and Vladimir, N. (2020). Stability, performance and power flow of active u-tube anti-roll tank. *Engineering Structures*, 211:110267.

Astrom, K. J. and Murray, R. M. (2008). *Feedback Systems: An Introduction for Scientists and Engineers*. Princeton University Press, USA.

DNV GL (2017). Offshore gangways. `https://rules.dnvgl.com/docs/pdf/DNVGL/ST/2017-09/DNVGL-ST-0358.pdf`.

Gunsing, M., Carette, N., and Kapsenberg, G. (2014). Experimental data on the systematic variation of the internal damping inside a u-shaped anti-roll tank.

Holden, C. and Fossen, T. I. (2012). A nonlinear 7-dof model for u-tanks of arbitrary shape. *Ocean Engineering*, 45:22–37.

Holden, C., Galeazzi, R., Fossen, T. I., and Perez, T. (2009). Stabilization of parametric roll resonance with active u-tanks via lyapunov control design. In *2009 European Control Conference (ECC)*, pages 4889–4894.

Holthuijsen, L. H. (2007). *Waves in Oceanic and Coastal Waters*. Cambridge University Press.

Journée, J. and Massie, W. (2001). *Offshore hydrodynamics*. Delft University of Technology.

Kornev, N. (2012). *Ship dynamics in waves*. University of Rostock.

Lloyd, A. R. J. M. (1989). *Seakeeping: ship behaviour in rough weather*. E. Horwood.

MARIN (2020a). Diffrac: Calculation of wave loads and motions using 3-d potential theory including wave diffraction.

MARIN (2020b). *Service operation vessel (75 m); Seakeeping tests*. MARIN.

MIT (2004). Understanding poles and zeros. `https://web.mit.edu/2.14/www/Handouts/PoleZero.pdf`.

Moaleji, R. (2006). *Adaptive control for ship roll stabilization using anti-roll tanks*. ProQuest LLC.

Neves, M. A., Merino, J. A., and Rodríguez, C. A. (2009). A nonlinear model of parametric rolling stabilization by anti-roll tanks. *Ocean Engineering*, 36(14):1048–1059.

Royal IHC (2020a). Sea-link motion compensated gangway. `https://www.royalihc.com/en/products/offshore-wind/operations-and-maintenance/motion-compensated-gangway-sea-link`.

Royal IHC (2020b). Service operation vessel. `www.royalihc.com/en/products/offshore-wind/operations-and-maintenance/service-operation-vessel`.

A - Appendix

A.1 Figures

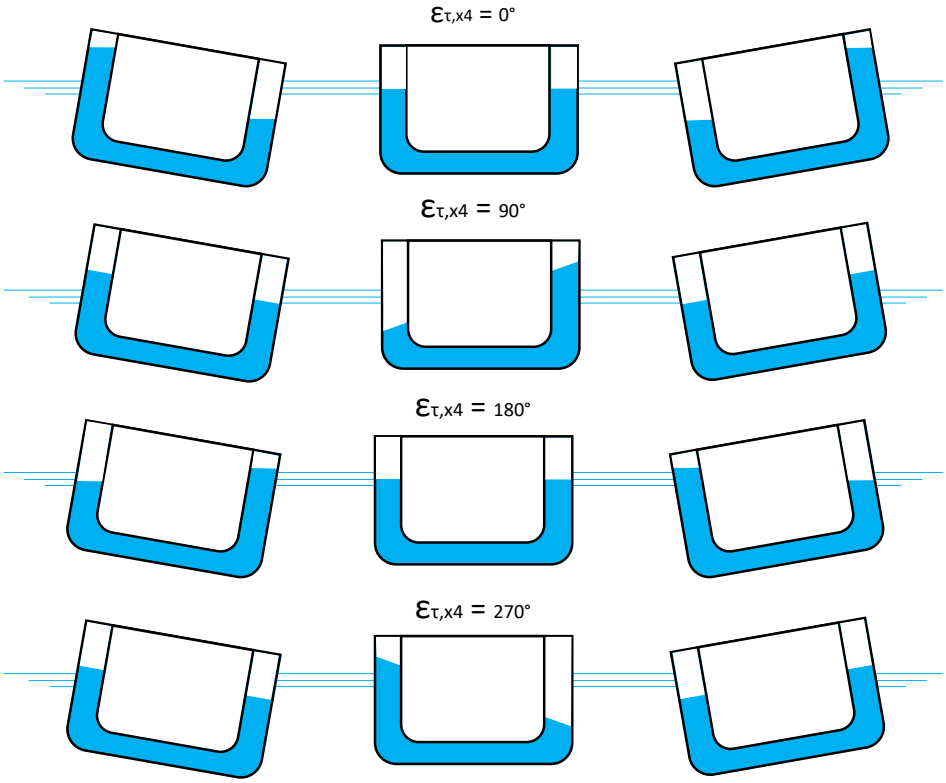

Figure A.1: Illustration of phase angles between the fluid angle (τ) and roll angle (x_4).

Figure A.2: Comparison between constant and real hydrodynamic coefficients.

A.2 Elaboration on equation for wave moment

To obtain an expression for the wave moment use is made of the work by Kornev (2012). The wave excitation force contains out of two parts:

- Froude–Krylov force: This part regards the integration of the wave induced pressure, without considering the interaction between the wave and the ship (the ship is transparent). This force contains out of two parts:
  - A hydrostatic part due to integration over the mean submerged area.
  - A hydrodynamic part due to integration over the instantaneous submerged area.
- Diffraction force: This part is a correction for the fact that in reality the waves are effected by the ship.

Froude–Krylov part Restoring hydrostatic moment corrected for wave induced hydrostatic moment:

$$F_{4,hs} = -\rho g \nabla_0 G M_\gamma (x_4 - \theta) \quad [\text{Nm}] \tag{A.1}$$

The hydrodynamic forces can be obtained by considering the Bernoulli pressure equation.

$$p = -\frac{\rho u^2}{2} - \rho g z - \rho \frac{\partial x_4}{\partial t} + p_a \quad [\text{Pa}] \tag{A.2}$$

In the above equation:

- $\frac{\rho u^2}{2}$ is a second order term and will not be considered.
- $\rho g z$ is the hydrostatic moment considered in Equation A.1.
- $\rho \frac{\partial x_4}{\partial t}$ is the hydrodynamic effect caused by waves. By working out this term (see Kornev (2012), p42) it will become clear that this is as second order term. Hence, it is left out of consideration.
- p_a is the atmospheric pressure and will not result in any forces if integrated over the submerged area.

So, the total Froude–Krylov moment contains only the wave induced hydrostatic component of Equation A.1:

$$F_{4,FK} = \rho g \nabla_0 G M \theta = \rho g \nabla_0 G M \frac{\omega^2}{g} \zeta_0 \sin(\omega t) \quad [\text{Nm}] \tag{A.3}$$

Diffraction part For the diffraction part of the wave moment, the accelerated flow is considered. For the roll motion this regards the angular velocity and angular acceleration of the free surface of the incident wave ($\dot{\theta}$ & $\ddot{\theta}$).

$$F_{4,dif} = a_{44}\ddot{\theta} + b_{44}\dot{\theta} = -a_{44}\frac{\omega^4}{g}\zeta_0 \sin(\omega t) + b_{44}\frac{\omega^3}{g}\zeta_0 \cos(\omega t) \quad [\text{Nm}] \tag{A.4}$$

Total wave moment The Froude-Krylov and diffraction parts combined lead to the total wave moment.

$$F_{w4} = F_{4,FK} + F_{4,dif} = \left(\rho g \nabla_0 GM - a_{44}\omega^2\right)\frac{\omega^2}{g}\zeta_0 \sin\omega t + b_{44}\frac{\omega^3}{g}\zeta_0 \cos\omega t \quad [\text{Nm}] \quad \text{(A.5)}$$

Simplified wave equation In the work by Alujević et al. (2020) the simplified wave equation is used as below.

$$F_{w4} = c_{44}\theta \quad \text{(A.6)}$$

Starting from the expression for the magnitude of the wave moment in Equation 2.22, the following steps can be taken:

$$\begin{aligned} |F_{w4}| &= \theta\sqrt{(\rho g \nabla_0 GM - a_{44}\omega^2)^2 + (b_{44}\omega)^2} \\ &= \theta\sqrt{(\rho g \nabla_0 GM)^2 - 2a_{44}\omega^2 \cdot (\rho g \nabla_0 GM) + {a_{44}}^2\,\omega^4 + {b_{44}}^2\,\omega^2} \\ &\approx \theta\rho g \nabla_0 GM = \theta c_{44} \quad [\text{Nm}] \end{aligned} \quad \text{(A.7)}$$

So, by neglecting the higher order terms of ω, the wave moment can be simplified to the equivalence of the wave slope multiplied with the restoring spring term. To determine whether this simplification is a good approximation, the phase and magnitude of the wave moment are plotted in Figure A.3. As seen, the difference between the simplified wave equation and the original equation is rather large. Therefore, the simplified wave equation is not used within this thesis.

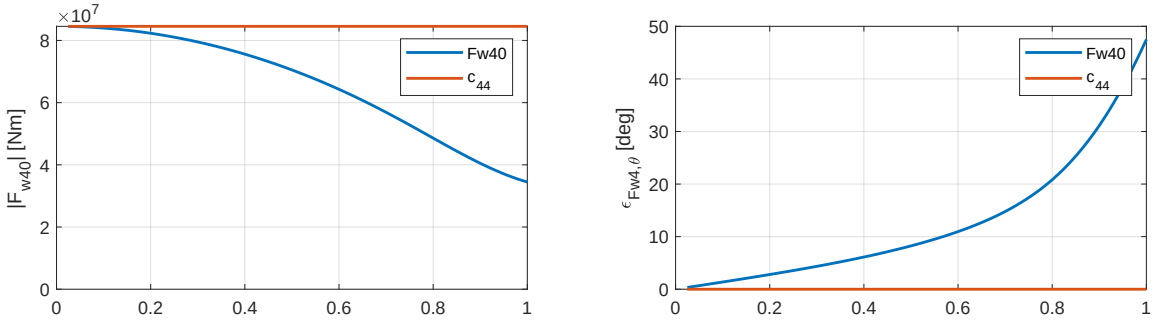

Figure A.3: Error in wave moment approximation.

A.3 Hexapod test

When comparing the model with the hexapod tests, it was found that the data points only match if a negative value for r_d is used. In Figure A.4 it can be seen what the effect is of a change in sign of r_d. As also stated by Lloyd (1989), the lower the value of r_d, the higher the moments caused by the ART.

All in all it is assumed that the data points contain a mistake in the translation from model to prototype.

Figure A.4: Comparison of data with positive value of r_d.

A.4 Graphical representation of coupled transfer functions

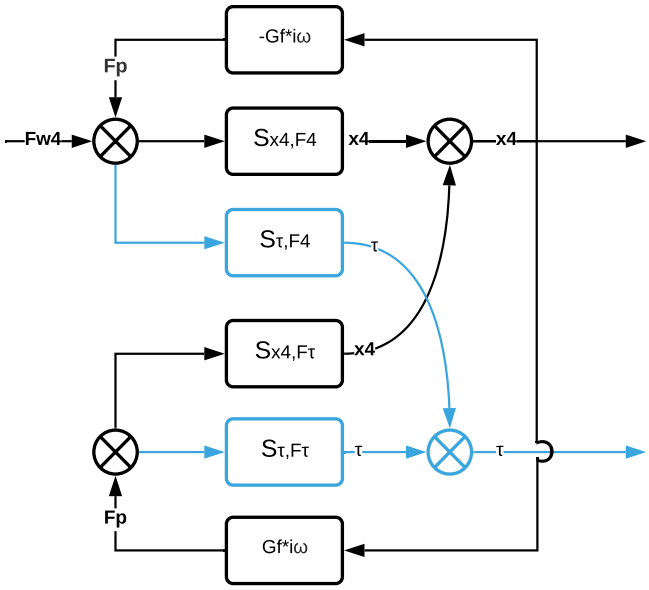

Figure A.5: Block diagram with transfer functions of active feedback controlled ART.

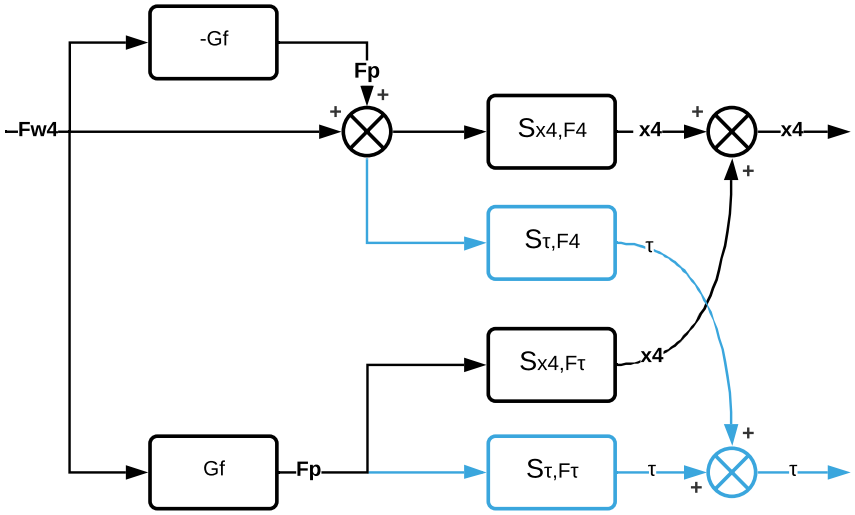

Figure A.6: Block diagram with transfer functions of active feed forward controlled ART.

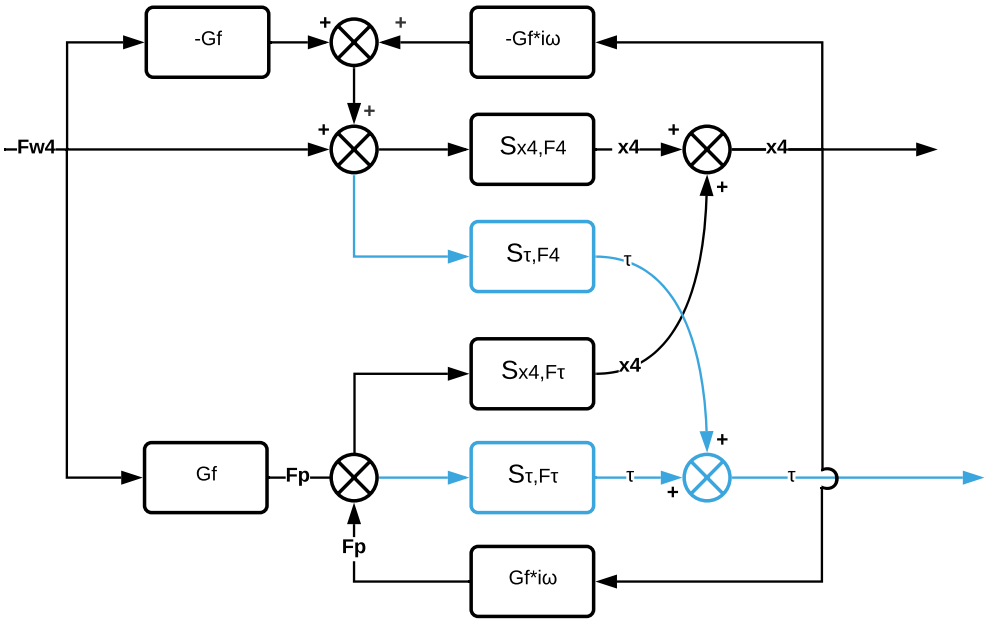

Figure A.7: Block diagram with transfer functions of 2DoF controlled ART.